

Report for 2002GA5B: Toxic Metalloid (As, Se, Sb) Enrichment from Coal-Fired Power Plants in the Chattahoochee-Apalachicola (ACF) & Etowah-Coosa (ACT) Rivers

- Dissertations:
 - Lesley, Michael P., 2002, "The Fluxes and Fates of Arsenic, Selenium, and Antimony from Coal Fired Power Plants to Rivers," Geochemistry, School of Earth and Atmospheric Sciences, Georgia Tech, Atlanta, GA, 133 pages.

Report Follows:

**The Fluxes and Fates of Arsenic, Selenium, and Antimony
from Coal Fired Power Plants to Rivers**

**School of Earth and Atmospheric Sciences
Georgia Institute of Technology**

prepared by:
**Michael Patrick Lesley
Philip N. Froelich, Jr.**

sponsored by:
**Georgia Water Resources Institute
and
The U.S. Geological Survey**

October 2002

ACKNOWLEDGEMENTS

I believe the completion of this thesis is due more to those around me than myself. I did the leg work, but you all pulled me through. I would like to thank the members of my thesis reading committee, Dr. Philip (Flip) N. Froelich, Dr. Ellery Ingall, Dr. Martial Taillefert, and Dr. Herb Windom for their advice and insight during this process. In particular, I would like to extend Flip a huge thanks. He has put up with me for two years and has driven me to produce a solid piece of science that I am very proud of.

I am extremely grateful to my wife Becca who has *also* put up with me for two years, and who has given up more than one Friday night to help me in the lab.

I would like to thank my fellow geochemistry graduate students (especially Jean Fracois Kopervnjak and Poloumi Sanigrahi) for their fellowship, advice, and support.

There are two people without whom this project would not have been completed. They are Dr. Stephany Rubin-Mason and Chris Bartley. Chris provided *all* the nutrient data for this project. He got up early with me for sampling trips, and worked late analyzing samples after I was able to go home. For this, I am grateful. Stephany has been a constant source of encouragement and advice. She has taught me more about the lab and doing science than I thought I would ever know. Stephany and Chris, I can't thank you enough.

And a final dubious thanks to the Foster Falls copperhead population, who got me busted for skipping school and who gave Flip verbal ammunition for a lifetime.

TABLE OF CONTENTS

ACKNOWLEDGEMENTS	iii
LIST OF TABLES	vii
LIST OF FIGURES	viii
LIST OF SYMBOLS	x
SUMMARY	xi

CHAPTER

I INTRODUCTION

1.1	Rational and Objectives	1
1.2	Clean versus Dirty Rivers	2
	1.2.1 Natural Backgrounds	2
	1.2.2 Metalloid Uses and Sources of Contamination	2
1.3	Solubility and Stability	4
	1.3.1 Speciation	4
	1.3.1.1 Redox Speciation	4
	1.3.1.2 Organometalloid Speciation	10
	1.3.2 Biotic Transformation	13
1.4	Toxicity in Biota	16
	1.4.1 Speciation	16
	1.4.2 Bioaccumulation	16
1.5	Coal and Coal Fired Power Plants	17
	1.5.1 Behavior in Coal Fired Power Plants	17

II	METHODS AND MATERIALS	19
	2.1 Materials	19
	2.1.1 Reagents	19
	2.1.2 Inductively Coupled Plasma-Mass Spectrometer	19
	2.1.3 Sampling and Storage	20
	2.2 Methods	23
	2.2.1 Cleaning	23
	2.2.2 Sample Gathering and Storage	24
	2.2.3 Direct Aspiration / Direct Nebulization Inductively Coupled Plasma Mass Spectrometry	25
	2.2.4 Hot Acid Extraction	34
	2.2.5 Nutrient Methods	35
	2.3 Sample Sites	35
	2.3.1 The Etowah-Coosa-Oostanualla River System	35
	2.3.2 The Chattahoochee River System	41
III	RESULTS	45
	3.1 River Metalloid Profiles	46
	3.1.1 Metalloid Concentration Profiles	46
	3.1.2 Metalloid Flux Profiles	47
	3.1.3 Delta (Δ Flux) Profiles	49

3.1.4 Suspended Sediment Load and Metalloid Concentration Profiles	50
3.2 The Etowah River and Plant Bowen	53
3.3 River Nutrient Profiles	66
IV DISCUSSION	75
4.1 Delta Fluxes	75
4.1.1 Ash Pond Effluent Evidence	75
4.1.2 Escape Efficiency	79
4.2 The Fate of Metalloids in Rivers	82
4.2.1 Biological Uptake	85
4.2.2 Sorption onto Sediments	86
4.3 Toxic Release Inventories and the PISCES Model	94
4.3.1 Toxic Release Inventories	94
4.3.2 The PISCES Model	95
V THE PLANT BOWEN ASH SPILL	99
VI CONCLUSIONS	105
APPENDIX I	107
APPENDIX II	119
APPENDIX III	127
REFERENCES	131

LIST OF TABLES

Table	Page
1-1 Arsenic ΔG_f Values	5
1-2 Selenium ΔG_f Values	8
1-3 Antimony ΔG_f Values	11
1-4 Metalloid Concentrations in Coal	18
2-1 Analytical Reagents	21
2-2 ICP-MS Settings	30
2-3 Reproducibility Results	33
4-1 Bowen Ash Pond Samples	76
4-2 Metalloid Δ Flux	80
4-3 Metalloid Loss Fluxes	83
4-4 Phosphate Loss Fluxes	83
4-5 Peak Sediment Delta Fluxes	89
4-6 TRI Aquatic and Total Release Reports	96
5-1 Above Euharlee Creek Metalloid Concentrations	100
5-2 Below Euharlee Creek Metalloid Concentrations	101
5-3a Above Euharlee Flux	104
5-3b Below Euharlee Flux	104
5-4 Etowah Δ Flux	104

LIST OF FIGURES

Figure	Page
1-1 As Eh-pH Diagram	6
1-2 Se Eh-pH Diagram	9
1-3 Sb Eh-pH Diagram	12
2-1 Metalloid Calibration Curves	29
2-3 Etowah-Coosa-Oostanuala Sampling Area	36
2-4 Plant Hammond Topography	38
2-5 Plant Bowen Topography	39
2-6 Chattahoochee Sampling Area	42
2-7 Plant Wansley Topography	43
2-8 Plant Yates Topography	44
3-1 Chattahoochee River Landmarks and Average Metalloid Concentrations	45
3-2 Etowah River Landmarks and Average Metalloid Concentrations	45
3-3 Chattahoochee River annual average metalloid flux	48
3-4 Chattahoochee River annual average metalloid Δ flux	48
3-5 Chattahoochee River annual average suspended sediment metalloid concentration	51
3-6 Chattahoochee River annual average suspended sediment load	51
3-7 Etowah River Metalloid Data, 21 May 2001	56
3-8 Etowah River Metalloid Data, 2 August 2001	57

3-9	Chattahoochee River Metalloid Data, 22 May 2001	58
3-10	Chattahoochee River Metalloid Data, 6 August 2001	59
3-11	Chattahoochee River Metalloid Data, 15 September 2001	60
3-12	Chattahoochee River Metalloid Data, 9 November 2001	61
3-13	Chattahoochee River Metalloid Data, 18 December 2001	62
3-13	Chattahoochee River Metalloid Data, 6 March 2002	63
3-14	Chattahoochee River Metalloid Data, 6 May 2002	64
3-15	Chattahoochee River Metalloid Data, 5 June 2002	65
3-17	Chattahoochee River average annual nutrient concentrations	69
3-18	Chattahoochee River Nutrient Data, 9 November 2001	70
3-19	Chattahoochee River Nutrient Data, 18 December 2001	71
3-20	Chattahoochee River Nutrient Data, 6 March 2002	72
3-21	Chattahoochee River Nutrient Data, 6 May 2002	73
3-22	Chattahoochee River Nutrient Data, 5 June 2002	74
4-1	Δ Flux Metalloid Ratios	77
4-3	Metalloid Loss Factors	84
4-4	As / PO ₄ Loss Ratio	87
4-5	Chattahoochee River Arsenic Box Model	90
4-7	Chattahoochee River Selenium Box Model	91
4-8	Chattahoochee River Antimony Box Model	92
5-1a	Etowah River-Euharlee Creek Metalloid Concentrations 7-31-02	102
5-1b	Etowah River-Euharlee Creek Metalloid Concentrations 8-2-02	102

LIST OF SYMBOLS

ppb	part per billion ($\mu\text{g} / \text{L}$)
ΔG_f	Gibbs Free Energy of Formation
ICP-MS	Inductively Coupled Plasma-Mass Spectrometry
C	Analyte Concentration
m	Slope of the Calibration Curve
R_s	Ratio of Analyte to Internal Standard
A	Isotopic Abundance of Analyte in Nature
C_{sus}	Concentration of Metalloids in Suspended Solids
C_{ex}	Metalloid Concentration of Filter Extract
M_{sed}	Mass of Sediment per Volume Water
F	Volume River Water Through Filter
E_{eff}	Metalloid Escape Efficiency
B	Mass of Coal Burned per Unit Time
R	Metalloid Release in Mass per Unit Time
Q	Stream Flow
F_{ss}	Suspended Sediment Metalloid Flux

SUMMARY

The toxic metalloids arsenic (As), selenium (Se) and antimony (Sb) are mobilized to their local aquatic environments during coal combustion. Measurements above and below power plants on the Chattahoochee River have allowed the quantification of this flux. From this flux I have been able to estimate the escape efficiency of As, Se, and Sb from power plants to rivers. Mass balance modeling has shown that the aqueous input from fly ash effluent is not sufficient to balance downstream loss. I hypothesize that this extra input is in the form of ash that sluices out of the holding ponds when they are released to rivers.

I have estimated the partitioning of As, Se, and Sb between the aqueous, suspended sediment, and biologic systems as the contaminant plume moves downstream. Calculations show that bio-removal of metalloid elements is the dominant metalloid sink in contaminated rivers.

This study compares estimates of metalloid release to EPA Toxic Release Inventories (TRI) and the PISCES model. My findings show that TRI estimates are too low by a factor of two or more. The PISCES model predicts that the majority of Se and Sb in coal are lost to the atmosphere via stack gas. Aqueous escape efficiency estimates show that Se and Sb are partitioned both onto fly ash and lost via stack gas.

Finally, a before / after comparison of metalloid flux has been made based on historic and recent samples of a large coal fired power plant that has been converted from a wet ash disposal system to a dry ash disposal system.

CHAPTER I

INTRODUCTION

1.1 Rationale and Objectives

The majority of electrical power in the United States is generated by power plants burning coal. With many nuclear power plants reaching the end of their projected lifetimes, the lack of new construction of nuclear power plants, the lack of funding for other renewable energy sources, and large US coal reserves (200-300 years at current rates of usage), this percentage will increase in the next 25-50 years. Coal combustion is a notoriously dirty process. Much attention has been paid to the airborne effects of coal combustion and to methods to control airborne pollutants. The effect of coal combustion on the aquatic environments immediately surrounding coal fired power plants (CFPPs) has received far less attention.

Work in the 1980's by Froelich (1985) showed enrichment in the metalloid element Germanium (Ge) in waters receiving ash pond effluent from coal fired power plants. It follows that these waters should also be enriched in the other toxic metalloids Arsenic (As), Selenium (Se,) and Antimony (Sb). The objective of this research has been to quantify the flux of metalloids from coal fired power plants to local receiving waters, to trace the fates of metalloids downstream through inorganic and biologic reactions, and to evaluate the accuracy of US EPA methods and estimates.

1.2 Clean versus Dirty Rivers

1.2.1 Natural Backgrounds

The metalloid concentration in contaminated rivers can be orders of magnitude higher than in rivers not impacted by anthropogenic change. The typical concentration ranges in clean rivers of As, Se, and Sb are 0.5-2.0 ppb (Francesconi and Kuehnelt 2002), 0.1 ppb (this study), and <1.0 ppb (Filella et al. 2002), respectively.

Metalloids in natural waters are the result of the weathering of rocks containing metalloid minerals. The high concentration of As in rocks is due to the substitution of As in the crystal lattices of silicate minerals, particularly in place of Si, Al, and Fe (Bhumbala and Keefer, 1994). Arsenic is commonly associated with pyrite, forming several arseno-sulfide (AsS) minerals; Arsenopyrite (FeAsS), Cobaltite (CoAsS), and Prousite (Ag₃AsS₃) (Francesconi and Kuehnelt 2002). High levels of Se in streams and rivers in the western United States have been associated with the weathering of certain Cretaceous and Tertiary age rock formations, particularly shales (Stephens and Waddell, 1998). Antimony in nature occurs mainly in the forms of Stibnite (Sb₂S₃) and Valentinite (Sb₂O₃) (Filella et al. 2002). These minerals are commonly associated with Barite bearing strata (Klien and Hulbut 1993).

1.2.2 Metalloid Uses and Sources of Contamination

Arsenic, selenium, and antimony have a wide variety of industrial uses. The manufacturing of commercial products is the main source of anthropogenic As to the environment, representing 40% of the total flux. (Bhumbala and Keefer 1994). One of the largest uses of As is in the wood preservative copper chromated arsenate (CCA). CCA

treated wood is used ubiquitously in outdoor building. The US EPA is currently requesting a voluntary industry-wide effort to phase out CCA use in lumber for domestic use by 2004 (www.epa.gov/pesticides/citizens/1file.htm). Release of As from coal combustion by products represents the second highest (20%) flux to the environment. Between 4% and 40% of the As in coal ash is water extractable. 100% of ash borne As is extractable at $\text{pH} < 7$ (Bhumbala and Keefer 1994).

Selenium has been used as an agricultural supplement for animals since its discovery as an essential micronutrient in the 1960's. These practices led to concerns regarding the toxicity of Se metabolites in livestock urine and manure. Subsequent studies revealed concentrations as high as 7.3% Se in dry matter and 133 ppb in the aqueous phase in manure lagoons (Oldfield 1998). Concentrations of this magnitude present serious concerns regarding the possibility of groundwater Se contamination in aquifers beneath livestock waste lagoons.

Selenium has also been the culprit behind fish reproductive failures and population declines in freshwater lakes receiving ash pond effluent. In the 1980s an in depth study of Hyco Reservoir, a reservoir receiving ash pond effluent from the Roxboro CFPP revealed water concentrations reaching as high as 15 ppb in 1985 (Crutchfield 2000). Subsequent studies conducted after the Roxboro plant converted to dry ash disposal have shown a decline in Se concentrations to near background levels in both water and fish tissue samples.

Antimony is widely used industrially. Alloying lead with Sb greatly increases its hardness and mechanical strength in applications such as batteries, small arms bullets,

and cable sheathing. Antimony trioxide (Sb_2O_3) has strong flame retardant properties and is widely used in plastics, adhesives, and cloth. Alloyed Sb is commonly reclaimed through recycling. However, recent trends towards the use of Sb in non-recyclable products such as paints, plastics, and adhesives have led to the release of more Sb to the environment (Filella et al. 2002).

1.3 Solubility and Stability

1.3.1 Speciation

This section discusses the major species of As, Se, and Sb found in nature. It includes Gibbs Free Energy of Formation (ΔG_f) values and Eh-pH diagrams for the major aqueous phases of these elements.

1.3.1.1 Redox Speciation

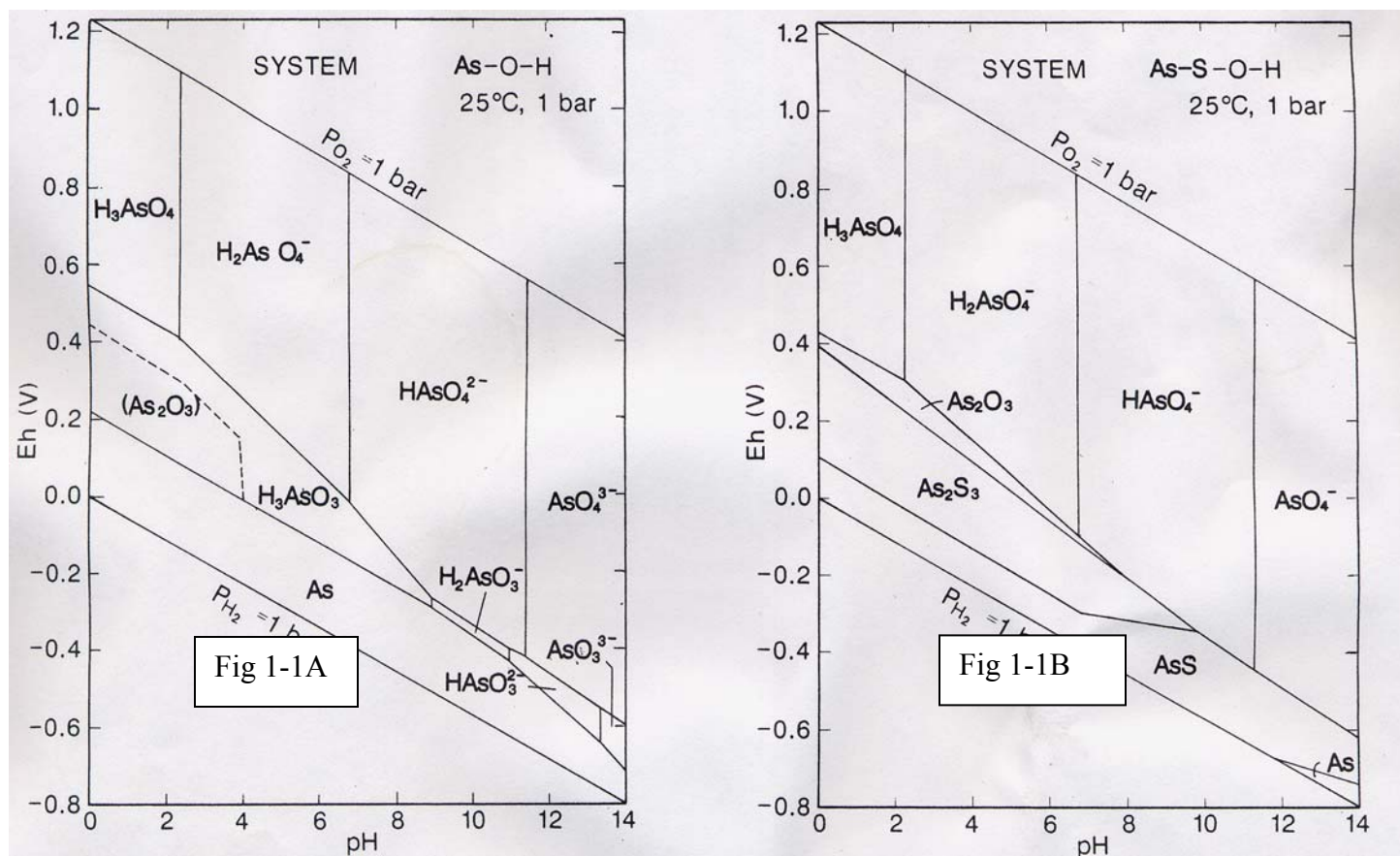
Arsenic has two major valence states, arsenite (As(III)) and arsenate (As(V)). As(-III) can be formed in certain reducing conditions, however, these conditions are not prevalent in natural systems. Table 1-1 contains ΔG_f in kcal / mol data for the major redox species of As in natural waters. This table contains data for a number of AsS compounds. These compounds are extremely important in reducing environments, such as swamps, where coal formation takes place. Figure 1-1 shows two Eh-pH diagrams. Figure 1-1A shows the As acid-base / redox speciation in a system with no S present. From the diagram it can be seen that in oxidizing / pH neutral waters the As(V) species HAsO_4^{2-} dominates. This is of critical importance as As(V) species have a high affinity for Fe and Mg oxyhydroxide minerals. These relationships play a critical role in the

Table 1-1 Arsenic ΔG_f values

Table 1-1 contains the ΔG_f values for the major As redox species found in natural water systems. In the state column, “c” is crystalline and “aq” is aqueous. ΔG_f is in units of kcal per mol.

Species	State	ΔG_f (kcal/mol)
As	C	0.00
AsS	C	-16.80
As ₂ S ₃	C	-40.30
As ₂ O ₃	C	-137.66
H ₃ AsO ₄	Aq	-183.08
H ₂ AsO ₄ ⁻	Aq	-180.01
HAsO ₄ ²⁻	Aq	-170.69
AsO ₄ ³⁻	Aq	-154.97
H ₃ AsO ₃	Aq	-152.92
H ₂ AsO ₃ ⁻	Aq	-140.33
HAsO ₃ ²⁻	Aq	-125.31
AsO ₃ ³⁻	Aq	-107.00

Data from Brookins 1988



From Brookins 1988

Figure 1-1 As Eh-pH Diagram. Figure 1-1 A shows the Eh-pH diagram for the simple As acid-base system $\{\text{As}\}=10^{-6}$ $\{\text{S}\}=10^{-3}$. Figure 1-1 B shows the As acid-base system but includes sulfur species in reducing conditions.

mobility of As in the environment.

As (V) is less mobile and more strongly attracted to hydrous iron oxides than As (III). Through adsorption onto and co-precipitation with hydrous iron oxides much of the As (V) can be removed from a contaminated river (Mok and Wai 1994). If As is sorbed onto the surface of sediment suspended in streams, it can be transported to downstream to a reservoir where it settles. If the bottom waters of the reservoir become anoxic, insoluble Fe(III) can be reduced to soluble Fe (II). If this occurs the As (V) sorbed onto the Fe (III) minerals is mobilized into the bottom waters of the reservoir, usually in the reduced form of As (III). A similar phenomenon occurring in tube wells in Thailand and Nepal has been responsible for thousands of cases of chronic As poisoning. Agget and O'Brien (1985) discovered evidence of this phenomenon in anoxic sediments in Lake Ohakuri in New Zealand. They noted that while As (III) and As (V) were both mobilized to the water column from the dissolution of hydrous iron oxide bearing sediments, in sediments with appreciable amounts of S some of the As was sequestered through the precipitation of arsenopyrite (FeAsS) and orpiment (As_2S_3).

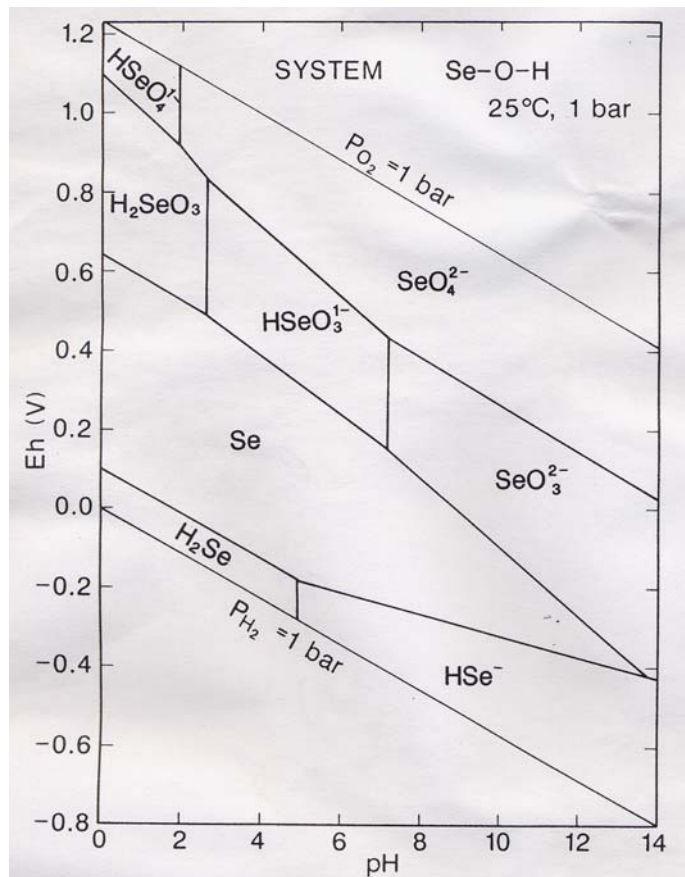
Selenium has oxidation states of Se (VI), Se (IV), Se (0) and Se (-II). However Se (-II) formation occurs outside the Eh-pH stability field for water. Table 1-2 contains the ΔG_f values for the major Se species in natural waters. Figure 1-2 shows the Eh-pH diagram for Se. The diagram shows that at neutral pH Se can exist in the +6, +4, and 0 valence states. Se (-II) can substitute for S(-II) in crystal lattices and in biological pathways (Brookins 1988). There is evidence that Se (IV) is more bioavailable because it is easier to reduce in cell pathways than Se (VI). All Se that crosses the cell

Table 1-1 Selenium ΔG_f values

Table 1-2 contains the ΔG_f values for the major Se redox species found in natural water systems. In the state column, “c” is crystalline and “aq” is aqueous. ΔG_f is in units of kcal per mol.

Species	State	ΔG_f (kcal/mol)
Se^{2-}	Aq	30.90
HSe^-	Aq	1050.00
H_2Se	Aq	3.80
H_2SeO_3	Aq	-101.85
HSeO_3^-	Aq	.98.34
SeO_3^{2-}	Aq	-88.38
HSeO_4^-	Aq	-108.08
SeO_4^{2-}	Aq	-105.47

Data from Brookins 1988



From Brookins 1988

Figure 1-2 Se Eh-pH Diagram. Figure 1-2 shows the Se Eh-pH diagram for the main inorganic Se species in natural waters. $\{\text{Se}\} = 10^{-6}$

membrane is reduced to Se (-II). Se (IV) is the favored species for uptake as it is energetically favorable to reduce as compared to Se (VI).

Table 1-3 contains the ΔG_f data for the major Sb species in natural waters. Figure 1-3 shows the Eh-pH diagram for the Sb-S system in natural waters. From this diagram, thermodynamics predict that Sb (III) should be the dominant species in anoxic conditions and Sb (V) should be the dominant species in oxic waters. However, studies have shown Sb (III) present in oxic conditions and Sb (V) in anoxic conditions. This suggests that the controls on Sb speciation are kinetic as well as thermodynamic (Filella et al. 2002). Little is known about the uptake of Sb by organisms.

1.3.1.2 Organometalloid Speciation

Arsenic, selenium, and antimony are known to have organometallic speciation as well as redox speciation. In the case of As, there are mono and di-methylarseno acids for both the +3 and the +5 redox states (Newman et al. 1998): monomethylarsonic acid and dimethylarsinic acid (As (V)) and monomethylarsonous acid and dimethylarsenious acid (As (III)). While these compounds are the most widely occurring, arsenic organometallic speciation is not limited to simple methyl compounds. Arsenobetaine, arsenosugars and other larger organoarsenic compounds are produced by macrofauna. However, these compounds make up little of the total concentration of As in natural waters.

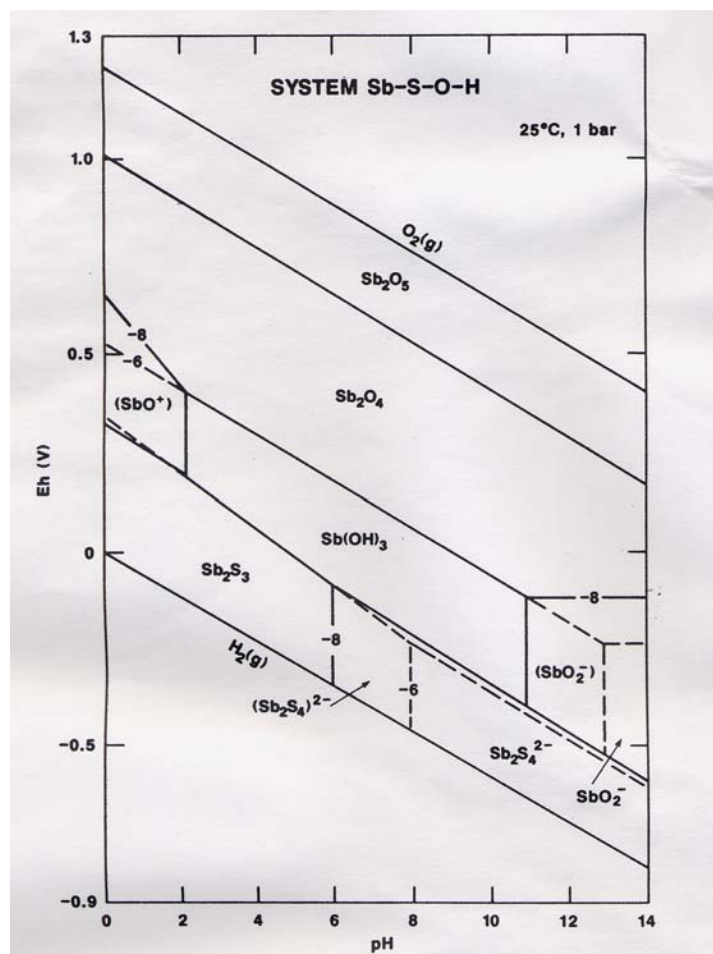
Like arsenic, selenium has a number of methyl and more complex organo species. Cooke and Bruland (1987) report nonvolatile seleno amino acids and a dimethylselenonium ion in addition to the volatile dimethylselenide and dimethyldiselenide species. They indicate that there is a biologically mediated pathway

Table 1-1 Antimony ΔG_f values

Table 1-2 contains the ΔG_f values for the major Sb redox species found in natural water systems. In the state column, “c” is crystalline and “aq” is aqueous. ΔG_f is in units of kcal per mol.

Species	State	ΔG_f (kcal/mol)
SbO ⁺	aq	-42.33
SbO ₂ ⁻	aq	-81.31
Sb ₂ S ₃	c	-41.49
Sb ₂ S ₄ ²⁻	aq	-23.78
HSbO ₂	aq	-97.39
Sb(OH) ₃	c	-163.77
Sb ₂ O ₄	c	-190.18
Sb ₂ O ₅	c	-198.18

Data from Brookins 1988



From Brookins 1988

Figure 1-3 Sb Eh-pH Diagram. Figure 1-3 shows the Eh-pH diagram for the main species of Sb-S system in natural waters. $\{\text{Sb}\}=10^{-6,-8}$ $\{\text{S}\}=10^{-3}$

from the dimethylselenonium ion to the volatile dimethyl selenide at neutral pH, and that this transformation may be an important process in the removal of Se from aqueous systems. Cutter and Bruland (1984) further distinguish that organo species of Se account for more than 80% of the total Se concentration in surface waters. They find that the maximum concentrations of reduced organo Se species (amino acids and sugars) in water column samples coincide with peaks in primary productivity, indicating that the formation of complex organo Se compounds is biologically mediated.

Evidence of biomethylation of Sb has been found in ocean water column studies (Andreae and Froelich 1984). However, these authors found no evidence of biomethylation by algae. This led them to hypothesize that biomethylation of Sb is a microbially mediated process. Recent studies show that certain fungi species can reduce and methylate Sb, releasing the volatile compound trimethylstibine in much the same manner some fungi species can reduce and methylate As to trimethylarsine (Andrewes et al. 2000).

1.3.2 Biotic Transformation

Recently much research has gone into the biotransformation of metalloids. This is due to the fact that metalloid toxicity depends greatly on speciation, and there is evidence that the organometallic species, produced exclusively biologically, may be more toxic to humans than inorganic species. There tend to be two classes of organisms that perform biological transformations, microbes and phytoplankton. Microbes, particularly in the case of As, seem to be responsible for the reduction of As (V) through respiration. Algae

and plankton are responsible for both reduction and the production of methylated and more complex organic compounds.

Oremland et al. (2000) report that in high salinity stratified lakes arsenate respiration can become nearly as important as sulfur reduction in anoxic waters. Their study shows that as much as 14% of the annual respiration in the lake may be due to arsenate reduction. This is particularly important in saline environments where sulfate reducing bacteria are forced to expend large amounts of internal energy maintaining cellular electrolyte balances. In these environments As reduction, as compared to S reduction, can be energetically more favorable for a factor of 30. Microbial reduction has also been hypothesized as a process contributing to the presence of arsenite in oxic waters where arsenate should be the dominant inorganic species (Newman et al. 1998). Whether the significant concentration of arsenite in oxic waters is a result of extremely rapid microbial production, or if the oxidation of As (III) is a slow kinetically controlled process has yet to be determined.

Methylated As compounds can account for as much as 59% of the total As concentration in some waters (Anderson and Bruland 1991). Sanders (1982) states that in some environments reduction and methylation by phytoplankton can be responsible for as much as 80% of the As speciation. Peaks in arsenite and methylarsenic concentration in areas of high primary productivity in water column samples support this hypothesis (Andreae 1978).

The environmental chemistry of Se, an essential micronutrient, is profoundly impacted by biological transformations. As with arsenic species, the concentration of

reduced and organo Se species in the water column peak in areas of primary production (Cutter and Bruland 1984, Takayanagi and Wong 1985). Recent research suggests that biological cycling of Se does not end with the release of methyl species followed by their degradation back to inorganic species. Baines et al. (2001) show that up to 53% of the organoselenides supplied to phytoplankton cultures were incorporated into biomass. The production of highly volatile organo Se compounds appears to be an extremely important factor in the flux of Se from the oceans to the atmosphere (Cooke and Bruland, 1987). It is this flux, and its subsequent transfer to the land via precipitation, that supplies the terrestrial biosphere with necessary Se.

Little is known about the biotransformations of Sb. Methlystibine species have been detected in natural systems, but their source is still unclear (Filella et al. 2002). Sb is not known to be used for respiration and is not known to be a micronutrient for any microbial or planktonic species.

Biotransformations can be a potentially useful tracer of the fate of fly ash effluent in river systems. Emissions from CFPPs are as inorganic metalloid species in the reduced form. The reduced metalloids should rapidly oxidize. If biological removal is a significant factor in the downstream fate of metalloids then the concentration of metalloid metabolites (organometallic and reduced species) should increase downstream with a parallel decrease in oxidized metalloid concentrations.

1.4 Toxicity in Biota

1.4.1 Speciation

While arsenic is used in some microbial respiration and Se is an essential micronutrient, both are toxic in trace amounts. For both, toxicity depends largely on speciation. Arsenic (III) is commonly thought to be the more toxic of the inorganic As species. This is based mainly on median lethal dose tests. In reality there is no great difference in toxicity between As (III) and As (V) (Yamauchi and Fowler 1994). Methylarsenic compounds are far less toxic than the inorganic species. In the past it has been thought that arsenic methylation was a detoxification pathway. Sordo et al. (2001) have shown that the metabolite dimethylarsonic acid (DMA) has the ability to damage DNA in human leukocytes. However, this is not a universal trait as susceptibility to DNA by DMA varied from individual to individual.

Little is known about the toxic effects of specific Se species. It stands to reason that, in excess amounts, Se (IV) will be more toxic than Se (VI) as it is more bioavailable.

1.4.2 Bioaccumulation

Both arsenic and selenium bioaccumulate up the food chain (Eisler 1994 and Crutchfield 2000). Arsenic bioaccumulation can cause damage to DNA (Eisler 1994 and Sordo et al. 2001) causing cancer and birth deformities. Exposure to high levels of As has been responsible for declines in fish and wildlife populations as well as birth abnormalities.

Se bioaccumulation, in association with coal fired power plants, was seen in Hyco reservoir, a reservoir that received fly ash effluent in the 1970's and 1980's. Se

bioaccumulation was responsible for the decline in sport fish and bird populations as well as birth abnormalities. Due in part to this contamination, the Roxboro CFPP changed from a wet ash disposal system to a dry ash disposal system. With the cessation of ash pond effluent inputs to the local reservoir Se levels in water and animal tissues have returned to near baseline levels.

1.5 Coal and Coal Fired Power Plants

Metalloids are important trace elements in coal. Average metalloid concentrations in coal are shown in Table 1-4.

1.5.1 Behavior in Coal Fired Power Plants

In coals Arsenic, Selenium, and Antimony are all associated with the mineral pyrite (Zeng et al. 2001). Metalloids are liberated from coal during combustion regardless of combustion temperature or oxidation state (Yan et al. 2001). Arsenic is partitioned almost exclusively onto fly ash (Sandelin and Backman 2001) while Se and Sb are partitioned between fly ash and loss to the atmosphere via stack gas. (Yan et al. 2001). This difference in partitioning between As and Se and Sb is partly a thermodynamic consideration, but is also strongly impacted by the kinetics of escape from the pyrite melt during combustion (Zeng et al. 2001). Due to the reducing environment inside the combustor, metalloids in the ash and gas flow are typically found in the reduced form (Yan et al. 1999). Ash ponds are pH treated to trap toxic metals such as Cd, Zn, and Cu. At the pH>7 necessary to trap Cd, Zn, and Cu examination of the Eh-pH diagrams for As, Se, and Sb (Figs 1-1, 1-2, 1-3) show that the reduced, and therefore more mobile species

Table 1-4 Metalloid Concentrations in Coal

Table 1-4 shows the average weight concentration of metalloids in coal

Element	Avg. Concentration (ppmw)	Range (ppmw)
As¹	10	0.5-80
Se¹	1	0.2-1.5
Sb^{2,3}	1	0.1-2

1-Sandelin and Backman 1999

2-Rubin 1999

3-Yan et al 2001

.

of the metalloids will be preserved. This facilitates the aquatic transport of metalloids from the ponds to local waters. It is possible that metalloid species can also be used as a tracer for ash pond effluent downstream, as one would expect to find the oxidized forms of these metalloids in an oxic stream flow.

CHAPTER II

METHODS AND MATERIALS

2.1 Materials

2.1.1 Reagents

All reagents used in this experiment are of trace metal grade. All standards are greater than or equal to 99% purity. Acid solvents are sub-boiling distilled by the manufacturer and are 99.9% impurity free. The distilled-deionized water (DDW, 18.3 MΩ) is produced in our lab. City water is distilled and allowed to cool. Once cool, the distilled water is passed first through a Barnstead-Thermolyne high-capacity cation exchange column. It is subsequently passed through two Barnstead Thermolyne ultra-pure cation exchange columns. This water is stored in HDPE carboys used exclusively for storing DDW. Table 2-1 contains a comprehensive list of reagents and manufacturers.

2.1.2 Inductively Coupled Plasma – Mass Spectrometer

In this study a Hewlett Packard HP-4500 Inductively Coupled Plasma – Mass Spectrometer (ICP-MS) is used exclusively for trace metal determination. This instrument uses a quadrupole mass filter that allows the near simultaneous determination of more than one analyte. The combination of ease of conversion between analytical methods, the ability to determine more than one isotope at a time, high sensitivity, and mass/charge (m/z) selectivity make this instrument ideal for studies such as this one.

2.1.3 Sampling and Storage Material

Samples taken in the field are stored in the vessels in which they are collected. Field collection vessels are 125 mL and 1 L high density polyethylene (HDPE) bottles manufactured by Nalgene. The bottles are cleaned by the method described in section 2.2.2.1. Water is drawn from the river using 50 mL Fortuna syringes. These are trace metal certified syringes with polyethylene bodies and polypropylene plungers. Gelman AcroDisc (GHP membrane, 0.45 μm pore size) syringe filters are used to filter samples in the field. These filters are not trace metal certified and are a potential source of error through surface exchange. Experiments were conducted to account for these possibilities. To test for filtrate loss a standard solution of known concentration was passed through a new AcroDisc and compared to an aliquot of the same solution not passed through the filter. There was a 3% loss of As, a 0.6% loss of Se, and a 0.3% loss of Sb as compared to the unfiltered solution. These losses are within the uncertainty of the experimental method and insignificant compared to the concentrations of the standards and samples. There is also the possibility of contamination through the leaching of metalloids from the filter. This phenomenon was consistently tested with field filter blanks. The metalloid concentrations in DDW passed through an AcroDisc in the field are the same (within error) as DDW and reagent blanks prepared in the lab under clean conditions. This confirms that there are no metalloids leaching from the AcroDiscs and validates cleanliness of the field methods.

Table 2-1 Analytical Reagents

Table 2-1. Analytical reagents. This table contains the instrumentation, reagents, and manufacturers used for elemental analysis during this study.

Element	Method	Reagents
As	Direct Aspiration / Nebulization ICP-MS	1, 2, Arsenic Standard (Aldrich), Yttrium Standard (Aldrich), Indium Standard (Aldrich)
Se	Direct Aspiration / Nebulization ICP-MS	1, 2, Selenium Standard (Greg Cutter), Yttrium Standard (Aldrich), Indium Standard (Aldrich)
Sb	Direct Aspiration / Nebulization ICP-MS	1, 2, Antimony Standard (Aldrich), Yttrium Standard (Aldrich), Indium Standard (Aldrich)

1 Optima HNO₃ (Fisher)

2 DDW

2.2 Methods

2.2.1 Cleaning

2.2.1.1 Sampling Materials

The bottles used for gathering and storing trace metal samples are new 125 mL high-density polyethylene (HDPE) bottles. Upon removal from their original packaging, they are rinsed with distilled-deionized water (DDW) to remove any particulate matter from the manufacturing process. They are then filled with 1 N HNO₃ and sonicated for 3-4 hours. After sonication the 1 N HNO₃ is removed and saved for use in later cleanings. The bottles, caps, and threads are then rinsed 3 times with DDW, once with 1% trace metal free HNO₃, followed with 3 more rinsings with DDW. After the last rinsing the bottles are filled with DDW and stored until use in the field.

New 1 L HDPE bottles are used to collect particulate samples. Prior to use, these bottles are partially filled with DDW and shaken vigorously to remove any particulate material. They are then filled with DDW and stored until use in the field. No other material used in the field was pre-cleaned.

2.2.1.2 Laboratory Materials

The autosampler vials used in direct aspiration / direct nebulization ICP-MS are cleaned using the same method for the 125 mL HDPE bottles. All standard solutions are placed in HDPE bottles that undergo similar treatment. All of the volumetric laboratory ware used in this study is plastic. Prior to use, the flasks are rinsed once with DDW, followed by a clean HNO₃ rinse, and finally a second DDW rinse. If they are not used

immediately after cleaning the mouths of the flasks are covered with Parafilm to prevent contamination.

All standards and samples are prepared under a bench-top clean bench to avoid contamination by dust or sand in the air. Any micropipettes used to transfer standards or samples are equipped with new trace metal free tips prior to every use.

2.2.2 Sample Collection and Storage

Two types of samples were gathered during this study; filtered water samples used for metalloid analyses, and particulate samples used to determine the amount of suspended sediment in the river.

Filtered samples are taken by the following method. A 50 mL Fortuna syringe is filled with river water and emptied three times. An AcroDisc syringe filter is placed on the syringe luer tip. A small amount of river water is filtered through the syringe into a 125 mL trace metal cleaned bottle. The bottle is capped and the water swirled around. The water is dumped from the bottle into the cap, then poured over the threads. The process is repeated two more times. The syringe is then emptied and a fresh 50 mL aliquot of river water is collected. The entire volume of the syringe is passed through the filter and collected in the bottle. 500 μ L of concentrated (69%-70%) Optima nitric acid is added to the sample. The amount of river water passed through the filter is recorded in order to calculate suspended metalloid concentrations.

Particulate samples are taken in cleaned 1 L bottles. The bottles, caps, and threads are rinsed three times with river water. The bottles are then immersed completely in the river and allowed to fill. Both filtered acidified samples and particulate grab samples

must be stored in the cold and dark immediately after collection. A cooler filled with ice or ice packs is sufficient for this purpose.

Field filter blanks were taken to account for contamination in the field from dust or other debris and to test for leaching of metalloids from syringe filters.

2.2.3 Direct Aspiration / Direct Nebulization Inductively Coupled Plasma-Mass Spectrometry

Direct aspiration /direct nebulization inductively coupled plasma mass spectrometry (DA/DN ICP-MS) is used to analyze samples for total dissolved As, Se, and Sb. This method takes advantage of the quadrupole mass filter's ability to determine multiple analytes simultaneously. As and Se are determined by analysis of the ^{75}As and ^{77}Se isotopes respectively. Two Sb isotopes are analyzed; ^{121}Sb and ^{123}Sb , to cross check calculations. It is commonly thought that As and Se cannot be determined by ICP-MS due to isobaric interferences on their stable isotopes. I have determined that it is possible to analyze both these elements in low matrix samples when care is taken not to introduce interference by addition of specific reagents during the preparation stage. In the case of As, Cl^- cannot be present in the solution for analysis. In the torch, ^{40}Ar combines with ^{35}Cl and ^{38}Ar combines with ^{37}Cl to form the ArCl^+ ion of mass 75. This ion interferes with the only stable isotope of As. Workers using atomic absorption spectroscopy (AAS) to determine As have preserved and analyzed samples in HCl solutions. HNO_3 was used to preserve samples and as a matrix for standards to avoid this interference. The isobaric interferences for Se are more complicated. The major isotopes of Se, ^{76}Se , ^{78}Se , and ^{80}Se

have interferences caused by the formation of Ar dimers ($^{40}\text{Ar}^{36}\text{Ar}$, $^{38}\text{Ar}^{38}\text{Ar}$, $^{38}\text{Ar}^{40}\text{Ar}$, $^{40}\text{Ar}^{40}\text{Ar}$) in the plasma torch. The only isotope without an Ar dimer interference is the rare (7.6%) ^{77}Se isotope. This however can have an interference caused by the combination ^{40}Ar and ^{37}Cl . Similar to the procedures used for arsenic analysis, the introduction of Cl must be avoided.

Internal standards are used to correct for instrument drift. It is possible that drift may not occur equally across the mass scale. This phenomenon is called differential mass drift. Samples are prepared volumetrically and an equal number of moles of the internal standard is added. All samples have an equal concentration of the internal standard. In this study 4.5 mL of sample is pipetted into an autosampler vial. 0.5mL of a 500 ppb internal standard solution is pipetted into the sample making the sample to exactly 10 ppb with respect to the internal standard. By calculating a ratio of the analyte counts to the internal standard counts it is possible to correct for any changes due to instrument drift. Correction of differential mass drift requires the use of multiple internal standards.

In this study, ^{89}Y is used as an internal standard for As and Se. Yttrium is extremely rare in nature, has no isobaric interferences, and has only one stable isotope, making it ideal for use as an internal standard for As and Se, which have masses of 75 and 77 respectively. Sb is standardized with ^{115}In . Indium is also extremely rare in nature but experiences isobaric interference from ^{115}Sn . However, the concentration of Sn in natural waters is in the 0-40 pM range (Byrd and Andrea, 1982) and ^{115}Sn is a tiny fraction of (0.34%) of the total concentration of Sn. The interference of ^{115}Sn on ^{115}In at 10 ppb In can be ignored.

Standards were prepared by serial dilution from commercially purchased primaries in the case of As and Sb. A 1000 ppm standard from Greg Cutter (Old Dominion University) was used for Se. All dilutions were done with 1% Optima HNO₃. First 0.1 L of a 1 ppm 2^o multi-element standard was prepared by diluting 100 μL of a 1000 ppm As (Aldrich) standard, 100 μL of a 1000 ppm Se (Cutter) standard, and 99 μL of a 1010 ppm Sb (Aldrich) standard to 100 mL. A 100 ppb 3^o standard was prepared by diluting 10 mL of the 2^o to 100 mL. 1, 2, 4, 6, and 10 ppb working standards were made by diluting 100 μL, 200 μL, 400 μL, 600 μL, and 1 mL of the 2^o, respectively, to 100 mL. A 0.1 ppb working standard was made by diluting 100 μL of the 3^o standard to 100 mL. 0 ppb standard was prepared by transferring 100 mL of 1% Optima HNO₃ to the volumetric flask used to prepare the working standards and then transferred to its own bottle.

The 0, 0.1, 1, 2, 4, 6, and 10 ppb multi-element standards were used to make a 7 point calibration curve. The multi-element standards were spiked with the internal standard in the same manner as the samples. Calibration is done by plotting the ratio of the element to its internal standard versus the response. A typical set of calibration curves is shown in figure 2-1. The isotopic abundance of the isotope being analyzed is reflected in the concentrations shown on the x-axis. The analytical data are corrected for isotopic abundance to reflect the total metalloid concentrations in the samples. Concentration is calculated from the calibration curves using the following equation:

Eq. 2-1 Analyte Concentration in Samples

$$C = \frac{R_s}{m \times A}$$

C is the concentration of the analyte in the sample. R_s is the ratio of the analyte counts to internal standard counts measured for the sample. m is the slope of the calibration curve. A is the natural isotopic abundance of the analyte.

The detection limits of this method (3 times the standard deviation of the blank) for As, Se, and Sb are 0.006 ppb, 0.06 ppb, and 0.010 ppb respectively. Blank levels in DDW are 0.003 ppb for As, 0.04 ppb for Se, and 0.005 ppb for Sb. Precisions of 3.2% for As, 4.4% for Se, and 4.1% for Sb were obtained for samples having concentrations \geq 0.1 ppb ($n=3$). See Table 2-4 for reproducibility data.

The acquisition is made in peak jumping mode ($m/z = 75$ (As), 77 (Se), 89 (Y), 115 (In), 121 (Sb), and 123 (Sb)) with three points per peak. Dwell time is 0.5 s, with an acquisition time of 17 s. The detector is set to pulse counting mode. The peristaltic pump runs at 0.3 rps for a sample feed rate of 1 ml per minute. The autosampler program is as follows: DDW, reagent blank, 0-10 ppb standards (as listed above), samples, DDW. Between each sample and standard there is a 10s rinse with DDW and a 1 minute rinse with 1% Optima HNO_3 . The plasma gas rate is 16 L / min, the auxiliary gas rate is 1 L / min, and the carrier gas rate is 1.15 L / min. See Table 2-3 for other ICP-MS instrument settings.

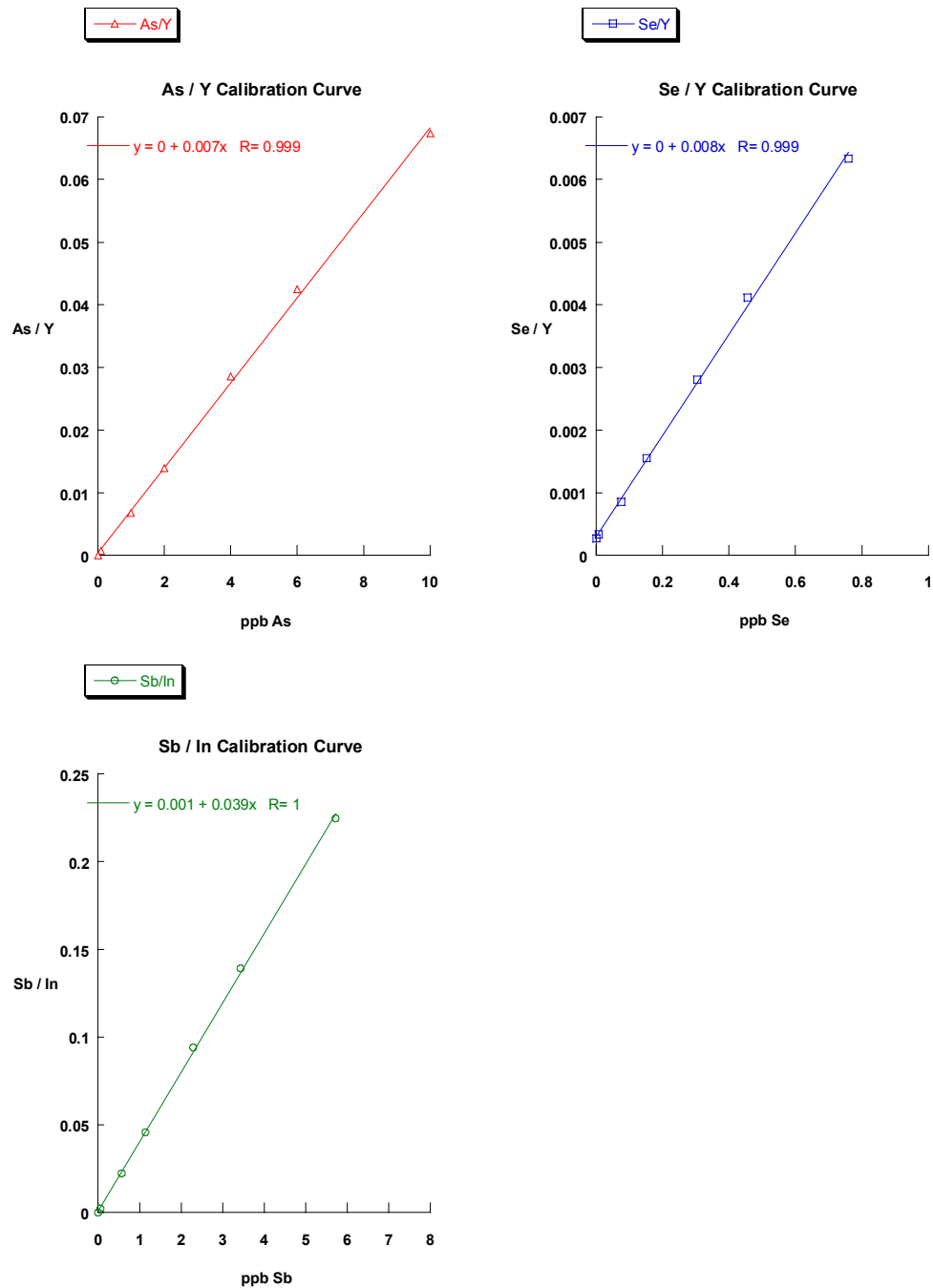


Figure 2-1 Metalloid Calibration Curves. Figure 2-1 shows a set of calibration curves for the multi-element standard. The x-axis is concentration in ppb. The y-axis is the count ratio of analyte to internal standard.

Table 2-3 ICP-MS Settings

Table 2-3. ICP-MS Settings. This is a table containing the settings of the ICP-MS instrument for a typical analysis run. These settings are particular to the HP-4500 and must be adjusted (re-tuned) each time the instrument is placed into standby mode.

Parameter	Setting	Parameter	Setting	Parameter	Setting
RF Power	1200 W	Extract 1	-250 V	AMU Gain	129
RF Matching	1.92 V	Extract 2	-100 V	AMU Offset	175
Sample Depth	5.5 mm	Einzel 1,3	-100 V	Axis Gain	1.001
Torch-H	-0.9 mm	Einzel 2	9.6 V	Axis Offset	-0.19
Torch-V	1.5 mm	Omega Bias	-50 V	Plate Bias	-4 V
Carrier Gas	1.15 L/min	Omega (+)	6 V	Pole Bias	0 V
Blend Gas	0 L/min	Omega (-)	-10 V	Discriminator	12 mV
Peristaltic Pump	0.3 rps	Quadrupole Focus	7 V	EM Voltage	-1910 V
Spray Chamber Temp	2 C	Ion Deflection	50 V	Last Dynode	-337 V
Sample Rate	1 mL / min	Peak Jumping (m/z)	75, 77, 89, 115, 121,123	Dwell Time	0.5s
Acquisition Time	17 s	Detector Mode	Pulse Counting	Plasma Gas	16 L / min

Table 2-4 Reproducibility Results

This table is located on the following page. It shows the reproducibility results for the storage and analysis methods used in the study. It is based on the original concentration calculated immediately after sample collection and a second quantification after some months of storage. “m” is the slope of the calibration curve for the day of analysis. ** indicates that no internal standard was used for these analyses. Original Concentration is the pre-storage calculation of concentration. The reanalysis concentrations are the calculated concentrations, in duplicate, of the samples after storage. The final reproducibility is the average of the standard deviations of the pre and post storage sample analyses.

Table 2-4 Reproducibility Results

R- Number	Date Collected	Element	Blank (ppb)	m (CPS/ppb)	Original Analysis Concentration (ppb)	Re-analysis Concentration 1 (ppb)	Re-analysis Concentration 2 (ppb)	Standard Deviation (n=3) (%)
R-1025	5/21/2001	As	0.003	11212 **	1.37	1.32	1.42	3.6
		Se	0.047	8937 **	1.40	1.33	1.45	4.2
		Sb	0.002	35627 **	0.61	0.65	0.60	4.2
R-1043	8/6/2001	As	0.002	0.016	1.89	1.95	1.84	2.9
		Se	0.010	0.011	1.25	1.34	1.36	4.5
		Sb	0.001	0.046	0.68	0.64	0.63	4.0
R-1048	9/15/2001	As	0.003	0.011	5.60	5.47	5.82	3.1
		Se	0.035	0.007	3.01	3.17	2.89	4.6
		Sb	0.002	0.043	1.41	1.35	1.46	3.9
R-1054	11/9/2001	As	0.002	0.011	3.72	3.55	3.79	3.3
		Se	0.027	0.008	2.02	2.12	2.19	4.1
		Sb	0.005	0.042	1.11	1.02	1.06	4.1
R-1060	12/18/2001	As	0.004	0.010	1.73	1.76	1.84	3.2
		Se	0.031	0.007	0.98	0.95	1.03	4.3
		Sb	0.002	0.040	0.52	0.53	0.57	4.5
R-1067	3/6/2002	As	0.001	0.009	0.40	0.43	0.42	3.4
		Se	0.042	0.007	0.64	0.62	0.67	4.0
		Sb	0.002	0.035	0.24	0.23	0.25	4.1
R-1079	5/6/2002	As	0.003	0.009	0.94	0.88	0.92	3.1
		Se	0.025	0.007	0.56	0.54	0.59	4.5
		Sb	0.002	0.033	0.33	0.34	0.36	4.2
R-1085	6/5/2002	As	0.002	0.008	5.67	5.40	5.35	3.2
		Se	0.034	0.006	1.99	2.08	1.90	4.6
		Sb	0.003	0.034	1.07	1.03	0.99	4.0
Reproducibility (Average Std. Deviation from re-analysis)							As	3.2
							Se	4.4
							Sb	4.1

2.2.4 Hot Acid Extraction

The concentration of metalloids on suspended sediments is determined by acid extracting the sediments from AcroDisk Filters used in the field. Suspended sediments collected on filters are extracted by passing a solution of hot nitric acid through the filter. A 10% HNO₃ solution is heated to 60° C and drawn into an acid cleaned syringe through an acid cleaned length of tygon tubing. The acid is passed through the filter at a rate of 1 mL/min and collected in an acid cleaned scintillation vial, diluted to 1% acid (10 x) with DDW, then analyzed by DA/DN-ICP-MS. The calculation for metalloid concentration in PPM(W) is as follows:

Eq. 2-2 Metalloid Concentration in Suspended Solids

$$C_{sus} = \frac{C_{ex}}{M_{sed} \times F}$$

C_{sus} is the concentration of metalloids on suspended solids in PPM(W). C_{ex} is the concentration of the filter extract. M_{sed} is the mass of suspended sediment in a volume of water, determined directly from a separate 1 L aliquot. F is amount of water passed through the filter in the field.

2.2.5 Nutrient Methods

Si is measured by spectrophotometry using the molybdate blue method. Dissolved reactive PO₄ is determined by using spectrophotometry by the method of Murphy and Riley (1962). This method has a detection range of 0.03 – 5.00 µM with a precision of $\pm 0.31/n^{1/2}$ where n is the number of analysis. Nitrite is analyzed by spectrophotometry after Murphy and Riley (1963). This method has a precision of $\pm 0.5/n^{1/2}$ where n is the number of analyses. Nitrite + nitrate was analyzed in the lab of Dr. Joe Montoya.

2.3 Sample Sites

2.3.1 The Etowah-Coosa-Oostanaula River System

This section provides specific details about the geographical area on the Etowah-Coosa-Oostanuala sampling transect.

2.3.1.1 Geology, Cities, and Coal Fired Power Plants

The Etowah-Coosa-Oostanaula (ECO) river system (Fig. 2-3) is located in northwestern Georgia. This study covers the Etowah River from its outlet (Allatoona Reservoir) at Allatoona Dam to Rome, GA. In Rome, the Etowah joins the Oostanaula River to become the Coosa River. From Rome, the Coosa flows southwest into Alabama. There are two major cities on the ECO transect, Cartersville and Rome, Georgia. Cartersville is located approximately 10 km (by river) west of Allatoona Dam. Rome is located approximately 85 km (by river) west of Allatoona Dam.

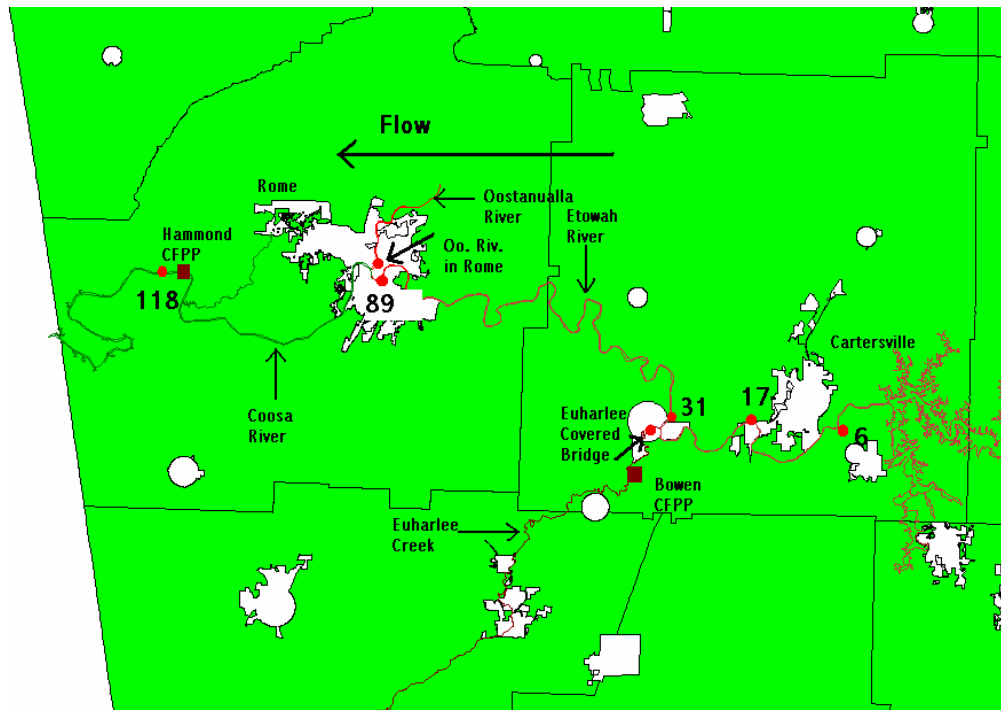


Figure 2-3 Etowah-Coosa-Oostanaula Sampling Area. Figure 2-3 shows the Etowah-Coosa-Oostanaula sampling area. Sample sites are indicated by orange circles. CFPP's are indicates by brown squares. The numbers next to the sample site markers are the km downstream (by river) of the site from the outlet at Allatoona Dam. The white areas are cities and towns.

In this area , the formation of particular interest is the Shady Dolomite, which outcrops in and around the Cartersville area. This formation contains veins and replacements of barite throughout its entire thickness. The barite is concentrated through weathering processes to the extent that the formation can contain 6-12% barite (Chowns 1983). The barite is strip mined and refined for use in making barium salt products. Of relevance to this study is the fact that barite is commonly associated with Sb minerals. The data gathered in this research suggest an input of metalloids to the Etowah River in the vicinity of these barite mines. We hypothesize that this input may be related to runoff from the mines and/or the barite bearing strata. Faulting processes heavily influence the stratigraphy and topography north of Rome.

There are two CFPPs on this transect of the ECO system, Plant Bowen and Plant Hammond. These two plants are radically different in both size and environmental impact. Plant Hammond (Figure 2-4) is a 800 MW plant while Plant Bowen (Figure 2-5) is a 3160 MW plant. Plant Hammond still uses wet ash disposal while evidence suggests that Plant Bowen has switched, at least partially, to a dry ash disposal system. While some ash is disposed of on site, about half is also being sold for other uses. A truck hauling ash from the ash field was followed to a housing development where the ash appeared to be used as ground fill beneath new houses. It is important to note that Plant Bowen is not situated directly on the Etowah River. A tributary stream (Euharlee Creek) receives any discharge from the fly ash settling pond and transports the resulting contaminants to the Etowah River.

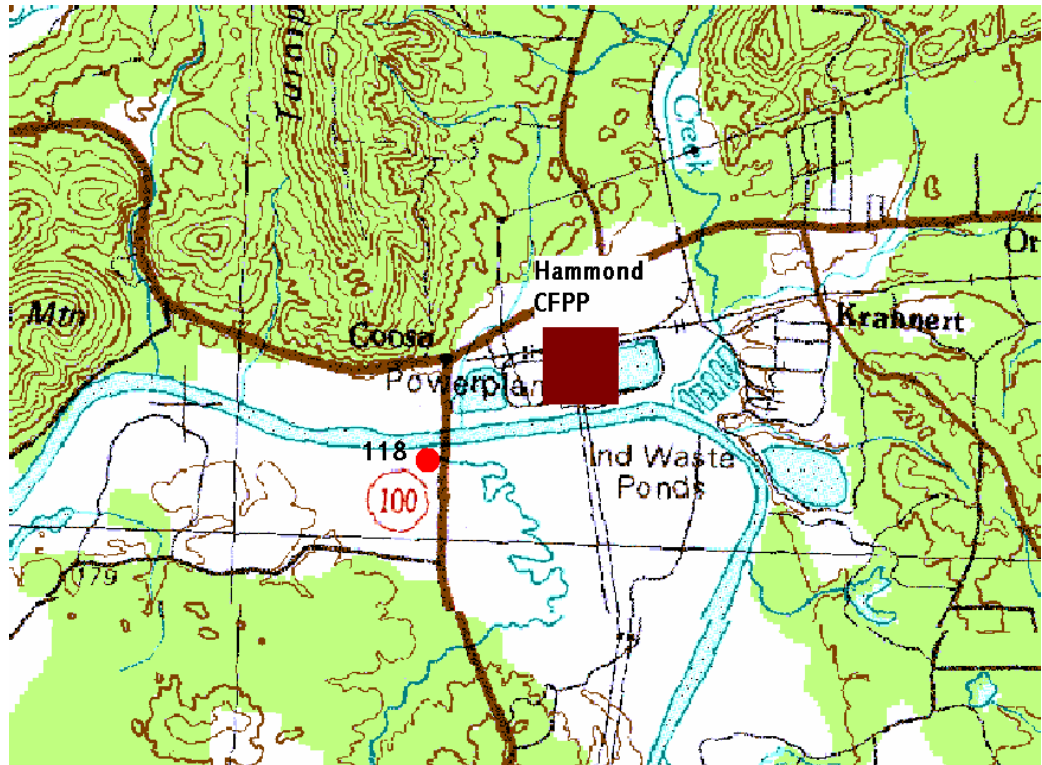


Figure 2-4 Plant Hammond Topography. Figure 2-4 shows the topography in the immediate vicinity of Plant Hammond. Sample sites are indicated by orange circles. CFPP's are indicated by brown squares. The numbers next to the sample site markers are the km downstream (by river) of the site from the outlet at Allatoona Dam. In this map the location of the site marker indicates the exact location of the sample site.

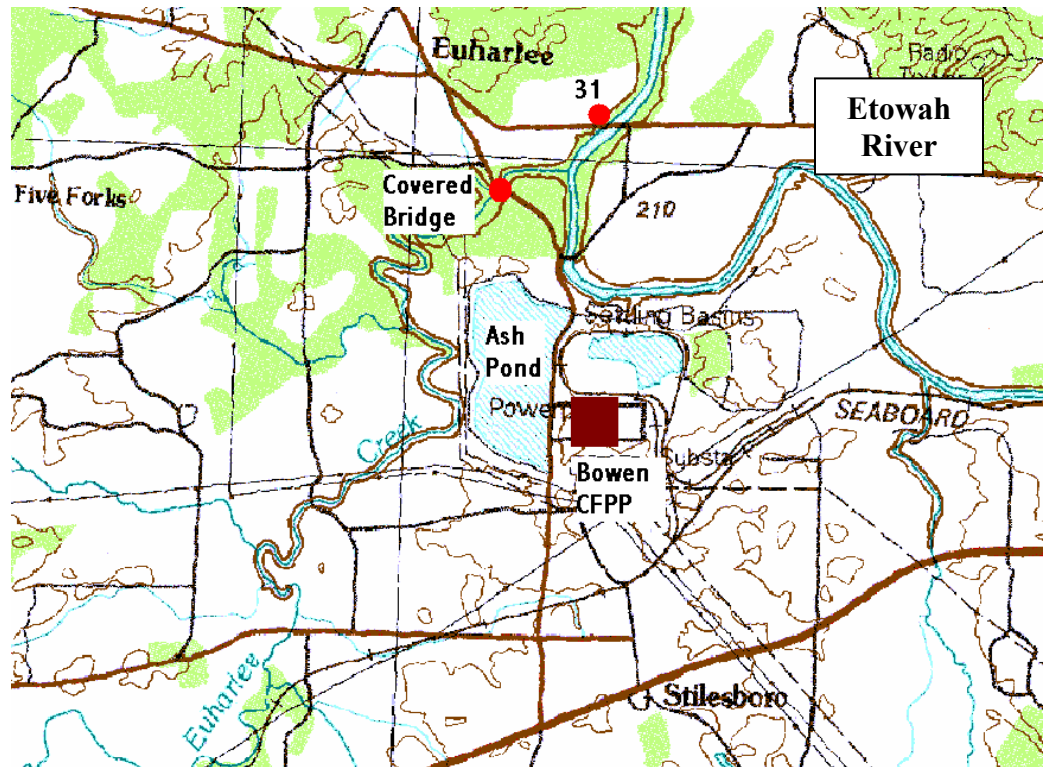


Figure 2-5 Plant Bowen Topography. Figure 2-5 shows the topography in the immediate vicinity of Plant Bowen. Sample sites are indicated by orange circles. CFPP's are indicated by brown squares. The numbers next to the sample site markers are the km downstream (by river) of the site from the outlet at Allatoona Dam. In this map the location of the site marker indicates the exact location of the sample site.

2.3.1.2 Sample Site Specifics The sample sites on this transect are taken above and below both power plants in order to assess the impact of the power plant on the rivers. There are seven sample sites on this transect, though only five of them fall on the Etowah or Coosa Rivers. Sample locations are named by their km marker downstream from the source reservoir (Fig 2-3). Sample site 118 is located on the Coosa River downstream from Rome and Plant Hammond. A sample of the Oostanaula is collected in Rome upstream of the junction where the Etowah and the Oostanaula Rivers join to become the Coosa River. Sample site 89 is located on the Etowah River in Rome. Sample site 31 is located on the Etowah River downstream of Euharlee Creek. Any metalloid signal from Plant Bowen should be evident in waters taken at this location. There is a sample from Euharlee Creek. This allows confirmation that any increase in metalloid flux in the Etowah is due to input from Plant Bowen. Sample Site 17 is on the Etowah River, above Euharlee Creek, west of Cartersville. It is this sample site that appears to be impacted by the barite strip mining southeast of Cartersville. Sample site 6 is located the Etowah River downstream of Allatoona Dam. This is considered the “clean” end member of the Etowah, as the river has not yet been impacted directly by effluent from fly ash ponds or barite mines. Specific driving directions to these locations as well as their latitude and longitude coordinates can be found in Appendix III.

2.3.2 The Chattahoochee River System

This section provides specific details about the geographical area on the Chattahoochee River sampling transect.

2.3.2.1 Geology, Cities, and Coal Fired Power Plants The section of the Chattahoochee River considered in this study begins at the outlet of Lanier Reservoir at Buford Dam and ends at the outlet of West Point Reservoir in West Point, Georgia (Fig. 2-6). There are several cities situated on the Chattahoochee in this transect, the largest of these being Atlanta, Georgia. The Chattahoochee flows through Atlanta for approximately 20 km (by river). In Atlanta the Chattahoochee is used for drinking water and also receives industrial, domestic, and sewage effluent. There is a small power plant, Plant McDonough (now Plant Atkinson), situated on the Chattahoochee in Atlanta. However, this plant has been converted to burn natural gas and is not considered in this study.

There are two major coal fired power plants on the river in this transect. They are Plant Wansley (1730 MW) (Fig 2-7) and Plant Yates (1250 MW) (Fig 2-8). Plant Yates is located 100 km downstream from Buford Dam. Plant Wansley is located 108 km downstream from Buford Dam. Both of these plants use wet ash disposal systems.

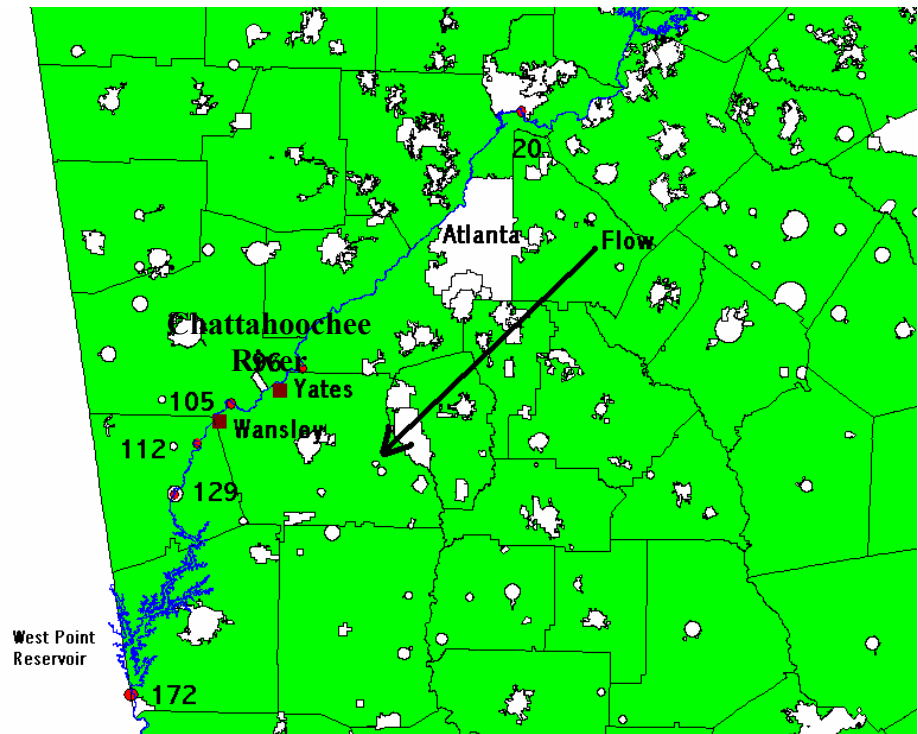


Figure 2-6 Chattahoochee Sampling Area. Figure 2-6 shows the Chattahoochee sampling area. Sample sites are indicated by orange circles. CFPP's are indicated by brown squares. The numbers next to the sample site markers are the km downstream (by river) of the site from the outlet at Buford Dam. The white areas are cities and towns.

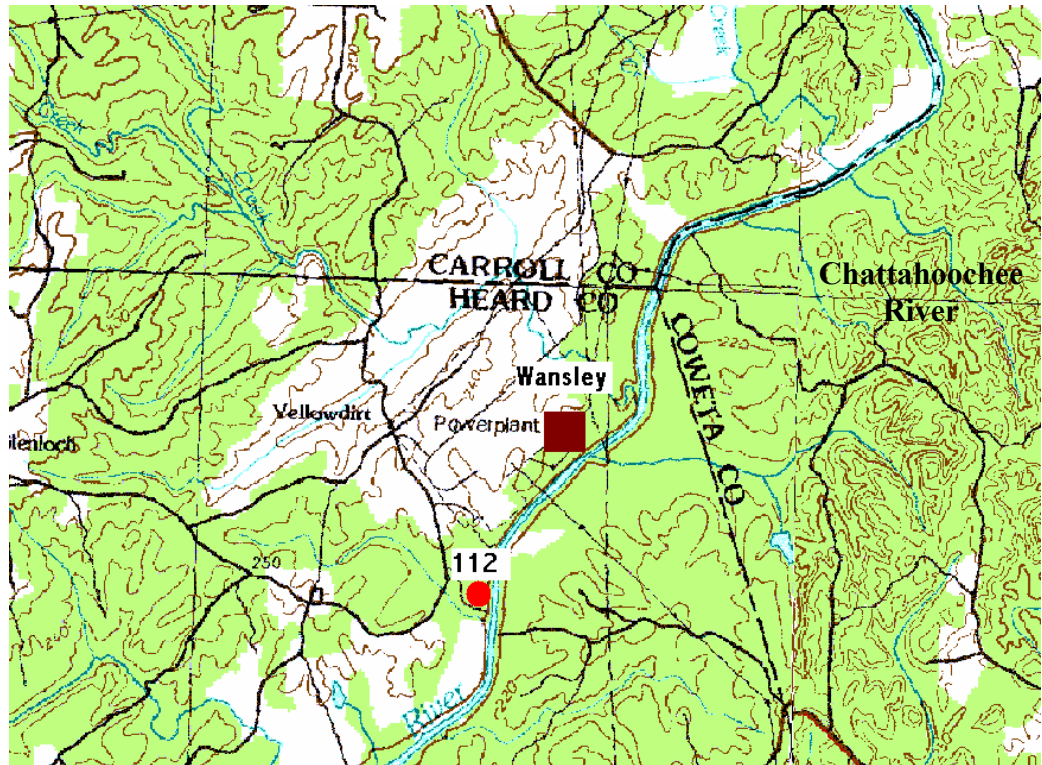


Figure 2-7. Plant Wansley Topography. Figure 2-7 shows the topography in the immediate vicinity of Plant Wansley. Sample sites are indicated by orange circles. CFPP's are indicated by brown squares. The numbers next to the sample site markers are the km downstream (by river) of the site from the outlet at Buford Dam. In this map the location of the site marker indicates the exact location of the sample site.

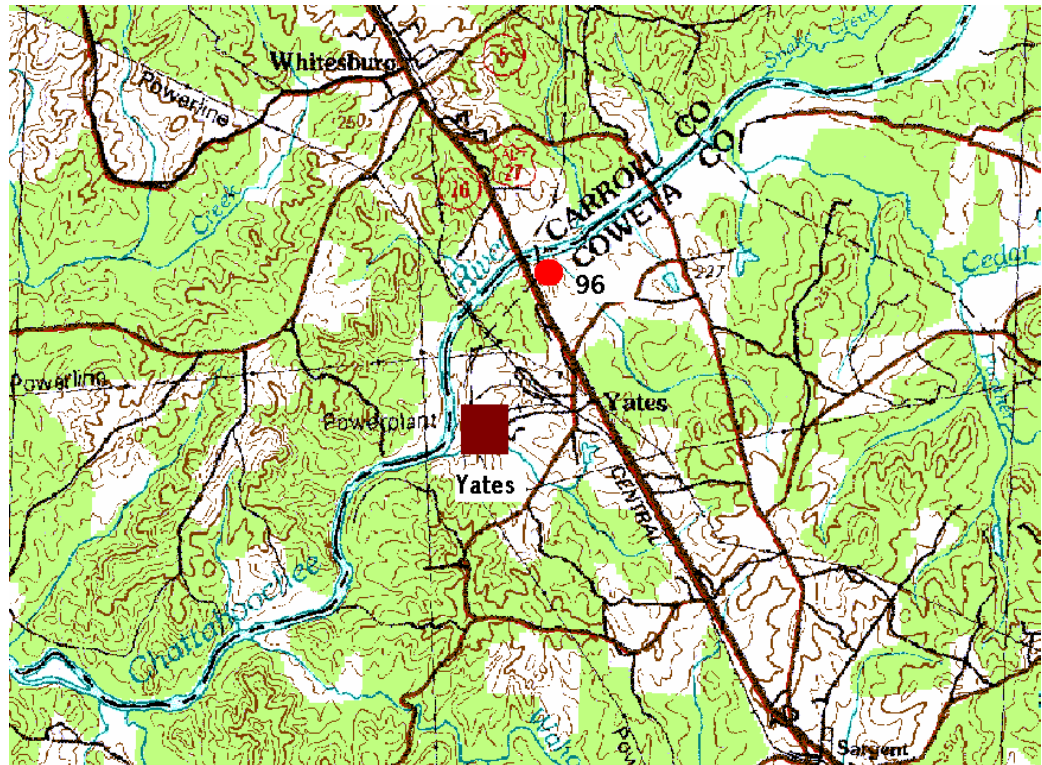


Figure 2-8 Plant Yates Topography. Figure 2-8 shows the topography in the immediate vicinity of Plant Yates. Sample sites are indicated by orange circles. CFPP's are indicated by brown squares. The numbers next to the sample site markers are the km downstream (by river) of the site from the outlet at Buford Dam. In this map the location of the site marker indicates the exact location of the sample site.

2.3.2.2 Sample Site Specifics Samples are taken above and below both power plants in order to assess the impact of these plants on the river receiving their ash pond effluent. There are six samples taken on this transect. They span the length of the river from Lanier Reservoir to West Point Reservoir, but focus on the last 72 km of the river Fig (2-6). A sample (sample site 172) is taken below West Point Reservoir to assess any changes in metalloid concentration from laucustrine processes. A sample is taken above West Point Reservoir (sample site 125) in order to gather information about the composition of the water flowing into West Point Lake. This site is also important because it gives a picture of metalloid behavior downstream of the power plants, but before the water is subject to any biological and chemical processes that may occur once water reaches the reservoir. A sample is taken approximately 4 km (by river) downstream of Plant Wansley (sample site 112). This sample has metalloid contamination from both power plants. A sample is taken upstream of Plant Wansley but downstream of Plant Yates (sample site 105). This allows separation, to some degree, the effect of the plants. Another sample is taken from upstream of both power plants (sample site 96). This gives a picture of the water composition immediately before the river is affected by power plant effluent. The sixth sample is taken far upstream approximately 20 km (by river) from the outlet of Buford Dam (sample site 20). This is considered the “clean” end member of the Chattahoochee. At this sample site the river has not been impacted directly by power plant pollution. Of note is the fact that this sample is taken at the main potable water intake facility for north Dekalb County, Georgia. Detailed driving directions to these sites can be found in Appendix III.

CHAPTER III

RESULTS

This chapter contains the analytical results of this project, presented as plots of downstream river transects. Appendices I and II contain the analytical data presented in these graphs. The dissolved and suspended metalloid and nutrient concentration data are presented in Appendix I. Flux calculation data are presented in Appendix II.

Figures 3-1 and 3-2 show average annual dissolved metalloid concentration profiles and the locations of important landmarks and features on the Chattahoochee (Fig 3-1) and Etowah Rivers (Fig 3-2). In both figures the x-axis is kilometers downstream of the river source reservoir. The y-axis is the dissolved metalloid concentration.

3.1 River Metalloid Profiles

This section discusses general trends in the metalloid profiles of the Etowah and Chattahoochee Rivers during the year of this study. While the degree of metalloid enrichment and loss varies from month to month, the general trends remain the same.

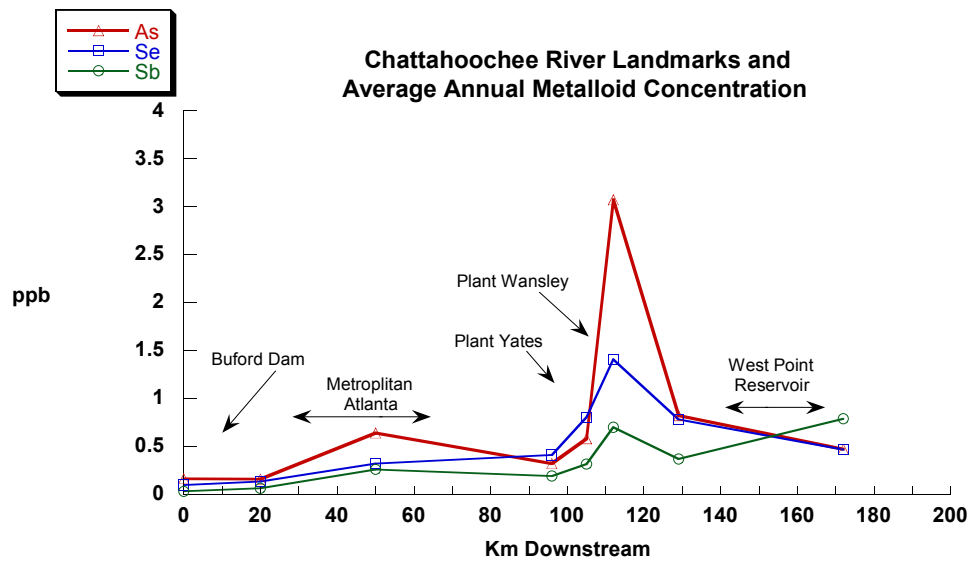


Figure 3-1. Chattahoochee River landmarks and typical (annual average) metalloid concentrations

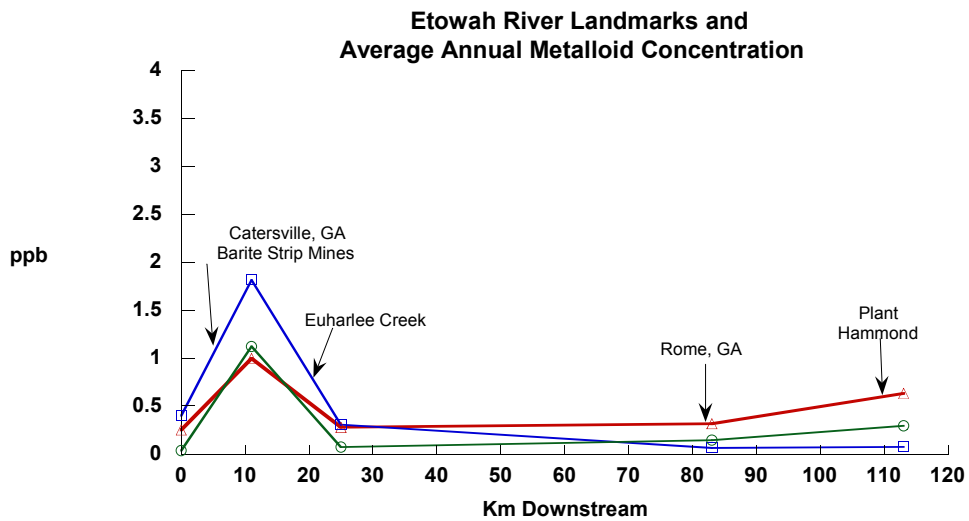


Figure 3-2. Etowah River landmarks and typical (annual average) metalloid concentrations.

3.1.1 Metalloid Concentration Profiles

The analytical data discussed in this section is located in Appendix I. The average annual metalloid concentrations in the Etowah River at its spill way from Allatoona Dam are 0.25 ppb As, 0.40 ppb Se, and 0.04 ppb Sb. An increase in total dissolved metalloid concentrations to 1.00 ppb As, 1.82 ppb Se, and 1.12 ppb Sb is found in the Etowah River (Fig. 3-7, 3-8) above Euharlee Creek (sample site 10). Downstream of Plant Hammond (km 112), As, Se, and Sb concentrations increase to 0.63 ppb, 0.8 ppb, and 0.30 ppb respectively. This is a marked increase compared to the concentrations of 0.32 ppb As, 0.63 ppb Se, and 0.15 ppb Sb found 30 km (by river) east in Rome, GA. We attribute the input of metalloids at km 10 to barite open pit quarries south of Cartersville, GA. Barite deposits are commonly associated with Sb bearing minerals. Fly ash leachate from Plant Hammond is believed to be the source of metalloid input at km 112.

Metalloid concentrations in the Chattahoochee River (Figs. 3-9 - 3-16) increase below Plants Yates and Wansley. The upstream concentrations of As, Se, and Sb are 0.16 (± 0.07) ppb, 0.13 (± 0.05) ppb, and 0.06 (± 0.06) ppb respectively at Holcomb Bridge above Atlanta (sample site 20). Downstream of Atlanta but upstream of the power plants (sample site 96), the As, Se, Sb concentrations are 0.32 (± 0.09) ppb, 0.41 (± 0.26) ppb, and 0.20 (± 0.06) ppb respectively, a two fold increase in As and a three fold increase in both Se and Sb relative to those at Holcomb Bridge. However, downstream of Plants Yates and Wansley (sample site 112) the average concentrations of As, Se, and Sb increase to 3.07 (± 2.6) ppb, 1.41 (± 0.82) ppb, and 0.70 (± 0.41) ppb respectively. This represents a 19 fold increase in As concentration, 11 fold increase in Se concentration,

and 12 fold increase in Sb concentration compared to above Atlanta. Compared to concentrations immediately above the plants (sample site 96), there are ten fold, three fold, and four fold increases in As, Se, and Sb respectively.

Evidence that this increase in concentration is due to fly ash leachate can be found in the ratios of the metalloid concentrations in the rivers downstream of the power plants. The concentration of As, Se, and Sb in coal is in the preceding order, with As being the most abundant. The Se/As and Sb/As ratios in average coals are 0.1. The input fluxes from the power plants (3.1.3) reflect the ratios of metalloid concentration found in coal. It stands to reason that the rivers impacted by CFPP discharge will also reflect these concentration ratios, as found on the Chattahoochee River (Se/As=0.27, Sb/As=0.13). These ratios are within the bounds of the common metalloid concentrations in coal (Table 1-4) This theory can be applied to the question of the source of the increased concentrations at sample site 10 on the Etowah River. In both transects the element of metalloid of highest concentration is Se, which is not consistent with ash pond effluent (3.2).

3.1.2 Metalloid Flux Profiles

The data discussed in this section is located in Appendix II. Dissolved metalloid fluxes (Figure 3-3) are calculated using USGS river flow data (l/s) and analytical concentration data (mg/l). Multiplying the flow at a site by the metalloid concentration at

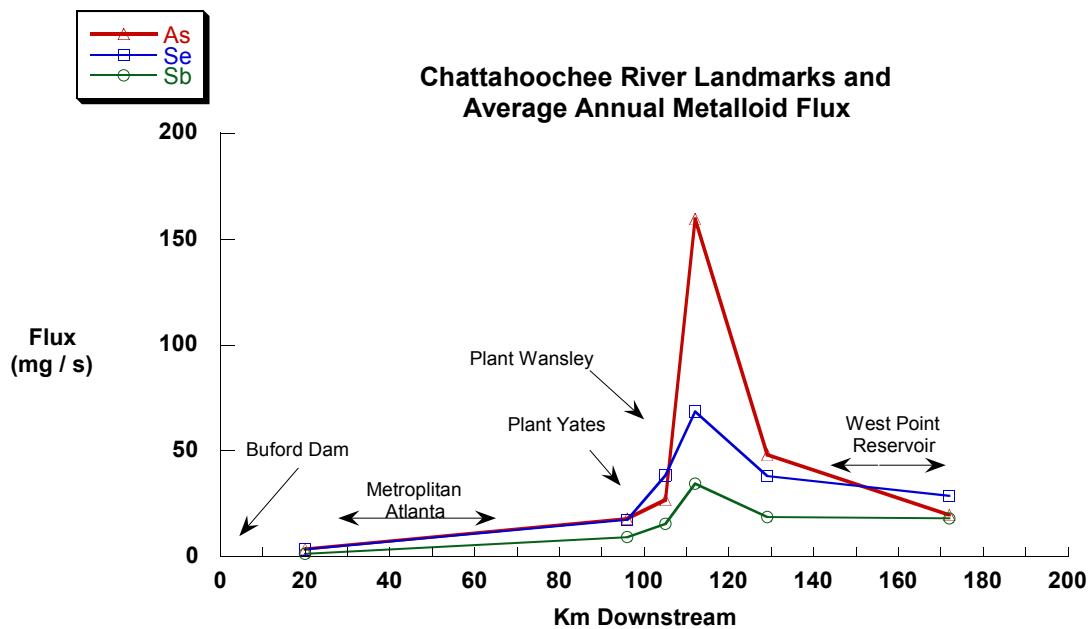


Figure 3-3. Chattahoochee River annual average metalloid flux

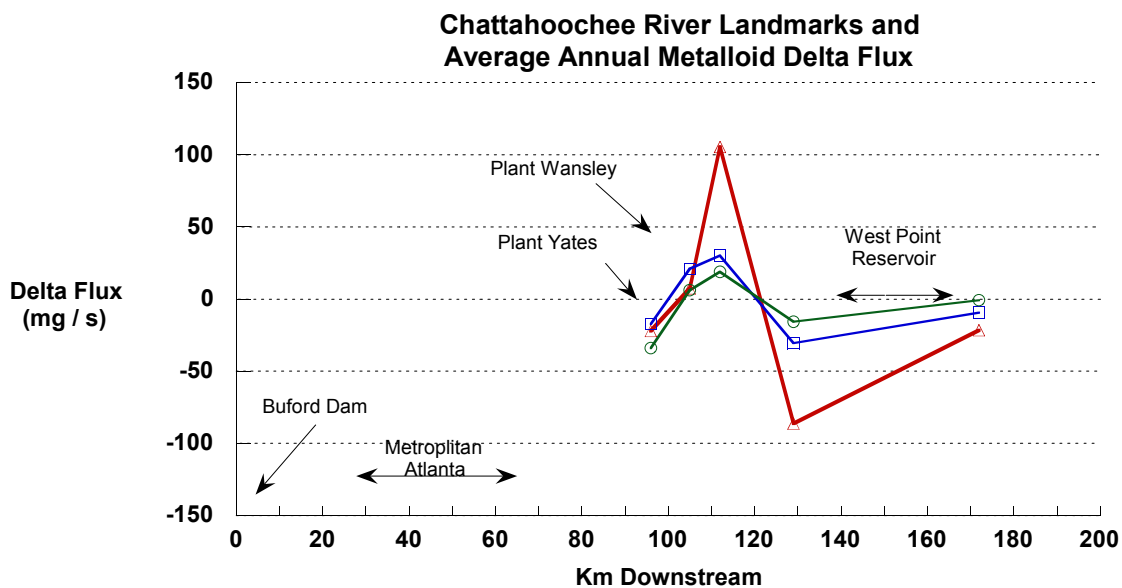


Figure 3-4. Chattahoochee River annual average metalloid Δ Flux

the site at the time of sampling yields metalloid flux, in units of mass per unit time (mg/s). Unlike concentration, which is a volume-dependant quantity, fluxes permit evaluations of the mass transport of metalloids through the river at the time and location of sampling.

On the Etowah River (Fig. 3-7, 3-8) there are two stretches of the river that show increasing metalloid fluxes. They occur at km 10 and km 112. The increase in flux at km 10 is attributed to the Cartersville barite mines. The increased fluxes at km 112 are the result of fly ash leachate from the Plant Hammond ash ponds.

On the Chattahoochee River (Figs. 3-9 - 3-16) there is an increase in metalloid flux beginning after sample site 95. This is presumably due to discharge from ash ponds. The same reasoning regarding the source of the increased metalloid concentrations on the Chattahoochee and Etowah Rivers can be applied to the flux calculations. However, there is also a sharp drop in flux from km 112 to km 125. This indicates that dissolved metalloids in the river are being removed from the system. The mechanism behind this loss and the fate of the metalloids in the river will be discussed in Chapter IV.

3.1.3 Delta Flux (Δ Flux) Profiles

The *Δ Flux data discussed in this section is located in Appendix II.* Delta flux (Δ Flux) is a measurement of the net loss or gain of dissolved metalloids over a stretch of river. Δ Fluxes are calculated by taking the difference of the downstream and upstream fluxes between any two points on a river. In profile (Figure 3-4) Δ Flux is displayed at the downstream sample site. The Δ Flux shown at km 96 is calculated using flux data from

sample site 20 and sample site 96. A positive Δ Flux indicates an input of metalloids to the river. A negative Δ Flux indicates a loss of metalloids from the river.

In the Etowah River (Fig. 3-7, 3-8) the Δ Flux profiles show an input of metalloids at km 10 and 112. These positive Δ Fluxes are a result of effluent from the barite mines and Plant Hammond respectively.

On the Chattahoochee (Figs. 3-9 - 3-16) there is an input of metalloids from km 95 to km 109. The sources of the metalloid input are the ash ponds associated with Plants Yates and Wansley. Downstream of km 109 there is loss of metalloids from the river. The mechanisms behind this loss and the fate of the metalloids in the rivers will be discussed in Chapter IV.

3.1.4 Suspended Sediment Load and Metalloid Concentration Profiles

The suspended sediment data discussed in this section is located in Appendix I.

The suspended sediment profiles (Fig. 3-6) and the suspended sediment metalloid concentration profiles (Fig. 3-5) show the concentration of metalloids on particles suspended in the river flow. Suspended sediment profile collections were begun in November 2001, thus there are no suspended sediment profiles for the Etowah River. The suspended sediment profiles in the Chattahoochee River (Figs. 3-9 - 3-16) show an increase in sediment metalloid loading downstream of the Plants Yates and Wansley. This is presumably due to two processes. The first is the input of solid ash material from the ash ponds to Chattahoochee from the ponds. The second is the sorption of dissolved

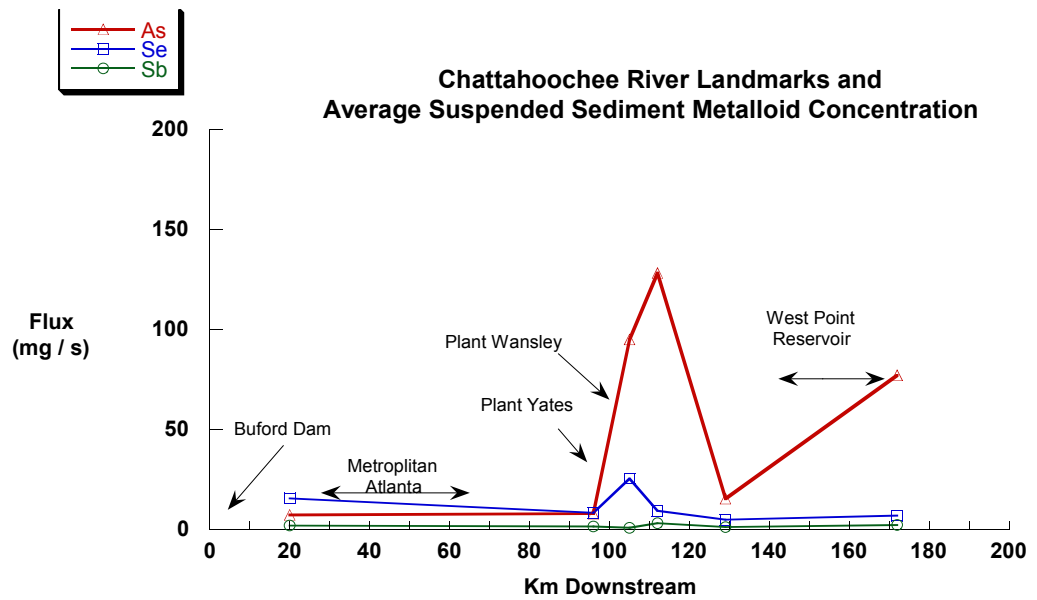


Figure 3-5. Chattahoochee River average annual suspended sediment metalloid concentration

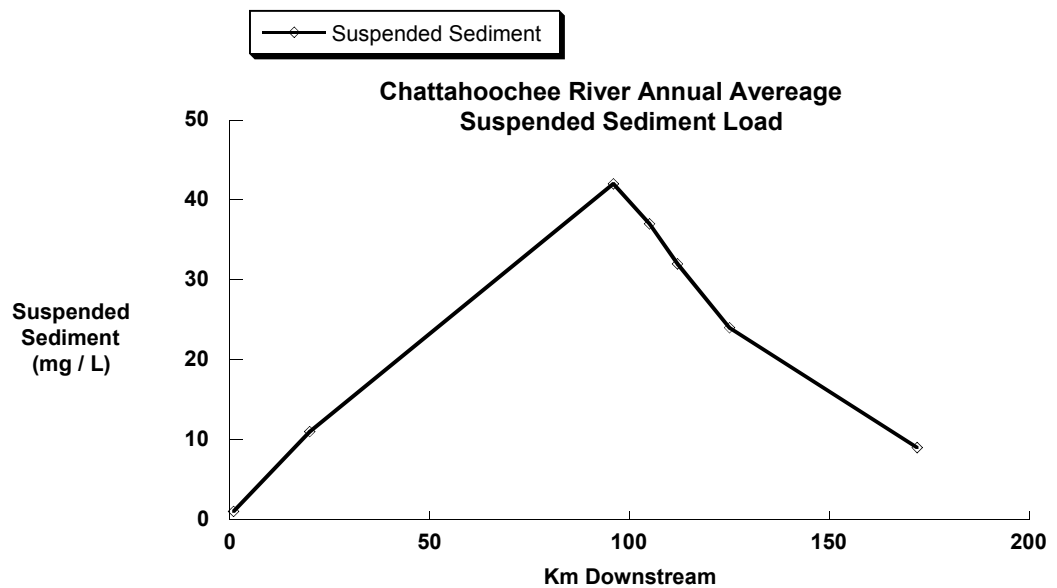


Figure 3-6. Chattahoochee River average annual suspended sediment load

As, Se, and Sb onto sediment suspended particles. Downstream of Yates and Wansley the suspended sediment metalloid concentrations decrease in a manner similar to the metalloid concentrations and fluxes. This is presumably due to the exchange processes that occur in river systems, i.e. the settling of metalloid laden sediment and the suspension of “clean” unaffected sediment from further downstream.

3.2 The Etowah River and Plant Bowen

In the late 1980's and early 1990's Froelich noted that Euharlee Creek, a tributary to the Etowah River that received ash pond effluent from Bowen CFPP was more contaminated with the metalloid Ge than any stream on the the planet. Presumably this Ge contamination was associated with the other more abundant and toxic metalloids As, Se, and Sb. It was the goal of this study to use the flux from plant Bowen as an integral part of the escape efficiency calculation. Transects of the Etowah above and below the mouth of Euharlee Creek (km 24 on figures 3-7 and 3-8) indicate there is no longer an appreciable flux of metalloids into the Etowah from Euharlee Creek and Plant Bowen. This is different from expectations based on the previous Etowah River transects. In the middle and late 1990's plant Bowen switched, at least partially, to dry ash disposal. During dry ash disposal, ash sluiced from the bag house and precipitator is allowed to dry and stored on site or sold for other industrial use. Because the ash is stored dry the sorbed metalloids do not enter the aqueous phase and cannot be transported to local rivers. The fly ash sold off site is used for many industrial purposes including the production of dry

wall and concrete. The author followed an ash truck from the Bowen site to a housing development where the ash was used as landfill beneath a new house. Georgia Power has informed the author that Bowen currently sells 50% of its ash, and wishes to eventually sell all ash produced at the plant.

Etowah River transects also reveal a surprising peak in metalloid flux at km 11 on figures 3-7 and 3-8. This peak is not located near a power plant, nor do the metalloid ratios ($\text{Se/As} = 1.85$, $\text{Sb/As} = 1.12$) agree with those in rivers clearly impacted by coal fired power plants ($\text{Se/As} = 0.27$, $\text{Sb/As} = 0.13$) (4.1.1). Research into the geology and history of the area shows that Cartersville area is actively involved in the barite (BaSO_4) mining industry. Barite is commonly associated with Sb (Klien and Halibut 1993) minerals such as stibnite and presumably other metalloid minerals. The abundance of barite nodules in the strata cut by the river in this area leads us to believe that this anomalous peak is the result of the weathering of barite bearing strata and minerals and water draining from water logged abandoned quarries.

Figures 3-7 – 3-16. Metalloid profiles vs. km downstream for each sampling transect.

Concentration of As, Se, and Sb in ppb ($\mu\text{g} / \text{L}$)

Flux of As, Se, and Sb in mg / s

Suspended sediment concentrations of As, Se, and Sb in ppm (mg / kg) and
suspended sediment load in mg / L

Delta Flux of As, Se, and Sb in mg / s

On each graph, As is represented by red open triangles; Se by blue open squares;
and Sb by green open circles. On the suspended sediment graphs suspended sediment
load is represented by black open diamonds.

On the Delta (Δ) Flux plots, Δ Flux is displayed at the downstream sampling site.
The Δ Flux at km 96 is calculated by subtracting the flux at km 20 from the flux at km
96. This Δ Flux is then displayed at km 96 in profile. This system is used for every station
on every Δ Flux profile.

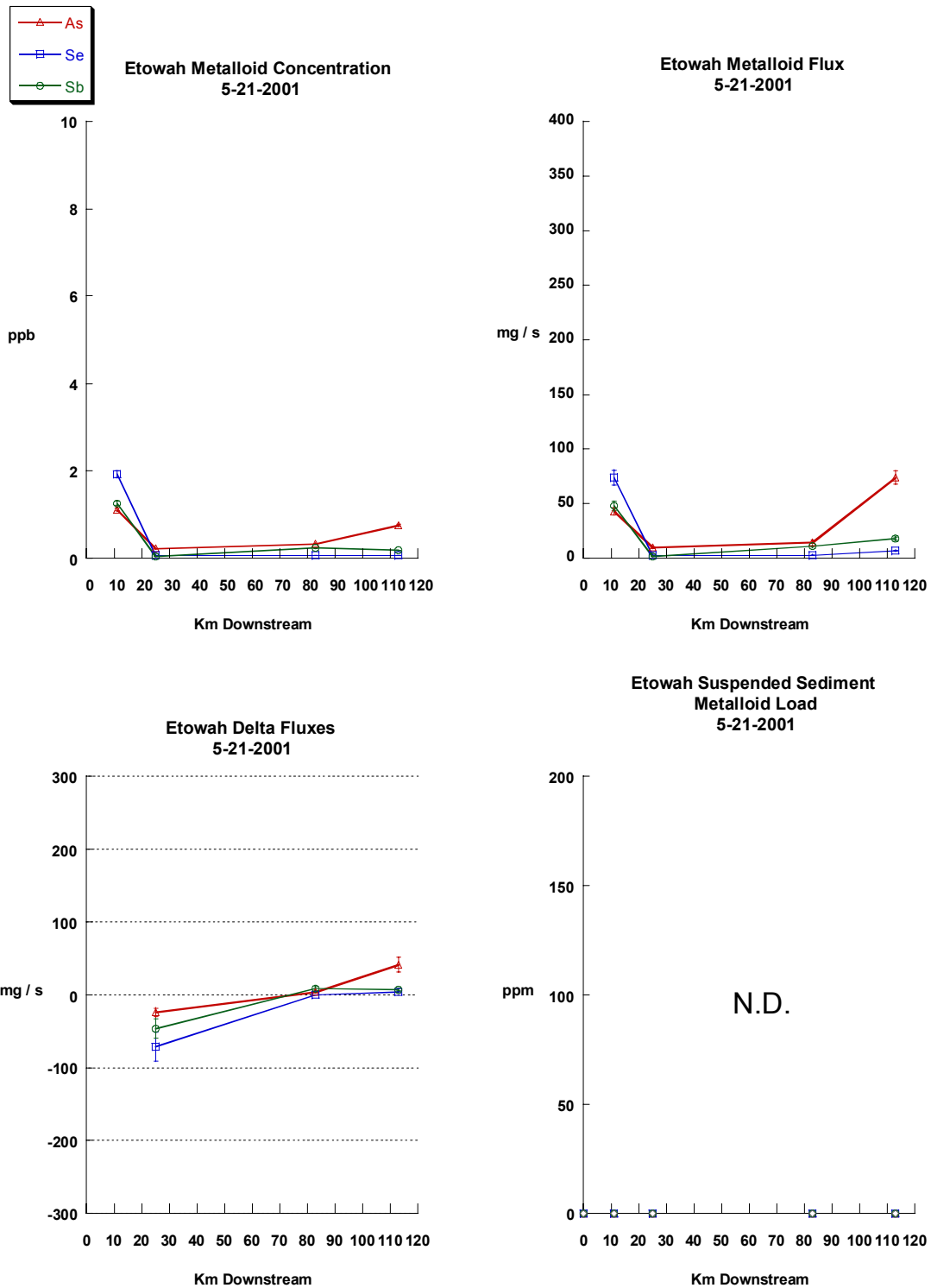


Figure 3-7. Etowah River Metalloid Data, 21 May 2001

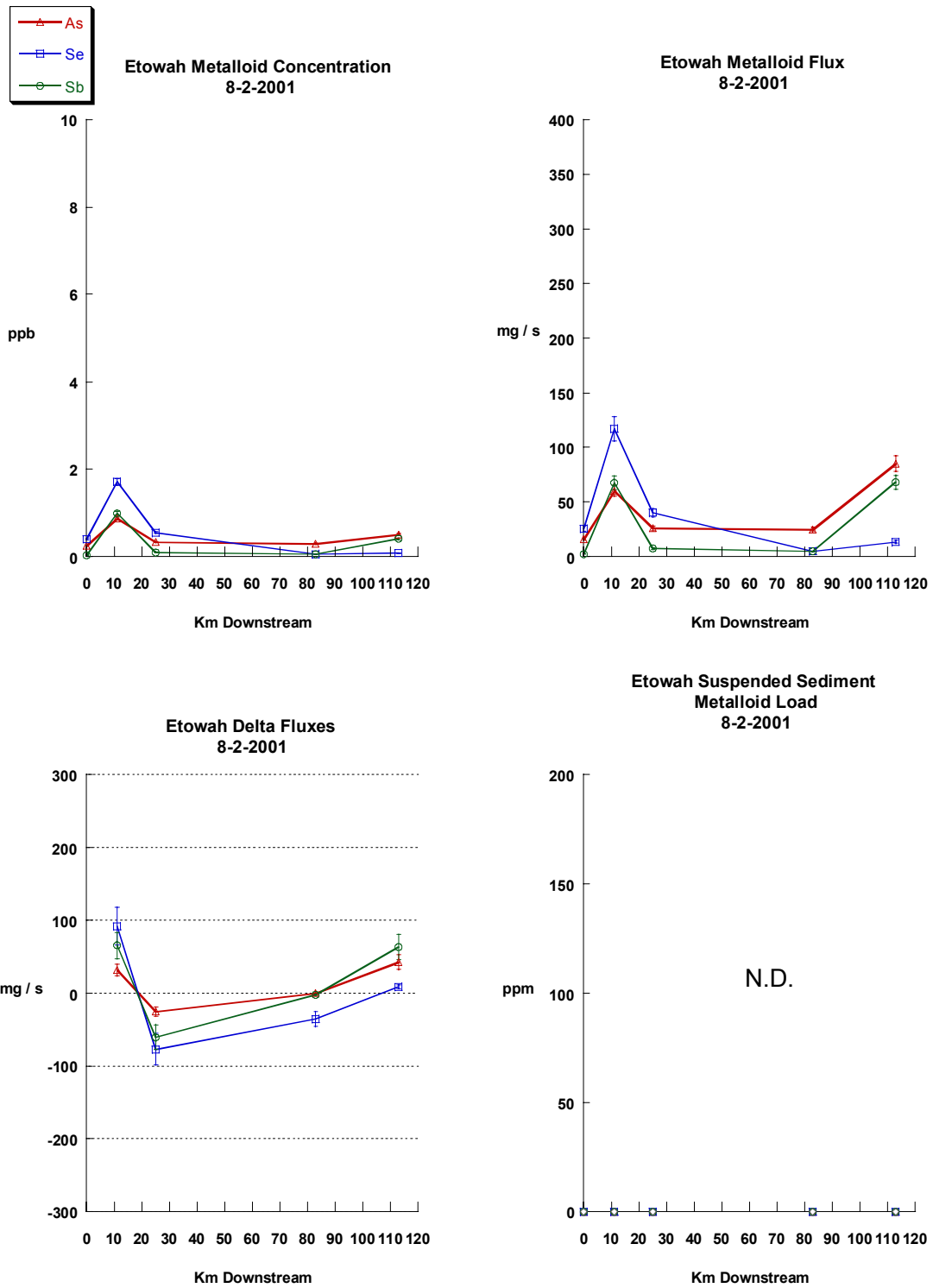


Figure 3-8. Etowah River Metalloid Data, 2 August 2001

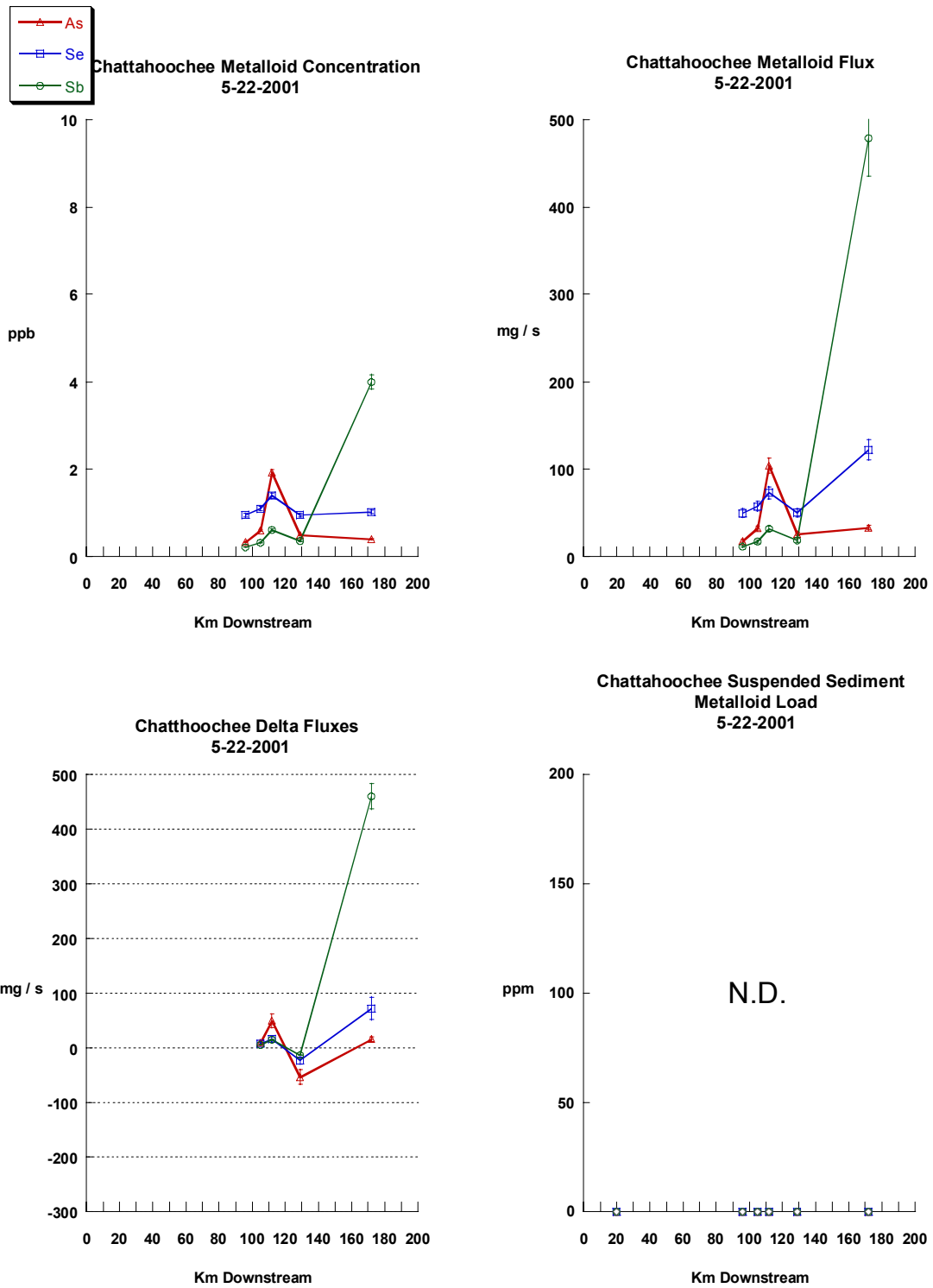


Figure 3-9. Chattahoochee River Metalloid Data, 22 May 2001

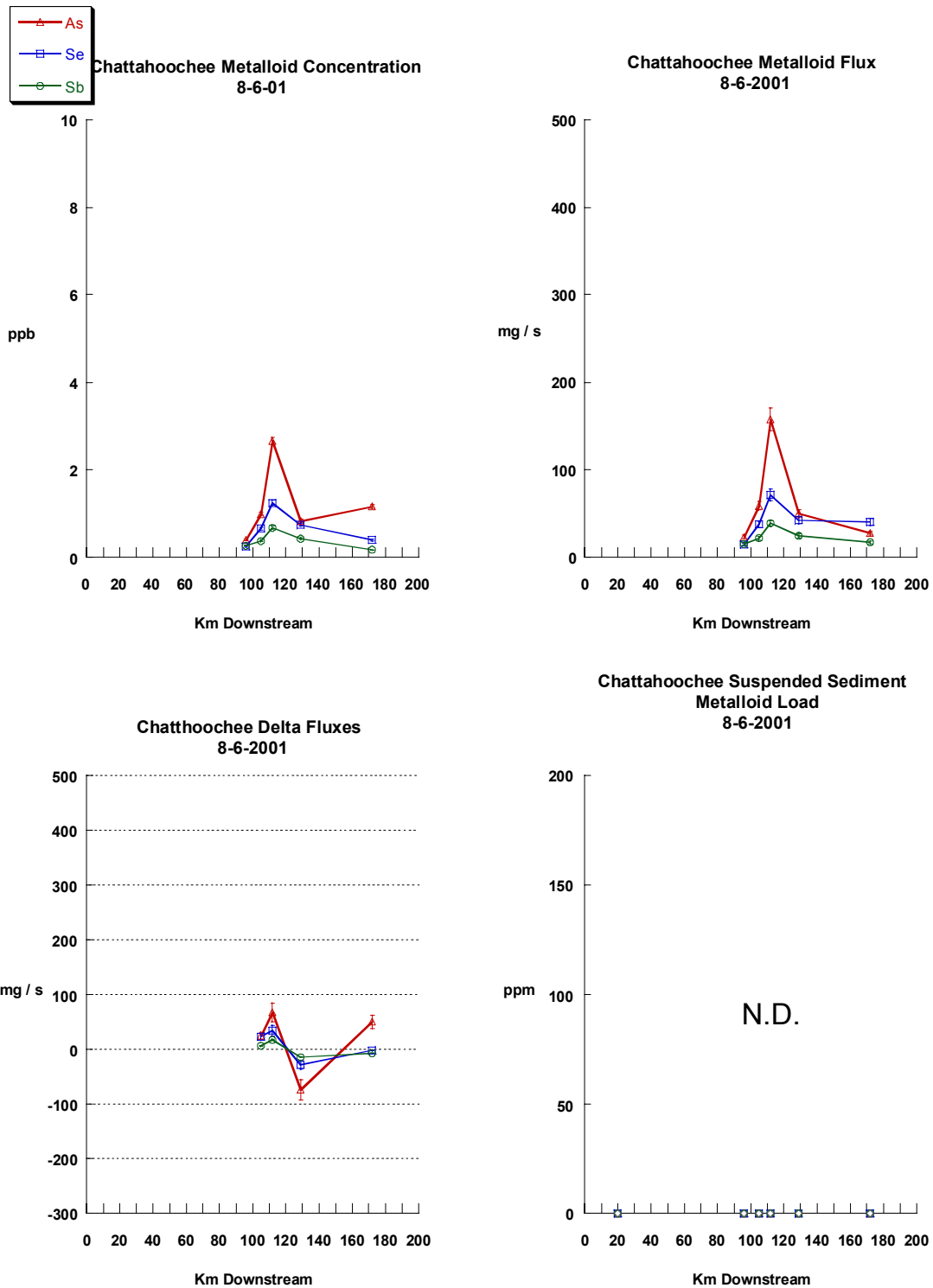


Figure 3-10. Chattahoochee River Metalloid Data, 6 August 2001

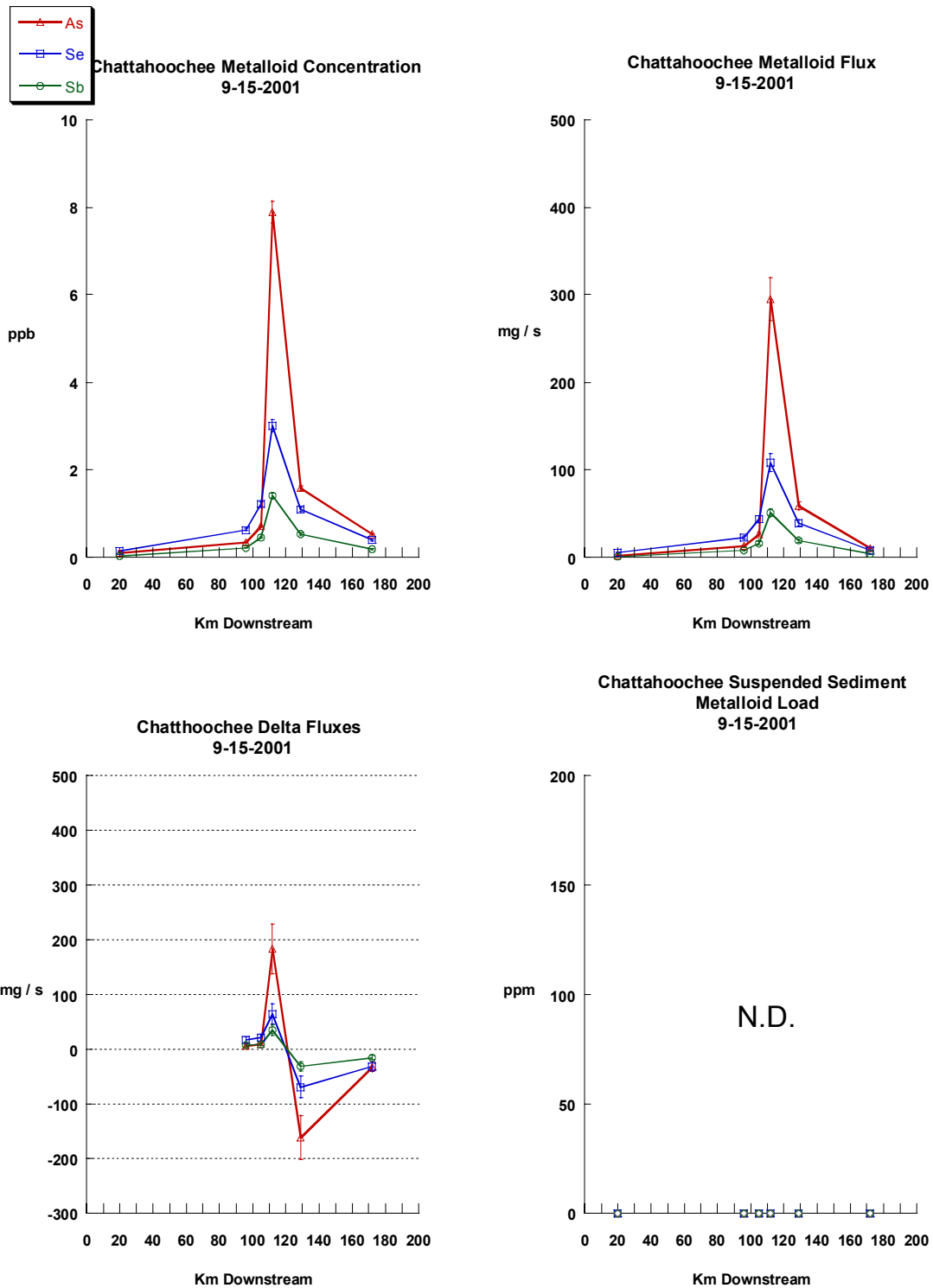


Figure 3-11. Chattahoochee River Metalloid Data, 15 September 2001

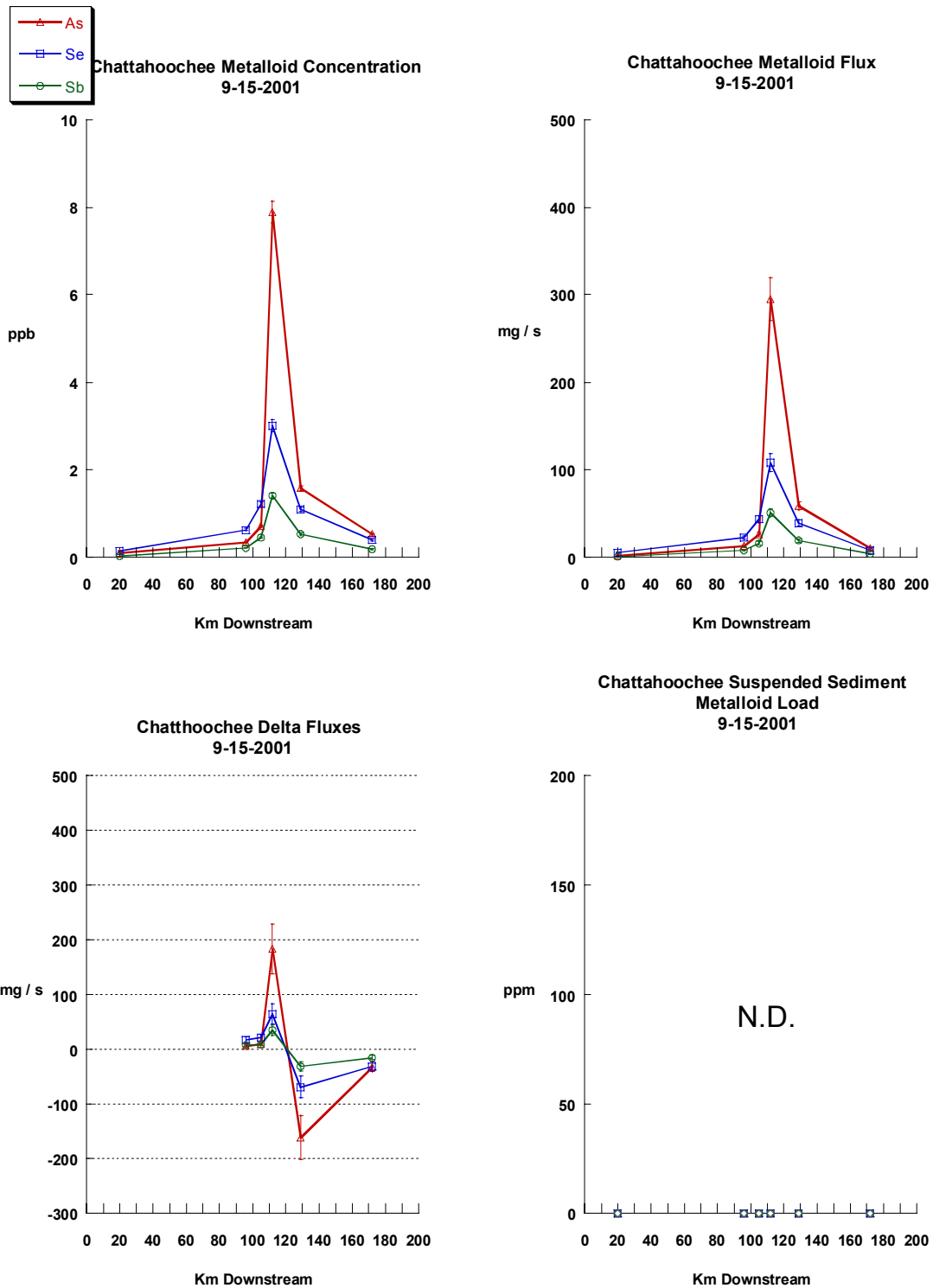


Figure 3-12. Chattahoochee River Metalloid Data, 9 November 2001

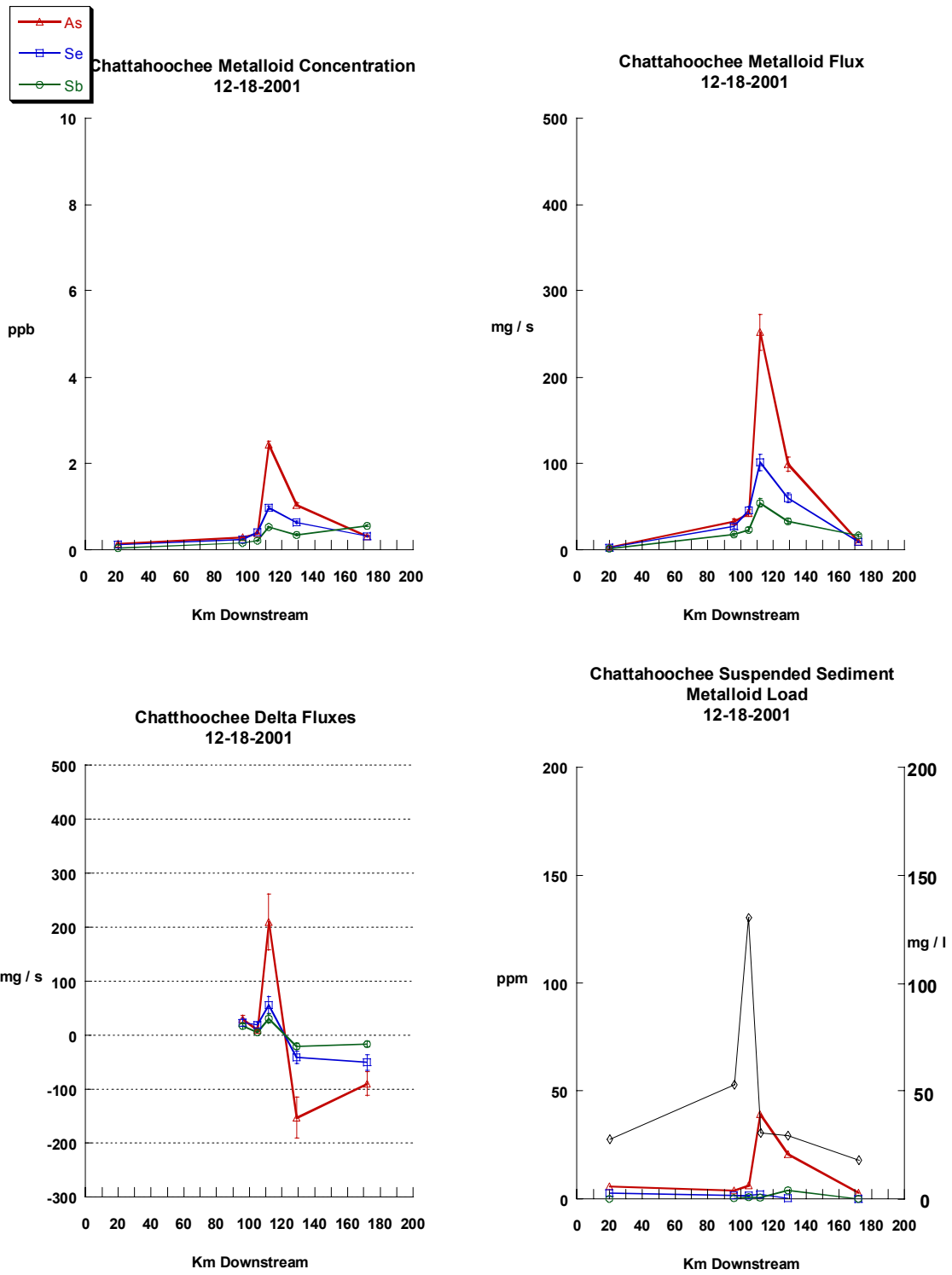


Figure 3-13. Chattahoochee River Metalloid Data, 18 December 2001

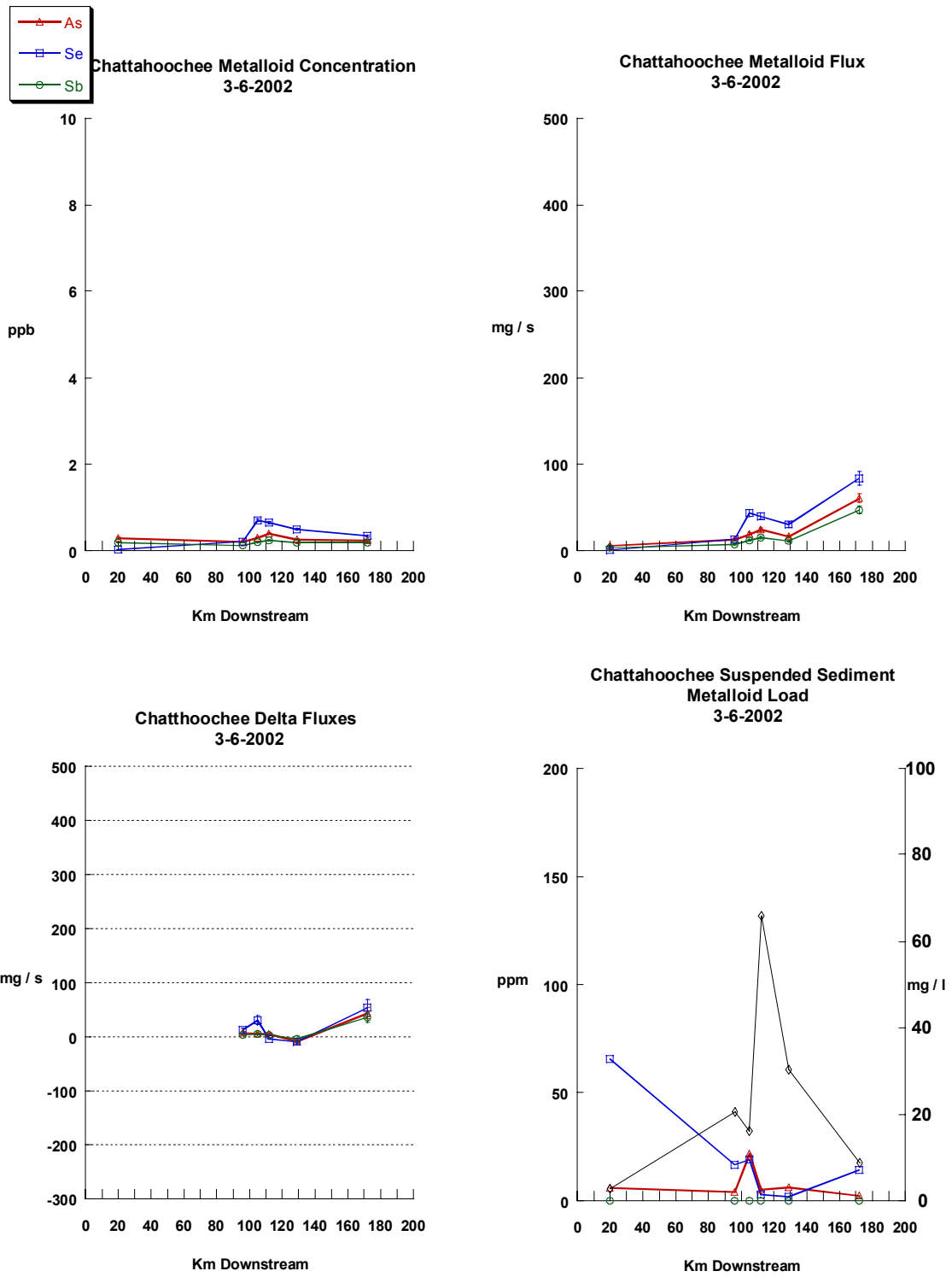


Figure 3-14. Chattahoochee River Metalloid Data, 6 March, 2002

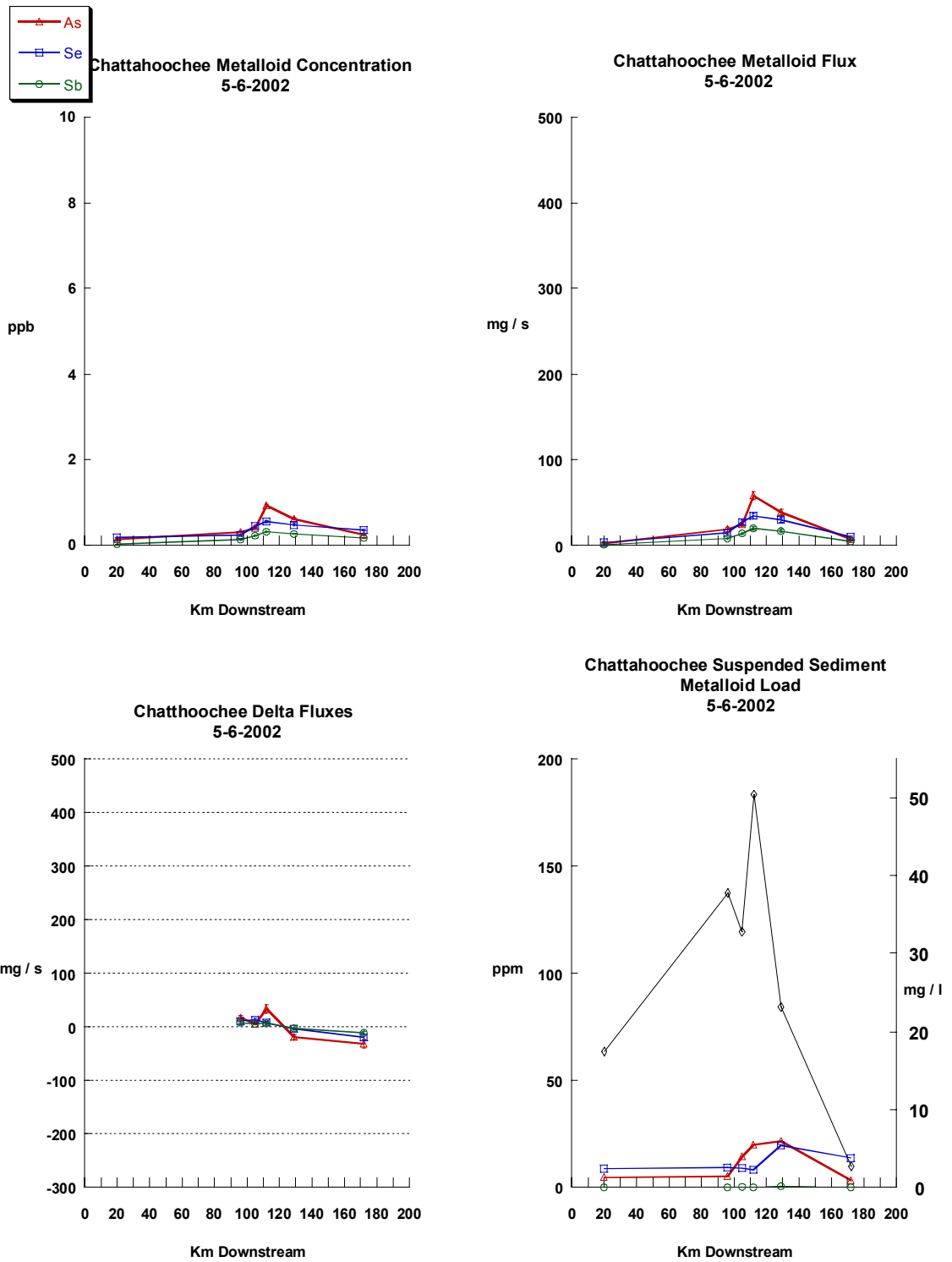


Figure 3-15. Chattahoochee River Metalloid Data, 6 May 2002

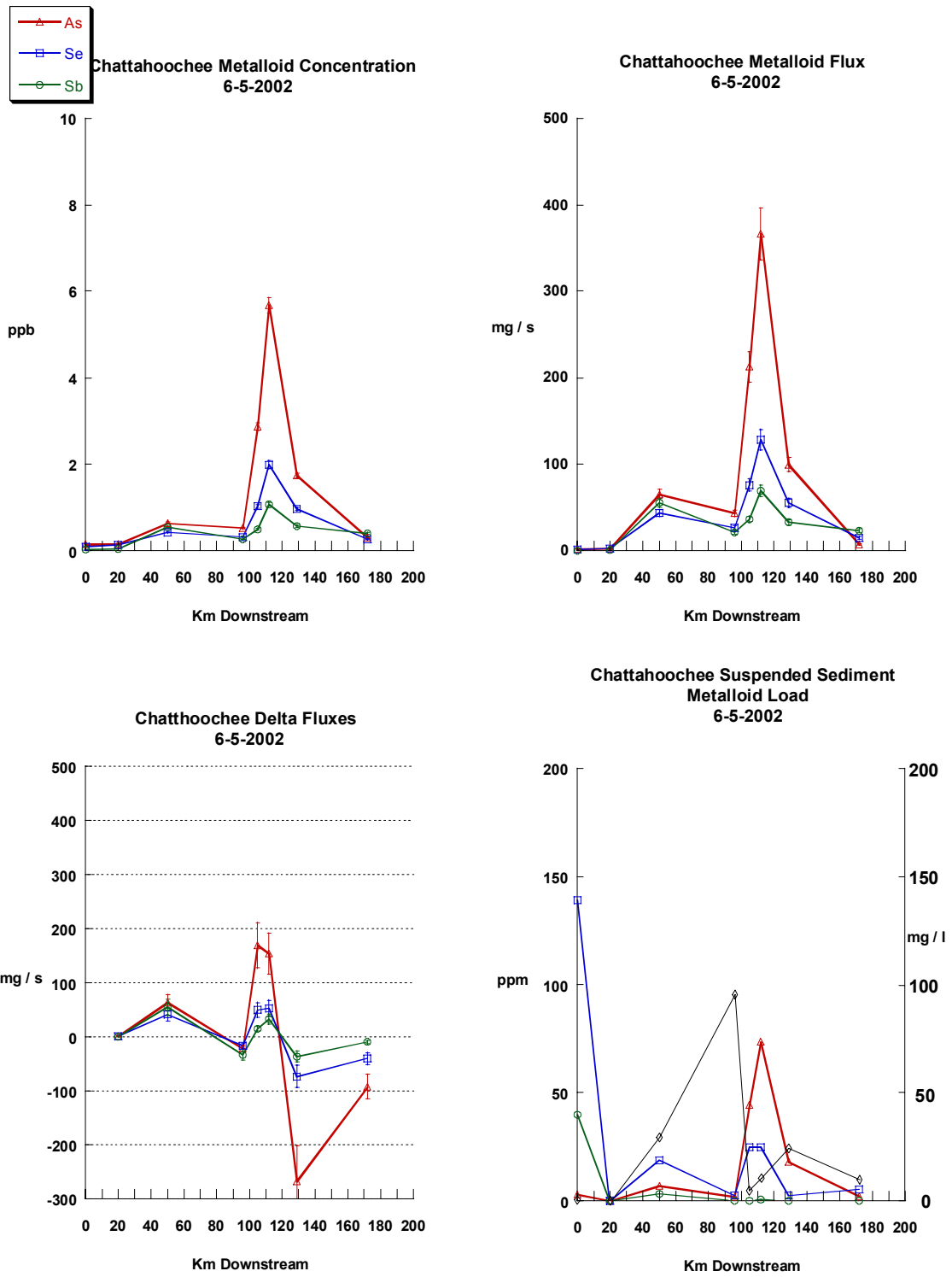


Figure 3-16. Chattahoochee River Metalloid Data, 5 June 2002

3.3 River Nutrient Profiles

This section discusses the Chattahoochee River nutrient profiles gathered during this study. Although the magnitude of the increases and decreases in river nutrients change from transect to transect, the general trends are the same. These trends are discussed below.

Five nutrients were analyzed during this research: dissolved reactive phosphate (PO_4^{3-}), nitrite (NO_2^-), ammonia (NH_4^-), silica (Si^-), and nitrite + nitrate ($\text{NO}_2^- + \text{NO}_3^-$). Average annual concentrations are shown in Fig. 3-17. Daily transect data is shown in Figs. 3-18 – 3-22. All nutrient profiles show an increase in nutrient concentration from above Atlanta to above Plants Yates and Wansley. Below Yates and Wansley all nutrient concentrations decrease. This decrease is similar to the observed decreases in all metalloid profiles across the same stretch of river.

Phosphate, ammonia, nitrite, and nitrate are nutrients essential to the growth and sustenance of photosynthetic communities. All can be limiting nutrients depending on the prevailing environmental conditions. These nutrients are released into the environment in and around major metropolitan areas. Phosphate is a major constituent in laundry detergent. The state of Georgia does not have regulations governing phosphates in detergents. The nitrogenous nutrients are by products of wastewater treatment. One of the major wastewater treatment plants for Atlanta discharges treated water to Utoy Creek, a tributary of the Chattahoochee in Atlanta. Silica is a ubiquitous nutrient in aquatic environments. It is mobilized into the aquatic environment through the weathering of silicate rocks and minerals. The data indicate that the decreases in nutrient concentration

across the stretch of the Chattahoochee River where Plants Yates and Wansley are sited is most likely a result of biological activity. This important has implications for the fate of metalloids in the environment, as will be discussed in Chapter IV.

Figures 3-13 – 3-17. Nutrient profiles vs. km downstream for each sampling trip arranged clockwise starting in the top left hand corner.

Dissolved Reactive Phosphate (PO_4) in units of μM

Ammonia (NH_4) in units of μM

Nitrite + Nitrate ($\text{NO}_2 + \text{NO}_3$)

Silica (Si) in units of μM

Nitrite (NO_2) in units of μM

On the graph of $\text{NO}_2 + \text{NO}_3$ and Si , $\text{NO}_2 + \text{NO}_3$ is represented by black open squares. Si is represented by green open inverted triangles.

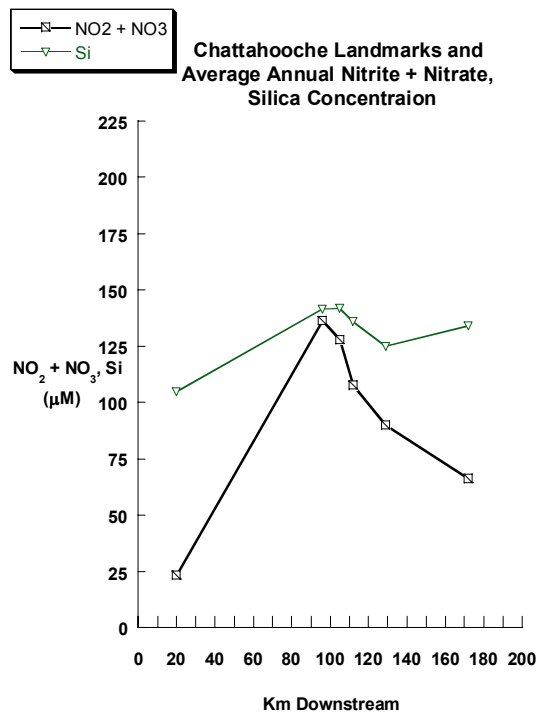
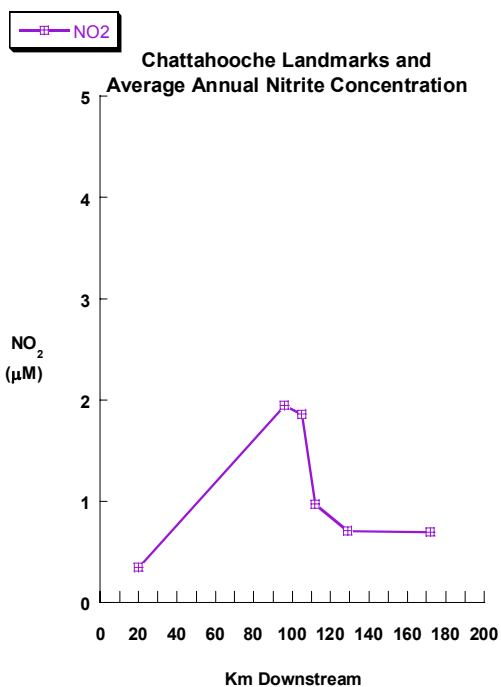
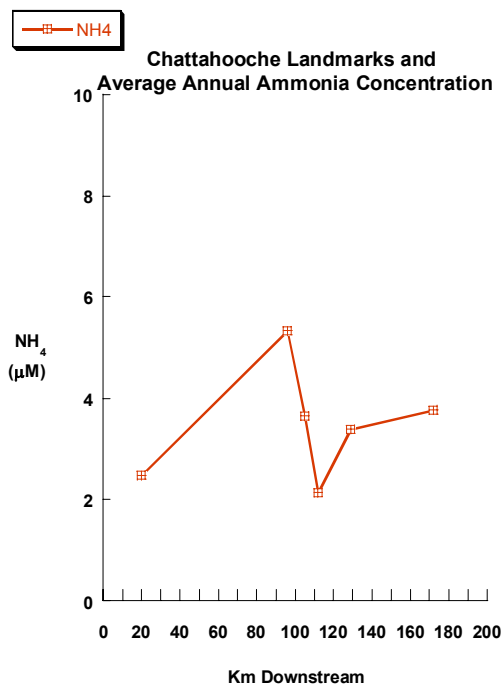
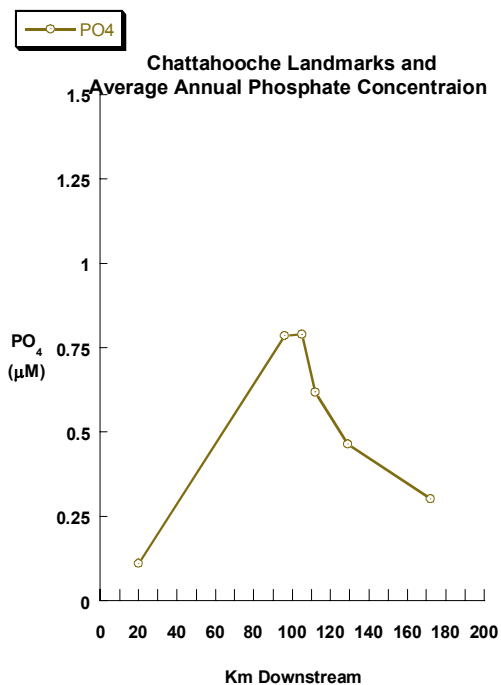


Figure 3-17. Chattahoochee River average annual nutrient concentrations

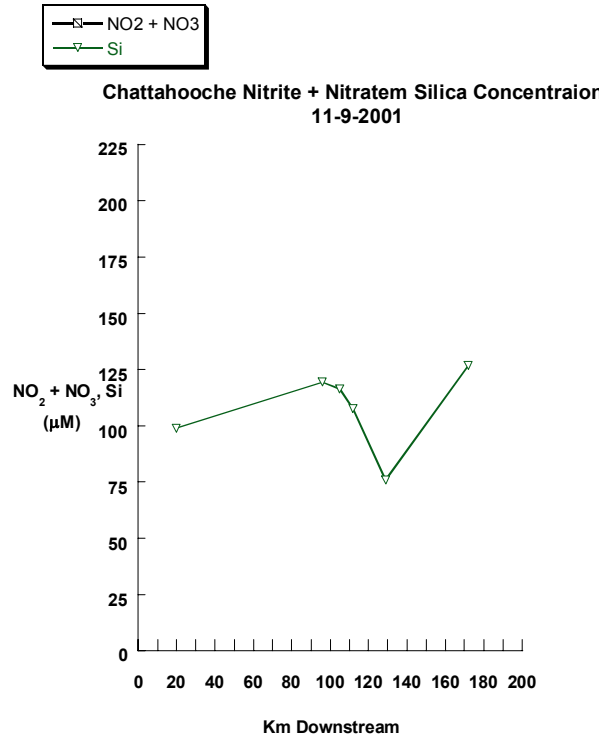
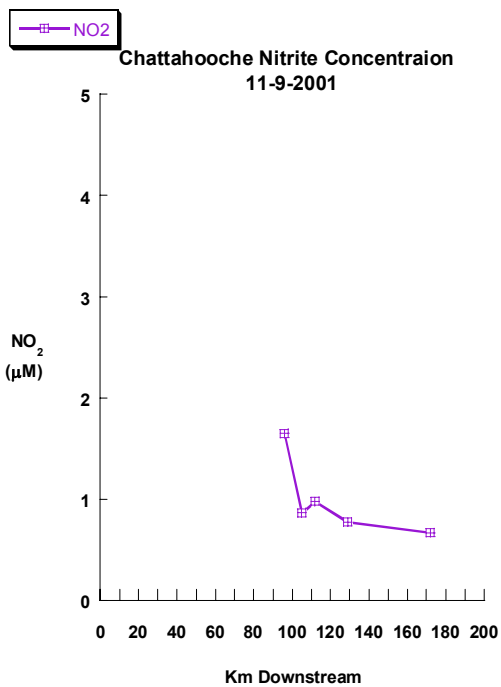
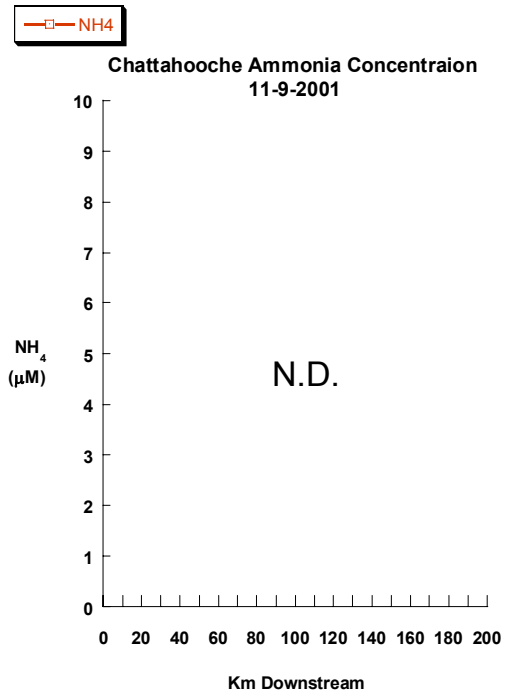
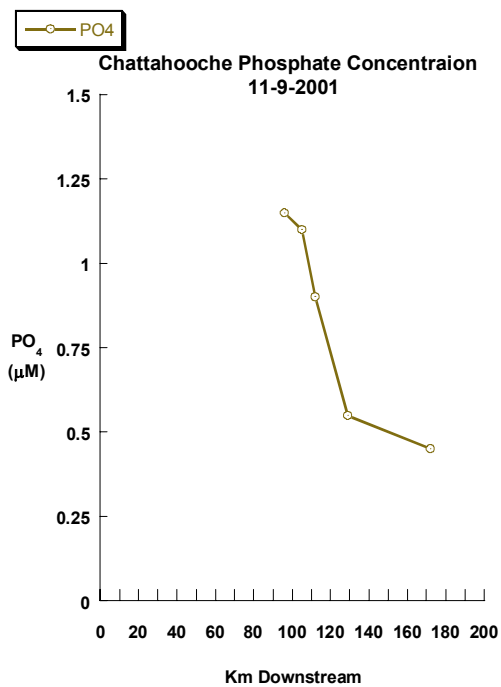


Figure 3-18. Chattahoochee River Nutrient Data, 9 November 2001

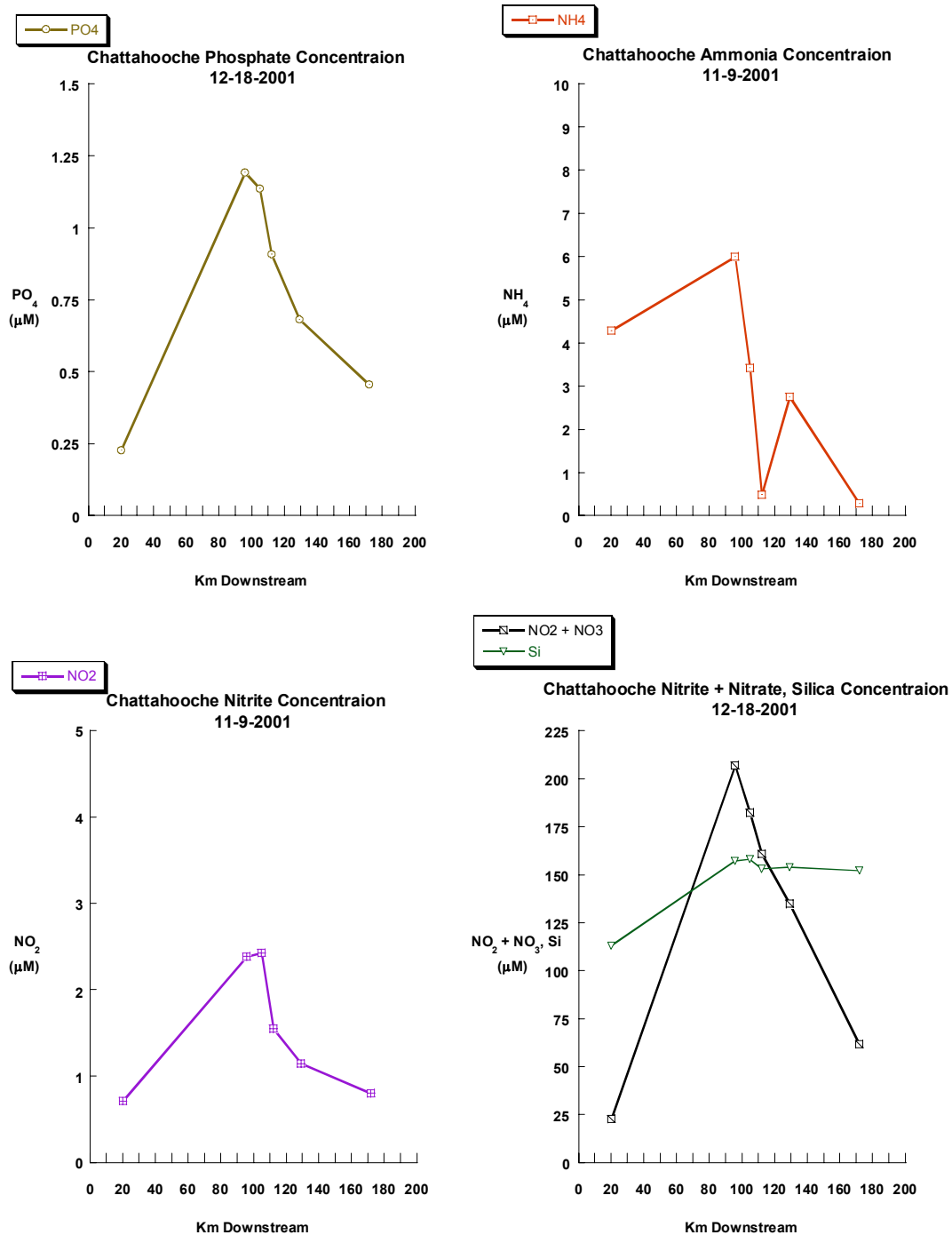


Figure 3-19. Chattahoochee Nutrient Data, 18 December 2001

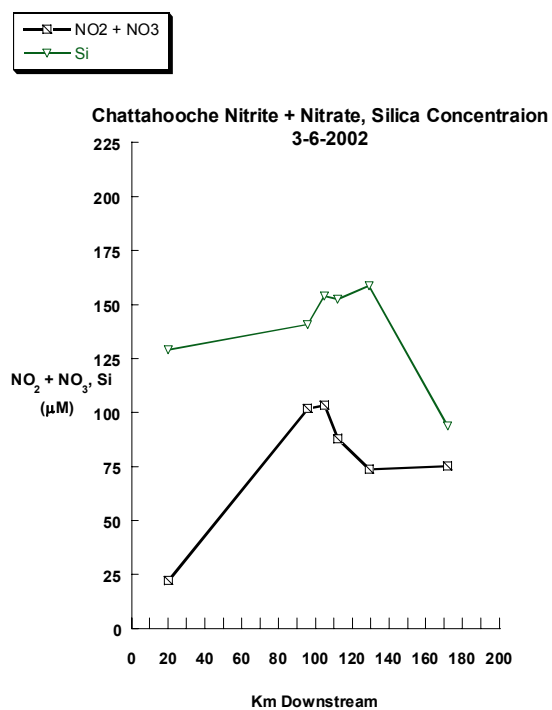
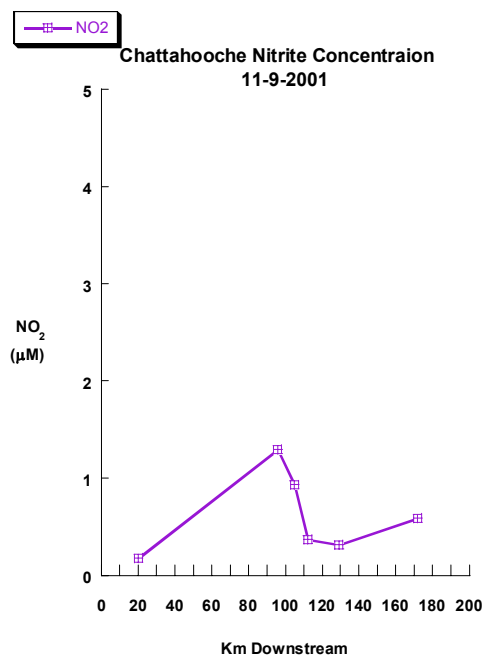
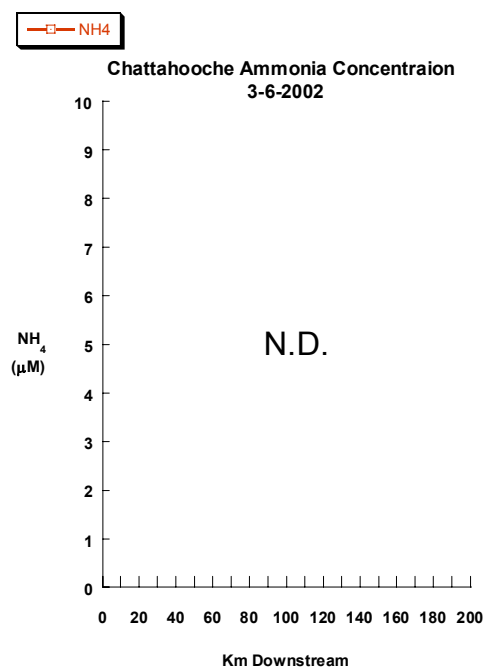
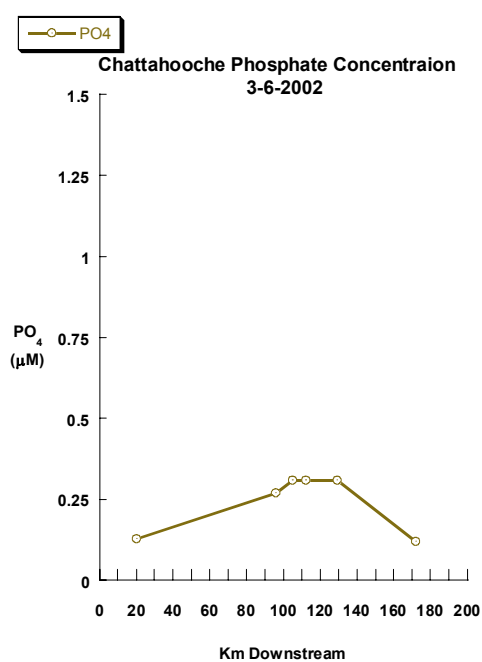


Figure 3-20. Chattahoochee River Nutrient Data, 6 March 2002

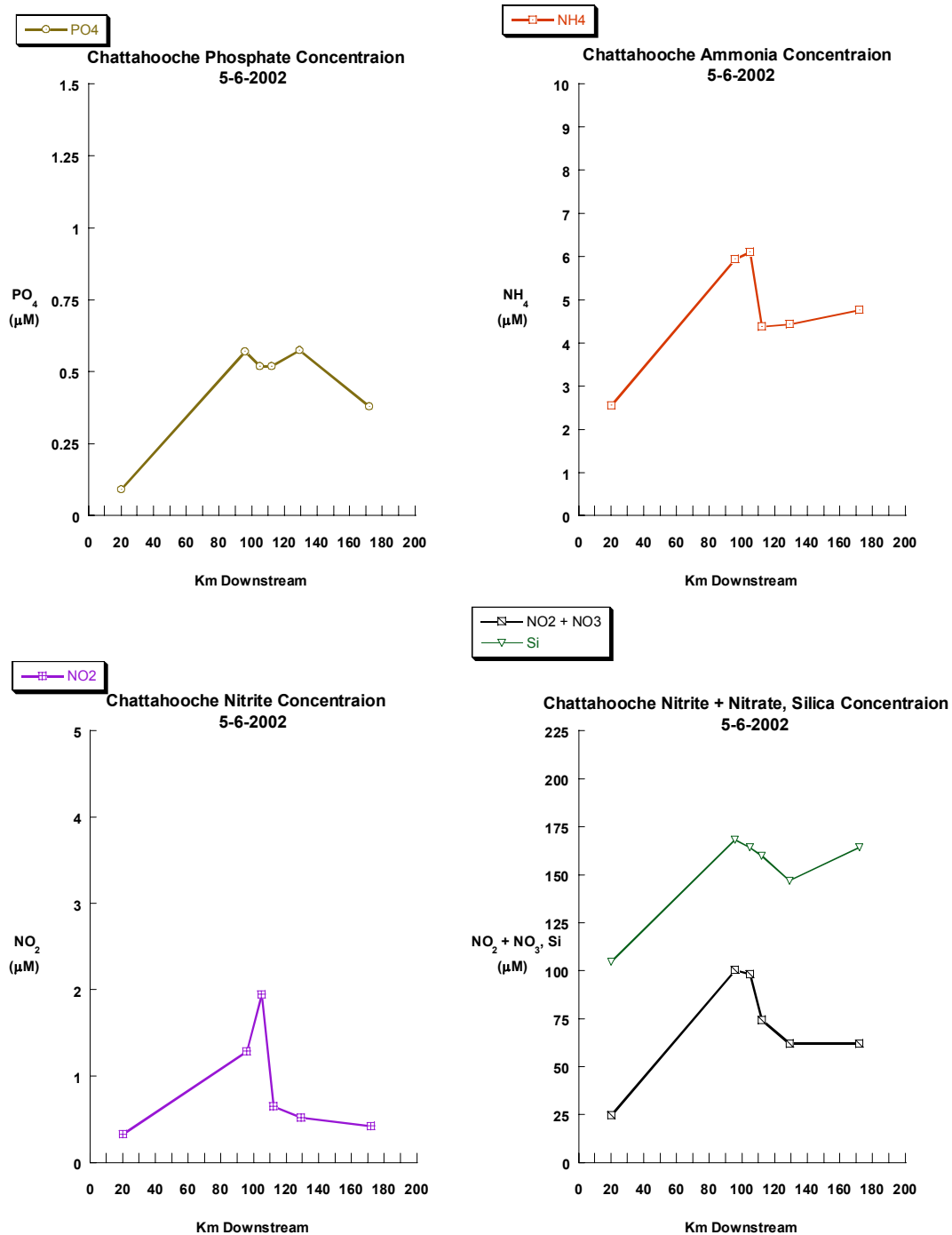


Figure 3-21. Chattahoochee River Nutrient Data, 6 May 2002

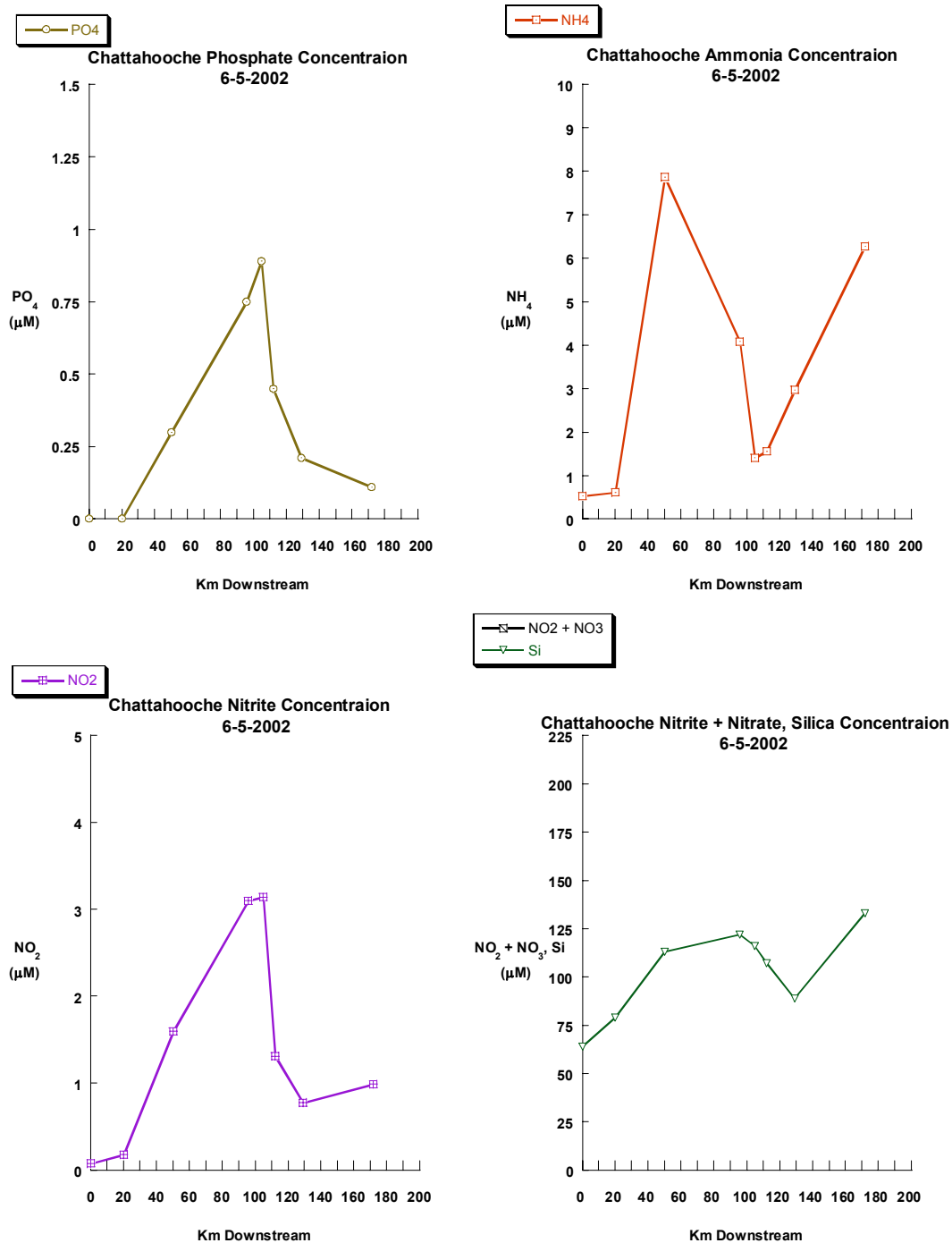


Figure 3-22. Chattahoochee River Nutrient Data, 5 June 2002

CHAPTER IV

DISCUSSION

This chapter discusses the implications of the data presented in the results section. I first focus on quantifying metalloid release from coal fired power plants. I follow with a discussion of the fate of metalloid contaminants in river systems.

4.1 Delta Fluxes

4.1.1 Ash Pond Effluent Evidence

Several conclusions can be drawn from examination of the Δ Flux data gathered during this study. Of critical import is evidence that the signal I have discovered can be attributed to ash pond effluent as opposed to a natural source or effluent from another type of industrial facility.

Table 1-4 contains the average concentrations of metalloids in coal and the reported ranges of those concentrations from the literature. If the peak in Δ Flux below plants Yates and Wansley is from ash pond effluent, then metalloid ratios in the receiving waters should reflect the ratios of the metalloid concentrations found in average coals. Figures 4-1a and b are “Redfield” style plots that show the ratios of Se and Sb to As in the Δ Fluxes calculated during this study. In both the Se / As and Sb / As plots there is a linear relationship. This relationship is expected if CFPP effluents discharge approximately constant As/Se/Sb ratios with time. The mass ratios of Se to As and Sb to As from the plots is 0.27 ppb / ppb and 0.13 ppb / ppb respectively. The metalloid

Table 4-1 Bowen Ash Pond Samples

Table 4-1 shows the metalloid concentration in historic ash pond samples (Froelich) taken from the Plant Bowen ash pond.

Location	Element	ppb	Se / As	Sb / As
Plant Bowen Fly Ash and Water Discharge (R-655)	As	242.5	0.29	0.24
	Se	69.4		
	Sb	57.8		
Plant Bowen Ash Pond Effluent (R-662)	As	61.3	0.21	0.22
	Se	12.7		
	Sb	13.4		

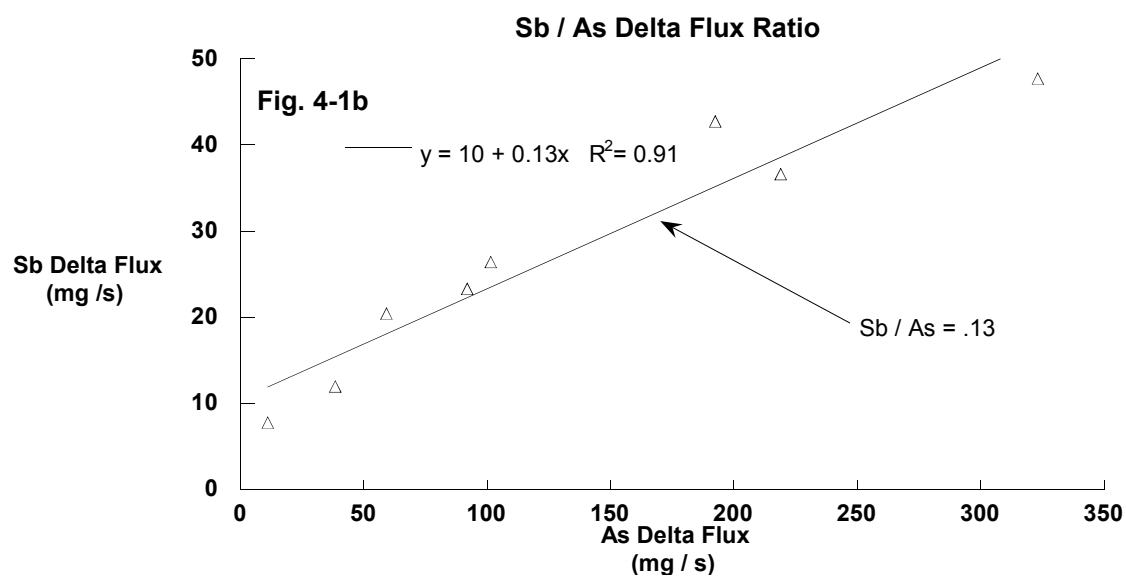
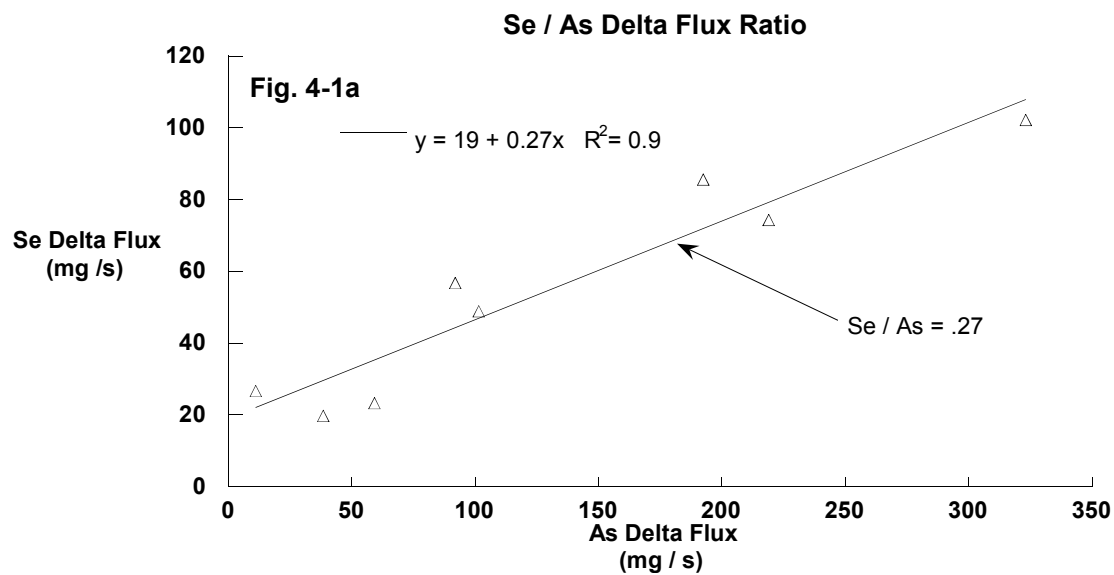


Figure 4-1 Δ Flux Metalloid Ratios. Figures 4-1a & b show the Se / As and Sb / As ratios of the Δ Fluxes calculated during this study.

concentrations in historic samples from the Plant Bowen ash pond (Table 4-1) show similar mass ratios (particularly Se / As) as compared to the Δ flux mass ratios. The mass ratios of Se to As and Sb to As calculated from the average values are both 0.1 (Table 1-4). In the case of the Sb / As ratio this is in close agreement with the ratio calculated from the Δ Fluxes. In all cases the differences in mass ratios fall within the ranges predicted by the concentration variability in coal. The positive intercepts of the Δ Flux plots (Se / As = 19 mg / s, Sb / As = 10 mg / s) suggest that As, Se, and Sb are removed from solution in the ash ponds at different rates (Fig. 4-1). Arsenic is apparently more efficiently. The lower intercept of the Sb line suggests that it is removed more efficiently than Se.

Some thermodynamic considerations may be used to explain these differential removal rates. The Eh-pH diagrams for arsenic, selenium, and antimony (Figs 1-1 through 1-3) show that in oxic river waters the oxidized species (As (V), Se (VI) and Sb (V)) will be the dominant inorganic forms of these elements. Although they are released from the ash ponds in their reduced states, thermodynamics predicts that they should oxidize to their higher valence states. This theory is supported by the rapid removal of As as compared to Se, and Sb. Arsenic (V) is strongly attracted to the iron oxyhydroxide clays which are suspended in the Chattahoochee River. Mass balance modeling supports this hypothesis. Little is known about the sorption characteristics of Se and Sb to mineral surfaces, however this data suggests that either the oxidation or the sorption processes of these elements is slower than As and may be kinetically limited as opposed to thermodynamically controlled.

4.1.2 Escape Efficiency

Using Δ Flux and CFPP coal flow data “escape efficiency” of the metalloid elements from coal fired power plants can be estimated. Escape efficiency is a measure of the steady-state fraction of the metalloids in fired coal that escapes into the aqueous phase from power plants.

Table 4-3 shows the peak Δ Flux calculations below plants Wansley and Yates on the dates sampled during this study. In order to estimate the escape efficiency, integrated Δ Fluxes over the period of the study must be calculated. The integrated Δ Fluxes over the time period of this study are the average of the highest Δ Flux values for each sampling trip. They are 130 mg / s, 55 mg / s, and 27 mg / s for As, Se and Sb respectively (See Table 4-3). Coal flow data obtained from Georgia Power (www.southernco.com/fuelservices/gapower.htm) states that Yates and Wansley together burn 5.6×10^9 kg of coal a year. The escape efficiency is the ratio of the Δ Flux (mass metalloid / time) to the coal flux (mass coal / time). This ratio yields a result with the dimensions of mass metalloid released / mass coal burned, or the mass metalloid released to the aquatic environment for every kilogram of coal burned. The escape efficiencies for As, Se, Sb are 0.73 mg / kg, 0.30 mg / kg, and 0.15 mg / kg respectively. Based on the average metalloid concentration in coal (Table 1-4) 7.3% of the As, 30% of the Se, and 15% of the Sb in combusted coal is released aquatically every year.

Table 4-2 Metalloid Δ Fluxes

Table 4-2 shows the peak Δ Fluxes in mg /s at the peak below Plants Yates and Wansley. These are the sums of the Δ Fluxes below Yates and the Δ Fluxes below Wansley. This permits the calculation of a “universal escape efficiency based on more than one power plant.

Peak Δ Fluxes (mg / s)									
	5/22/2001	8/6/2001	9/15/2001	11/9/2001	12/18/2001	3/6/2002	5/6/2002	6/5/2002	Integrated
As	59	92	192	102	219	11	39	323	130
Se	23	57	86	49	74	27	20	102	55
Sb	20	23	43	26	37	8	12	48	27

Eq. 4-1 Metalloid Release

$$E_{eff} \times B = R$$

Equation 4.1 is used to calculate the rate of release of a metalloid element into the environment based on the escape efficiency and the amount of coal burned per unit time. E_{eff} is the metalloid escape efficiency in units of mg metalloid released / kg coal burned. B is the amount of coal burned per unit time. R is the rate of metalloid release in units of mg per unit time. Using the escape efficiency of 0.73 mg / kg for As and the estimated 5.6×10^9 kg coal burned by plants Wansley and Yates I calculate that 4.1×10^9 mg or 4.1 tons arsenic is released in to the Chattahoochee River every year. Similar calculations for Se and Sb reveal that 1.7 tons of Se and 0.87 tons of Sb are released annually to the aquatic environment. Over a 20-year period, approximately the lifetime of these power plants, this is equivalent to 81 tons As, 34 tons Se, and 17 tons Sb discharged into the Chattahoochee River.

4.2 The Fate of Metalloids in Rivers

While there is clearly a source of metalloids to the Chattahoochee River from plants Yates and Wansley, there is also a loss of metalloids from the dissolved phase downstream of the power plants. The same calculations used to determine the integrated peak Δ Flux can be used to quantify the amount of metalloids lost downstream.

Table 4-4 shows the Δ Flux values between the sampling site below Wansley and Yates (sample site 112) and the sampling site in Franklin, GA (sample site 125). The Δ Flux values show a decrease in metalloid flux between the site below Yates and Wansley and the site in Franklin. Treating this data in the same manner as the peak Δ Flux data yield integrated values of -103 mg / s As , -35 mg / s Se , and -18 mg / s Sb . Assuming that this loss rate is the same over the last 20 years, these loss fluxes represent a removal of 65 tons As, 22 tons Se, and 11 tons Sb. These removal fluxes represent 80% of the As input and 65% of the Se and Sb inputs from the power plants. Plots (Fig. 4-3) of peak Δ Flux (Table 4-3) vs. metalloid loss flux (Table 4-4) confirm the integrated loss estimates. There is a linear relationship between the Δ Flux and the loss flux. The slope of -1.2 for each of the loss plots indicates that metalloid input is 1.2 times greater than the loss and that 80% of the input flux is lost from the aqueous phase. For As, this agrees exactly with the integrated estimate. For Se and Sb there is close agreement with the integrated loss estimate. The question now becomes the fate of the metalloids in contaminated river systems. I hypothesize that there are two fates for these metalloids. The first is incorporation into the planktonic and benthic biologic systems through incidental uptake.

Table 4-3 Metalloid Loss Fluxes

Table 4-3 shows the metalloid loss fluxes between the sample site below Wansley and Yates and the sample site in Franklin. A large fraction of the metalloid input from the ash pond effluents is lost over this 17 km length of river.

Metalloid Loss Fluxes (mg / s)									
	5/22/2001	8/6/2001	9/15/2001	11/9/2001	12/18/2001	3/6/2002	5/6/2002	6/5/2002	average
As	-54	-74	-161	-90	-153	-8	-19	-267	-103.134
Se	-23	-29	-69	-28	-41	-10	-5	-73	-34.661
Sb	-13	-14	-32	-19	-21	-4	-3	-36	-17.7918

Table 4-4 Phosphate Loss Fluxes

Table 4-4 shows the loss flux of phosphate between the sample sites below Wansley and Yates and the sample site in Franklin.

PO₄³⁻ Loss Fluxes (mg / s)					
11/9/2001	12/18/2001	3/6/2002	5/6/2002	6/5/2002	Integrated
-1123.12	-2783.22	-16.70	333.17	-1621.20	-1042.21

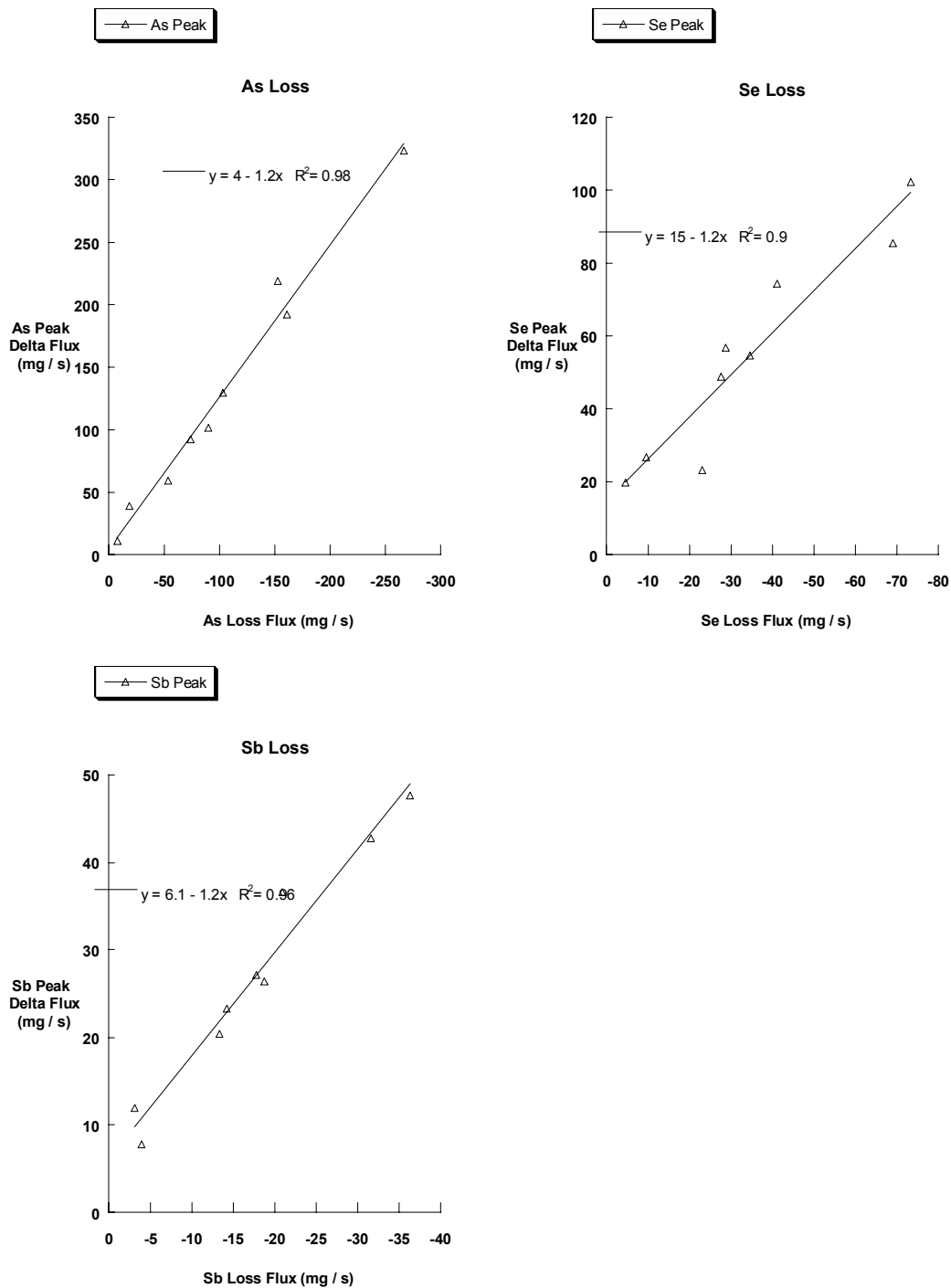


Figure 4-2Metalloid Loss Factors. Figure 4-2 shows the loss factors for As, Se, and Sb. A negative *loss* factor indicates that input is greater than loss.

The second is sorption onto suspended sediment particles followed by transport downstream.

4.2.1 Biological Uptake

All of the Chattahoochee nutrient profiles (Figs. 3-17 – 3-22) show dramatic increases in nutrient concentration between Atlanta (sample site 20) and sample site 96, above Yates and Wansley. Between this sample site and the site below Yates and Wansley (sample site 112) there is a drop in the concentration of all the nutrients analyzed during this study. This may be due to either dilution or biological uptake. Analyses of USGS stream flow data reveal that there is insufficient increase in water flow in the Chattahoochee over this stretch of river to explain the dilution of nutrients. This clearly suggests that aquatic flora and fauna are taking up nutrients.

It is known that metalloids can be incidentally incorporated into biomass in place of nutrient elements. Two well-documented examples are the substitution of Ge (germanic acid) for Si (silicic acid) in diatom shells and the incidental uptake of As (arsenate) into P (phosphate) biochemical pathways. There is also evidence for the uptake of Se into the biochemical pathways for S. All profiles of Si and PO_4^{3-} (Figs. 3-17 – 3-22) show decreasing concentrations across the stretch of river where the CFPPs are sited. These two facts coupled with concurrent decreases in NO_2^- , NO_3^- , and NH_4^+ suggest increases in phytoplankton are occurring in the river. The magnitude of the nutrient uptake suggests that a large percentage of the metalloid loss flux could be due to loss into aquatic and benthic organisms. Table 4-5 shows the loss of PO_4^{3-} between Wansley and Yates and Franklin. If biological uptake is a factor in the loss of As from the

river one would expect to see a relationship between PO_4^{3-} loss and As loss (Figure 4-4). With only 5 data points a definitive quantitative relationship cannot be made between these two loss fluxes. However, the estimated 6.5 atoms of As uptake for 100 atoms of PO_4^{3-} uptake appear reasonable, particularly in a PO_4^{3-} limited system.

4.2.2 Sorption onto Sediments

Suspended sediment profiles of the Chattahoochee River (Figs. 3-9 through 3-16) show an increase in the mass of metalloids on suspended sediments. This is presumably due to effluent from ash ponds. The concentrations of metalloids in the suspended phase show the same characteristic order ($\text{Se} / \text{As} = 0.16$, $\text{Sb} / \text{As} = 0$) found in the river. This is farther evidence that this loading is due to CFPPs and is not carried down the river from further upstream. As the metalloid concentrations in the river increase the mass of metalloids on suspended particles will also increase in an attempt to maintain equilibrium between the metalloids in the dissolved phase and in the particulate phase.

Mass balance modeling has revealed that the power plants also discharge solid ash material in the effluent from ash ponds. In the case of Plant Yates the metalloid discharge in the ash phase is greater than in the dissolved phase.

Using river flow data and suspended sediment data it is possible to calculate the flux of metalloids on suspended sediments. By comparing up and downstream fluxes, i.e. calculating a Δ Flux for suspended sediment metalloids, it is possible to estimate partitioning between metalloid loss into the biological system and sorption onto suspended sediments. The sediment flux calculation is as follows:

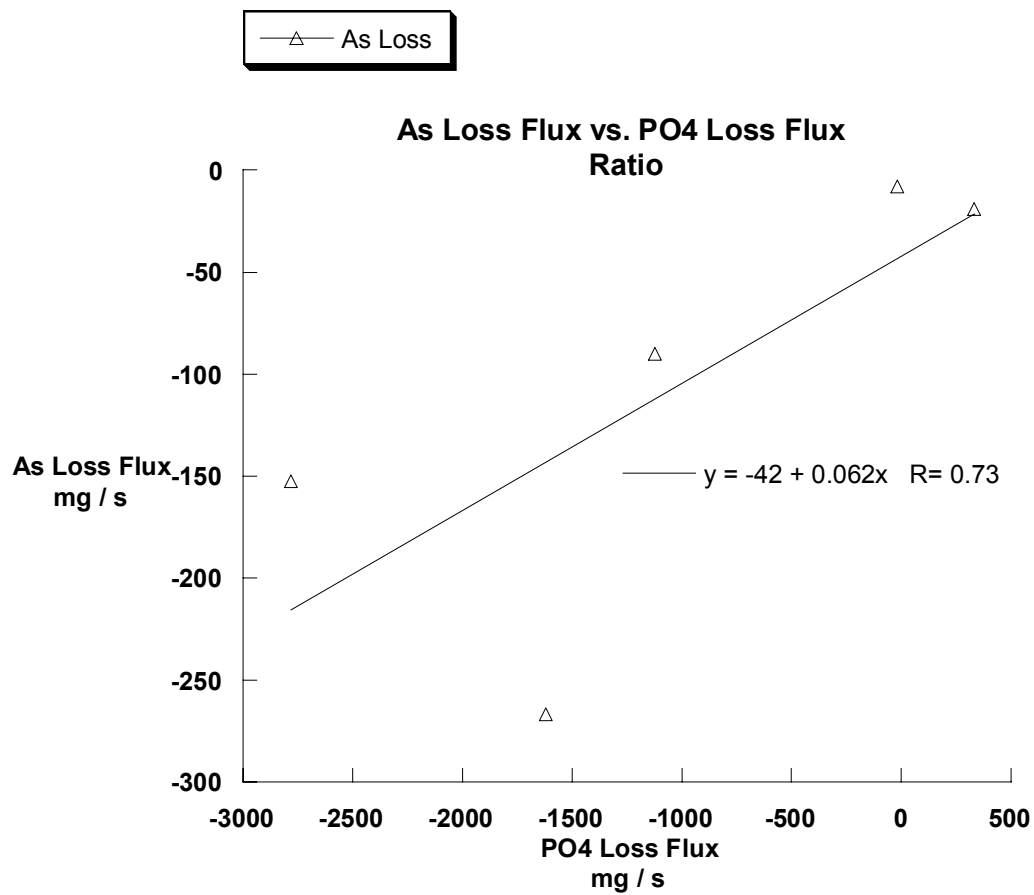


Figure 4-3 As / PO₄ Loss Ratio. Figure 4-3 shows the ratio of As loss and PO₄ loss between site 112 and site 129.

Eq. 4-2

$$M_{sed} \times Q \times C_{sed} = F_{ss}$$

M_{sed} is the mass of sediment per volume water (kg / L). Q is the river flow in L / s. C_{sed} is the metalloid concentration on the suspended sediment (mg / kg). F_{ss} is the flux of metalloids on suspended sediments in units of mg suspended metalloid / s. Table 4-5 contains the suspended metalloid Δ Fluxes as between the sample site above Wansley and Yates and the peak suspended metalloid concentration. With the exception of 5/6/2002 the peak concentration is at the site below Wansley and Yates. On this day the peak concentration suspended metalloid concentration was recorded in Franklin, GA.

From the values in this table the integrated suspended sediment Δ Flux can be calculated. They are 49 mg / s, 8 mg / s, and 0 mg / s for As, Se and Sb respectively. It is important to notice that the integrated value for Se is skewed by the high flux on 5/6/2002. This table shows that there is little change in the particulate flux of Se and Sb across the power plants. Along with the thermodynamic considerations put forth earlier (4.1.1), this suggests that the riverine chemistry of these elements is different than that of As.

Figures 4-5 – 4-7 are box models of metalloid fluxes through the Chattahoochee River system. These models show the two main metalloid reservoirs in the Chattahoochee system: the dissolved phase, and the suspended phase. The most important fluxes into, out of, and between these systems are the input of dissolved and solid metalloid phases from ash ponds, sorption of metalloids onto material suspended in the stream flow, desorption of metalloids off of suspended material, the settling of

Table 4-4 Peak Sediment Delta Fluxes

Table 4-4 shows the peak sediment Δ Fluxes for the Chattahoochee River below plants Wansley and Yates

Peak Sediment Delta Flux (mg / s)						
	11/9/2001	12/18/2001	3/6/2002	5/6/2002	6/5/2002	Integrated
As	39	101	16	55	35	49
Se	0	0	0	39	0	8
Sb	0	1	0	2	0	0

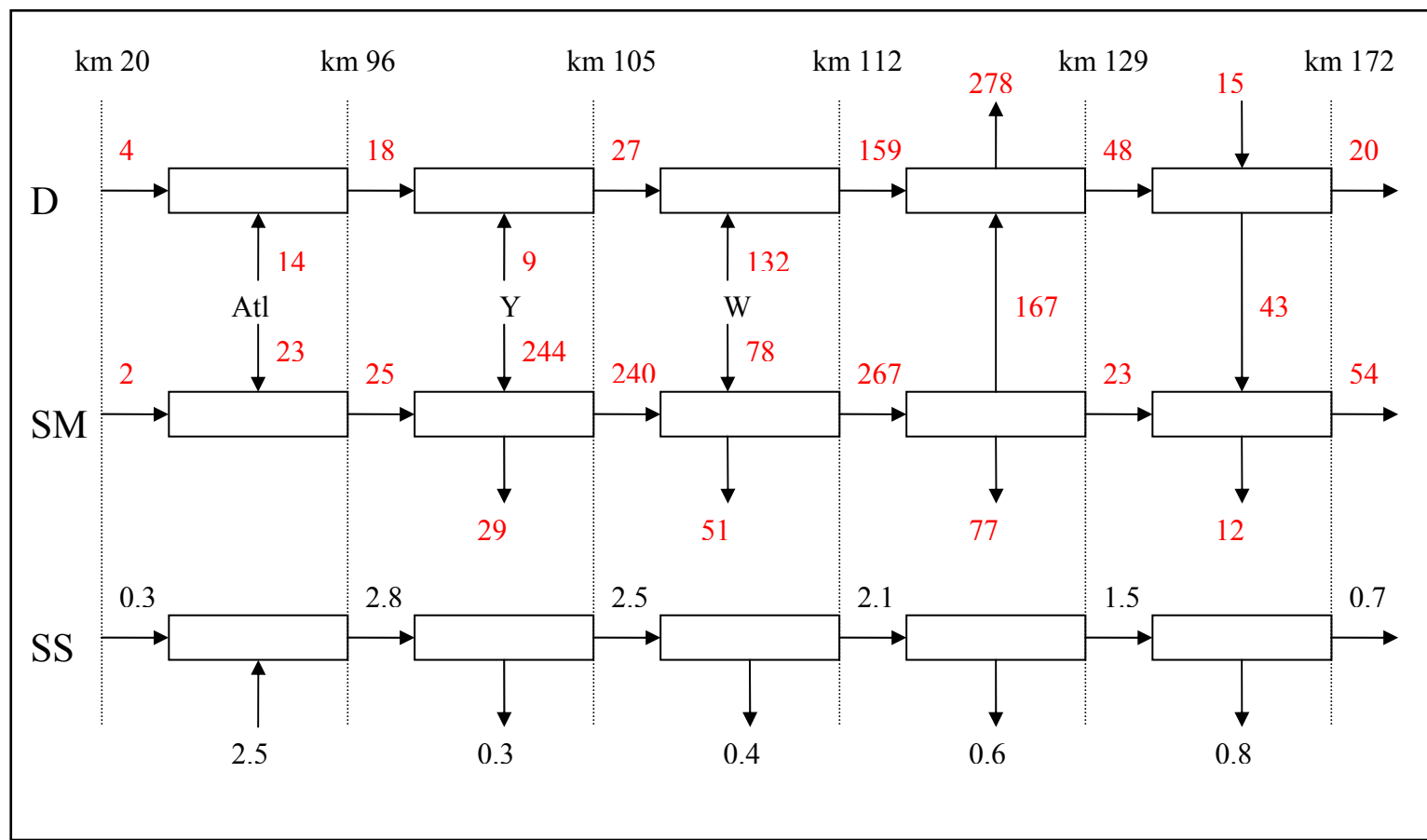


Figure 4-4 Chattahoochee River Arsenic Box Model. Figure 4-4 shows a box model of metalloid fluxes on the Chattahoochee River system. D is the dissolved phase. SM is the suspended material phase. SS shows the input and settling of suspended sediment in the river. Atl is Atlanta, GA; Y is Plant Yates; and W is Plant Wansley. D and SM Fluxes are in mg / s. SS Fluxes are in kg / s.

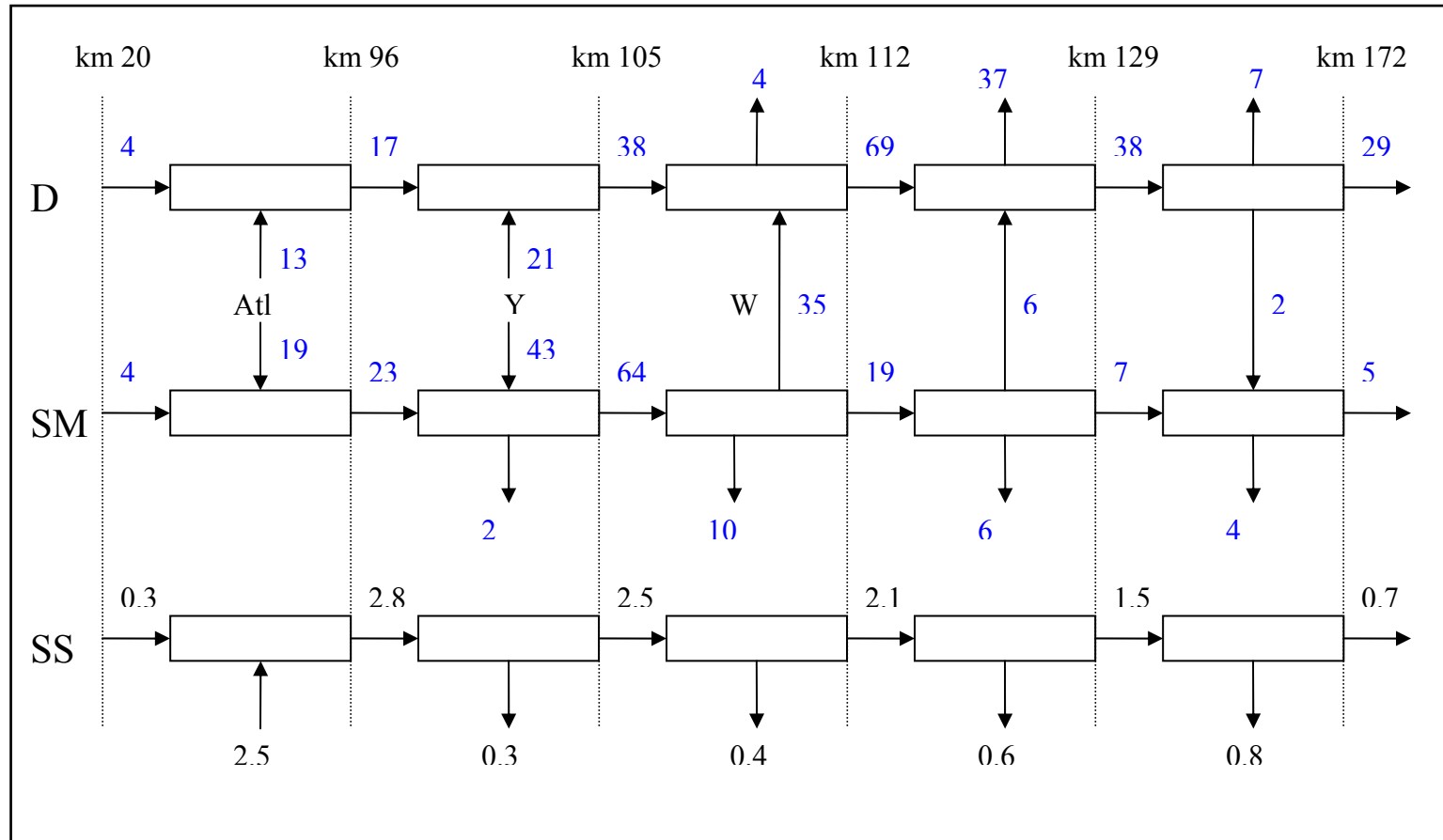


Figure 4-5 Chattahoochee River Selenium Box Model. Figure 4-5 shows a box model of metalloid fluxes on the Chattahoochee River system. D is the dissolved phase. SM is the suspended material phase. SS shows the input and settling of suspended sediment in the river. Atl is Atlanta, GA; Y is Plant Yates; and W is Plant Wansley. D and SM Fluxes are in mg / s. SS Fluxes are in kg / s.

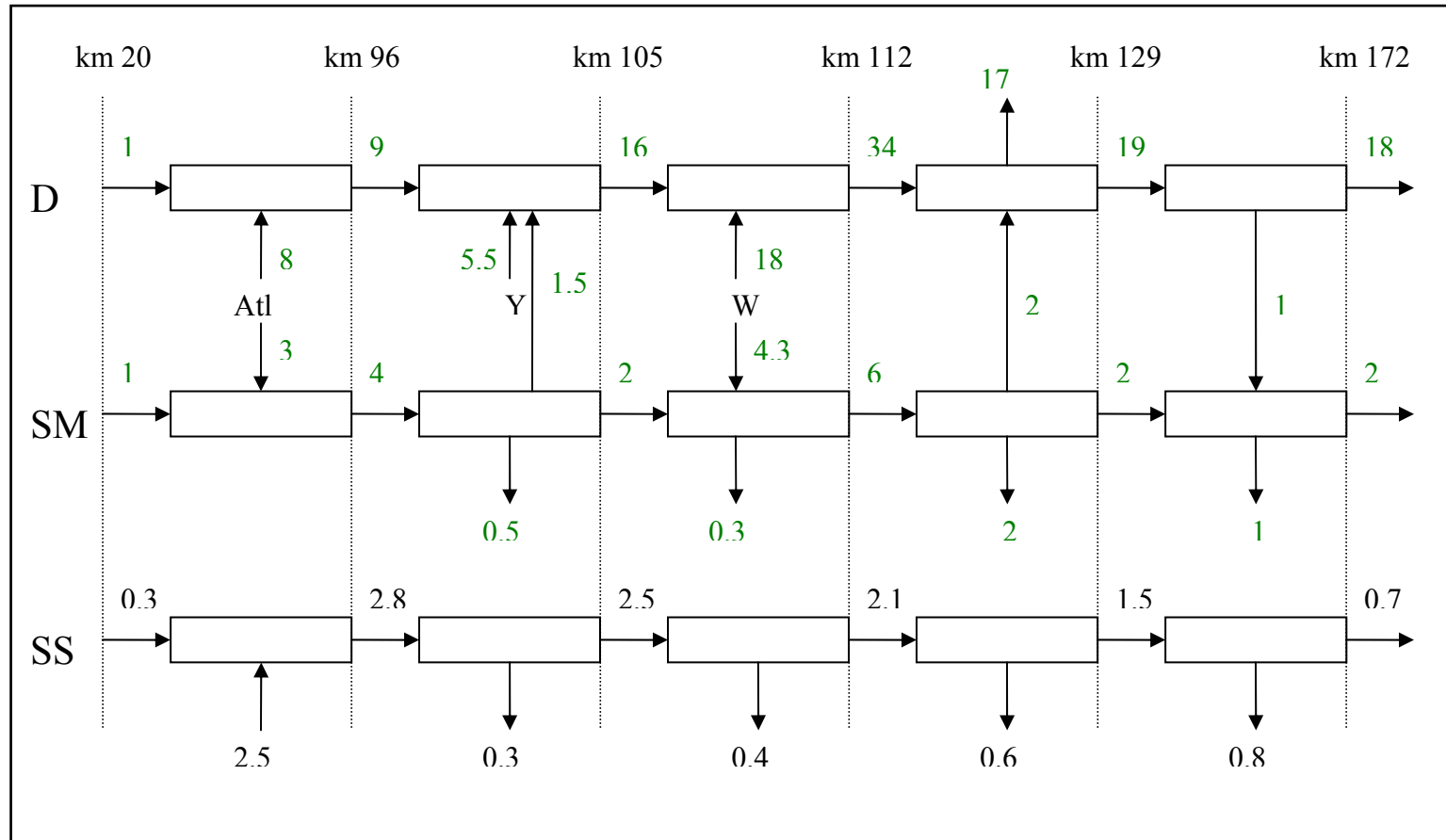


Figure 4-6 Chattahoochee River Antimony Box Model. Figure 4-6 shows a box model of metalloid fluxes on the Chattahoochee River system. D is the dissolved phase. SM is the suspended material phase. SS shows the input and settling of suspended sediment in the river. Atl is Atlanta, GA; Y is Plant Yates; and W is Plant Wansley. D and SM Fluxes are in mg / s. SS Fluxes are in kg / s.

suspended material onto the bed of the Chattahoochee River, and uptake of metalloids by micro and macro organisms. It is important to note that these models represent year long net fluxes and may not accurately describe the short term cycling of metalloids between the reservoirs.

Dissolved and suspended fluxes are calculated using the methods described previously (3.1.2 and 4.2.2). The rate of setting of metalloid laden sediment is calculated by multiplying concentration of metalloids on the sediment (mg / kg) by the loss of sediment (kg / s) in the river (SS out arrows in Figs. 4-5 through 4-7) to obtain the rate in units of mg / s.

The models reveal that the input of solid ash material from the ash pods is major source of metalloid contamination in the Chattahoochee River. In the case of arsenic, the suspended metalloid flux from CFPPs to the river is greater than the dissolved flux by a factor of two. The models also reveal that biological uptake is the principal metalloid sink in contaminated systems. The rates of biological uptake of As, Se, and Sb are 278 mg / s, 48 mg /s, and 17 mg / s respectively. Over the year of this study these fluxes represent biological uptake of 8.7 tons arsenic, 1.5 tons selenium, and 0.5 tons antimony. The models also show that the settling of metalloid laden sediment is an important process. This is of concern due to the fact that the sediment is eventually transported downstream to the upper reaches of West Point Lake, an important drinking water source for west central Georgia, and a popular sport fishing locale.

4.3 Toxic Release Inventories and the PISCES Model

4.3.1 Toxic Release Inventories

Beginning in 1998, coal fired electric plants are required to report their toxic releases. The reporting and the subsequent release of data is done through the US Environmental Protection Agency's (EPA) Toxic Release Inventory (TRI) program. In the case of CFPP's, TRI requirements are based on the size and power output of the power plant. Arsenic is required to be reported for plants 400 MW and larger; Se, for 1200 MW and larger; and Sb, for 4500 MW plants and larger (Rubin, 1999). Under these guidelines, Arsenic TRI reports would be required by every power plant in this study. Selenium TRI's would be required for Plants Bowen, Wansley and Yates. The 4500 MW requirement for Sb reporting in the TRI is larger than the rating of any of the power plants in this study.

Table 4-7 contains the TRI information for the power plants this study. It shows the TRI estimates for As, Se, and Sb for the years 1998, 1999, and 2000. The lag between the collection year and the publication of the data is approximately two years. The data for the year 2001 will be available in 2003. The latest year available at this writing is 2000. These TRI estimates can be compared to my estimated aquatic releases based on the mass of coal burned per year at each power plant and the escape efficiency calculated in section 4.1.2. This table shows that with the exception of the Yates Arsenic estimate for the year 2000 all of the TRI estimates are lower than the escape efficiency estimate by a factor of two or greater. It is interesting to note that the As estimates for Yates and Wansley increase from zero or near zero in the years before 2000 to approximately 1500

kg per year emission into the aqueous phase in the 2000 reporting year. I believe this reflects a change in the methods used for estimating the partitioning of toxic releases to the environment. It is of note that due to analytical uncertainty and the $\pm 5\%$ uncertainty in the USGS river flow data there is a $\pm 25\%$ uncertainty in my escape efficiency estimate for arsenic, a $\pm 28\%$ uncertainty for selenium, and a $\pm 28\%$ uncertainty for antimony. The 1474 kg arsenic release estimate from Plant Yates (2000) falls within this uncertainty. None of the other TRI estimates for any of these plants are within the escape efficiency uncertainty. It is also of note that a TRI for Sb is not required for these plants. While there is comparatively little known about this element and its riverine chemistry, it is known to be toxic and shown here to be released to the environment in significant amounts from coal fired power plants.

4.3.2 The PISCES Model

The Power Plant Integrated Systems: Chemical Emissions Studies (PISCES) Model is a model that the US EPA allows the electrical industry to use to estimate its toxic releases. The PISCES model is a thermodynamic model of the CFPP combustor train that attempts to minimize Gibbs free energy through mass and energy balances. The data base contains equilibrium constants for 21 elements and a total of 698 species (Sandelin and Backman 2001). A study of two power plants was conducted by these workers. They compared the measured results of trace element partitioning during coal combustion and the results of the PISCES calculations. These results showed that the experimentally derived exclusive partitioning of As onto fly ash was largely adequately by the model. However, this study showed a large discrepancy between the Se

Table 4-5 TRI Aquatic and Total Release Reports

Power Plant MW kg Coal / year	Element	CFPP Aquatic Release (This Study) 2001-02 (kg/yr)	1998 TRI Aquatic (Total) Estimate (kg/yr)	1999 TRI Aquatic (Total) Estimate (kg/yr)	2000 TRI Aquatic (Total) Estimate (kg/yr)
Bowen 3160 7.27x10⁹	As	<i>5300</i>	0 (14500)	0 (11600)	0 (24200)
	Se	<i>2200</i>	0 (14250)	0 (13200)	8 (18800)
	Sb	<i>1100</i>	NR*	NR	NR
Hammond 800 1.91x10⁹	As	<i>1400</i>	NA**	NA	NA
	Se	<i>570</i>	NR	NR	NR
	Sb	<i>280</i>	NR	NR	NR
Wansley 1730 3.64x10⁹	As	2650	0 (16400)	0 (17500)	1474 (23600)
	Se	1100	507 (8100)	207 (7600)	209 (7800)
	Sb	550	NR	NR	NR
Yates 1250 2.00x10⁹	As	1450	4 (110)	4 (9650)	1573 (13800)
	Se	600	NA	NA	NA
	Sb	300	NR	NR	NR

*Not Required by TRI

**Required by TRI but not available in published data

Data from www.epa.gov/tri/

Table 4-5 shows EPA TRI estimates as compared to the aquatic estimates from this study. Numbers in parenthesis indicate total release estimates. Numbers in italics indicate release estimates calculated from the Wansley / Yates escape efficiency estimate. These estimates may not be appropriate for Plants Bowen and Hammond.

partitioning of the model and the measured results. The model predicts that 100% of the Se in coal is lost from fired coal to the gas phase and lost via flue gas. Measurements show 75% of the Se is sorbed onto fly ash. Sandelin et al. (2000) attribute this discrepancy to the incomplete treatment of the thermodynamics for Se. This problem in the model for Se could be the source of the low TRI estimates for Se.

Another group of workers (Yan et al. 2001) have performed a similar experiment using a different model with a more extensive thermodynamic database (54 elements, 3200 species). The trace element partitioning results of their calculations agree with our results from Δ Flux calculations and escape efficiency estimates. They predict that As is partitioned almost exclusively onto fly ash while Se, and Sb are both sorbed onto fly ash and lost via stack gas. However, they do not quantify the exact Se and Sb partitioning. The larger thermodynamic database appears to make a difference in the models ability to correctly predict trace element fate during coal combustion.

However, we believe that it is not simply a matter of thermodynamics to predict trace element partitioning in CFPPs. The models used are equilibrium thermodynamic models. Within the confines of the boiler or the scrubber chambers an equilibrium model may be appropriate. As gases and ash move from one part of the plant to another they experience drastic changes in temperature, pressure, and gas and particulate phase chemistry. The temperature in the boiler is approximately 1200 K while the temperature in the particulate scrubber is only 300 K. The process occurring as the temperature drops 900 K are not thermodynamic equilibrium processes, they are kinetic processes. In order to have a complete understanding of the processes governing trace element partitioning

during coal combustion detailed kinetic models and studies must be undertaken along with thermodynamic treatments.

CHAPTER 5

THE PLANT BOWEN ASH SPILL

On July 28, 2002 a 4 acre sink hole collapsed under the 250 acre ash pond at Plant Bowen. Over a 3 day period 2.2 million gallons of ash pond effluent and 1.87 million pounds of ash was discharged from this sinkhole to Euharlee Creek a tributary of the Etowah River above Rome GA's drinking water intake. I performed sampling transects on the 31st of July and the 1st of August to establish the fluxes of metalloids downstream, and to quantify the release of metalloids to the environment. The sampling transects for these days were slightly different than normally taken on the Etowah River. The sample sites and locations are described below.

Sample 1: Etowah River. Sample site is located below Allatoona Dam 0 km from the spillway.

Sample 2: Etowah above Euharlee Creek. Located off Euharlee road at a public fishing bank, 15 km from spillway.

Sample 3: Euharlee Creek. Sample taken at the Historic Covered Bridge in Euharlee, GA. Euharlee Creek enters the Etowah 24 km below the Allatoona spillway

Sample 4: Etowah River below Euharlee Creek. Sample collected 1 km downstream of Euharlee creek. Site is located 25 km from the spillway

Sample 5: Etowah River at Hardin Bridge. Sample collected below the one lane bridge on Hardin Bridge Road. Site is located 30 km from the Allatoona spillway

Sample 6: Etowah River at GA Hwy. 20 / 411. Sample is collected under the bridge over the river. Site is located 50 km from the Allatoona Spillway

Sample 7: Etowah River in Rome. Sample site is located in downtown Rome, GA just upstream of the Oostanuala entry to the Etowah. Site is located 83 km from the Allatoona spillway.

Table 5-1 Above Euharlee Creek Metalloid Concentrations

Above Euharlee				
Date	Sample	As (µg/L)	Se (µg/L)	Sb (µg/L)
07/31/2002	1	0.184	0.880	0.038
	2	0.347	0.916	0.142
08/01/2002	1	0.236	0.891	0.036
	2	0.288	0.854	0.250

Average	0.26	0.89	0.12
Std. Dev (±)	0.07	0.03	0.102
RSD (%)	26.56	2.92	87.55

Table 5-1 Analytical data for the metalloid concentrations above Euharlee Creek 7-31-01 and 8-01-02. The numbers below the chart are the average values, standard deviations and relative standard deviations for the metalloid concentrations.

Table 5-2 Below Euharlee Creek Metalloid Concentrations

Below Euharlee				
Date	Sample	As (µg/L)	Se (µg/L)	Sb (µg/L)
07/31/2002	4	1.188	1.300	0.362
	5	1.460	2.594	1.300
08/01/2002	4	0.564	1.358	0.484
	5	0.677	1.484	0.552
	6	0.424	1.105	0.251
	7	1.193	1.546	0.566

Average	0.92	1.57	0.57
Std. Dev (±)	0.42	0.53	0.37
RSD (%)	45.41	33.72	63.13

Table 5-1 Analytical data for the metalloid concentrations below Euharlee Creek 7-31-01 and 8-01-02. The number below the chart are the average values, standard deviations and relative standard deviations for the metalloid concentrations.

Figures 5-1a and 5-1b Etowah River Concentration Profiles

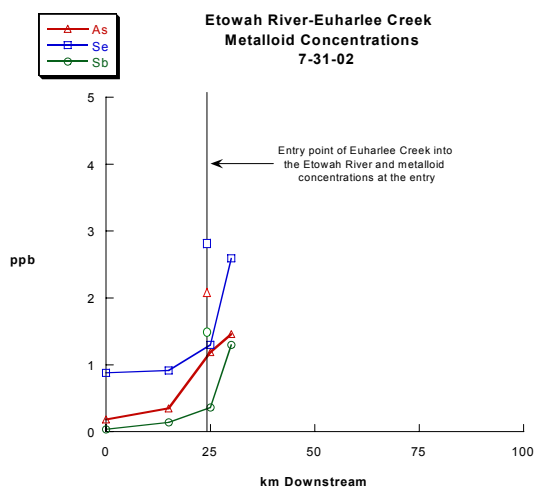


Figure 5-1a shows the metalloid concentrations for the Etowah River and Euharlee Creek on 7-31-02. The vertical line represents the inlet of Euharlee Creek to the Etowah. Metalloid concentration in ppb ($\mu\text{g/L}$) is on the y-axis. Km downstream in on the x-axis.

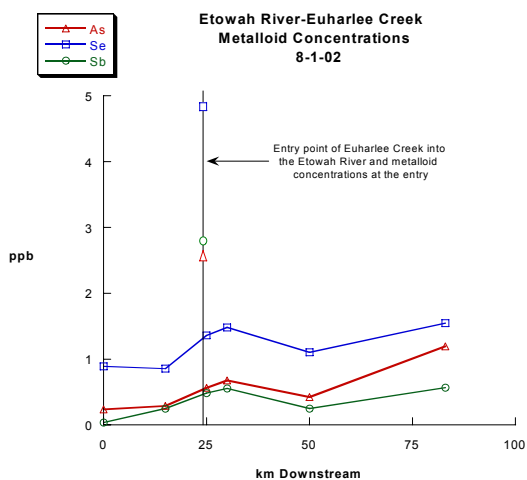


Figure 5-1b shows the metalloid concentrations for the Etowah River and Euharlee Creek on 8-1-02. The vertical line represents the inlet of Euharlee Creek the to Etowah. Metalloid concentration in ppb ($\mu\text{g/L}$) is on the y-axis. Km downstream in on the x-axis.

Table 5-1 shows the analytical data for the Etowah River upstream of Euharlee Creek. Table 5-2 shows the analytical data for the Etowah River downstream of Euharlee Creek. cursory examination of the data shows that the average metalloid concentrations below Euharlee creek are approximately two fold higher than above Euharlee Creek. Figures 5-1a and 5-1b are metalloid profiles of the Etowah. The vertical lines show the input concentration of Euharlee Creek. On both days the metalloid levels in Euharlee Creek are well above those in the upstream Etowah. The peaks in metalloid concentration downstream of the Euharlee inlet are clear evidence of the release of ash pond effluent to the river.

Using the average mean daily flow of 36,860 L/s for 7-31 and 8-1 and the stream concentration data we can calculate riverine metalloid fluxes and their upper and lower bounds. These data are shown in Tables 5-3a and 5-3b. The flux of metalloids is higher downstream of Euharlee Creek. Figure 5-4 shows the Δ Flux across Euharlee Creek. The centric values for As, Se, and Sb are 24 mg / s, 25 mg / s, and 17 mg / s respectively. This amounts to a total release of 6.3 kg As, 6.5 kg Se and 4.5 kg Sb over the three days of the spill.

Tables 5-3a and 5-3b Euharlee Creek Metalloid Fluxes

Above Euharlee Fluxes (mg/s)			
	As	Se	Sb
Centric	9.73	32.67	4.23
Upper Bound	12.32	33.62	8.04
Lower Bound	7.15	31.71	0.53

Table 5-3a

Below Euharlee Fluxes (mg/s)			
	As	Se	Sb
Centric	33.87	57.73	21.62
Upper Bound	49.24	77.20	35.26
Lower Bound	18.49	38.26	7.97

Table 5-3b

Tables 5-3a and 5-3b show the flux data for above and below Euharlee Creek in mg / s. Upper and lower bounds are the statistical high and low estimates for the fluxes. The centric is the median value.

Table 5-4 Etowah Δ Flux

Delta Fluxes (mg/s)			
	As	Se	Sb
Centric	24.13	25.06	17.33
Upper Bound	42.09	45.49	34.73
Lower Bound	6.17	4.64	0.00

Table 5-4 shows the upper, lower, and centric estimates for the Δ Flux across Euharlee creek in mg / s.

CHAPTER 6

CONCLUSIONS

This study has established and quantified the flux of the toxic metalloids arsenic, selenium, and antimony from coal fired power plant ash ponds to local receiving waters. Calculation of metalloid escape efficiencies have show that 4.1 tons of arsenic, 1.7 tons of selenium, and 0.9 tons of antimony were released to the environment in the dissolved reactive form during the year of this study. Detailed mass balance models of metalloid fate in the riverine environment were developed. These models revealed that there is also a metalloid flux from ash ponds in the form of solid ash material. These fluxes are 10.1 tons of As, 1.4 tons of Se, and 0.1 tons of Sb released on ash material during the year of this study. Over the course of 20 years the combined dissolved and solid releases have amounted to 284 tons of As, 62 tons of Se, and 20 tons of Sb. Mass balance has shown that the primary sink of metalloids in contaminated rivers is biological uptake. Over the year of this study 8.7 tons, 1. tons, and 0.5 tons of As, Se, and Sb entered the biological system respectively. Concern has also been raised regarding the settling of metalloid laden sediment in the upper reaches of West Point reservoir.

These fluxes have been compared to the EPA Toxic Release Inventory (TRI) estimates. Comparison of escape efficiency estimates to TRI estimates has shown that TRI estimates typically underestimate metalloid release by a factor of two.

Comparison of recent data to historic data at a CFPP that has converted to a dry ash disposal system has shown the cessation of metalloid input to local surface waters. These facts combined with studies at other CFPPs that have converted to dry ash disposal have shown this method to be an effective means of stopping the contamination of surface water with metalloid elements.

While this study has quantified metalloid release from CFPPs to the Chattahoochee River, it has only touched on the downstream fates of metalloids. Detailed metalloid speciation studies downstream of the power plants would allow a more comprehensive estimate of metalloid spiraling through the biological system. Seasonal water column studies in West Point Reservoir need to be undertaken in order to assess the impact of the settling of metalloid laden sediments from CFPPs on the ecology of the reservoir and the quality of the drinking water taken from the reservoir.

APPENDIX I

These tables contain the analytical data gathered during this study. Each table represents a sampling sequence (one day or contiguous dates). In all tables the row labeled “km downstream” indicates how far downstream from the origin the sample was taken. “Time” denotes the time of day the sample was taken. In the case of the Etowah River, the origin is the outlet from Allatoona Dam below Allatoona Reservoir. For the Chattahoochee River the origin is Buford Dam below Lanier Reservoir. Specific Site location and driving directions are found in Appendix 3. In all tables “nd” denotes “not determined”.

TDC: Total dissolved concentration in ppb ($\mu\text{g/L}$) of As, Se, Sb, and Ge at each sampling location.

As, Se, Sb, Ge: Concentration of dissolved metalloids for each sampling location in $\mu\text{g/L}$

Nuts: Nutrient concentrations at each sampling location in $\mu\text{mol/L}$

PO₄: Dissolved reactive phosphate

NH₄: Ammonia

NO₂: Nitrite

NO₂+NO₃: Nitrite plus nitrate

Si: Dissolved silica

Solids: Suspended solids and metalloid concentrations of the solids at each sample location.

Sus. Solid: Suspended solid concentration in each river sample in mg/L

As, Se, Sb, Ge: Concentration of acid extractable metalloids in the suspended solid in $\mu\text{g/g}$

WQ: Water quality parameters for each sampling location

pH: $\text{pH} (-\log \{H^+\})$

DO (%): Percent oxygen saturation at insitu temperature

O₂ (μM): Concentration of dissolved oxygen in $\mu\text{mol/L}$

Cond: Conductivity in $\mu\text{S/cm}$

Chlor: Concentration of chlorophyll in $\mu\text{g/L}$

Turb: Turbidity of the water in normalized turbidity units (NTU)

T: Temperature of the water in degrees Celsius.

Please see Tables 1 and 2 for location of relevant sites at kilometers downstream

Table 1

Chattahoochee River	
Km downstream	Power plant
20	Yates Wansley
96	
105	
112	
129	
172	

Table 2

Etowah River	
Km downstream	Power plant
0	Bowen
11	
25	
83	
113	Hammond

5-21-2001, Monday Etowah River

	R-Number		R-1017	R-1019	R-1020	R-1021
	km downstream	0	11	25	83	113
Time			11:00 AM	12:45 PM	2:15 PM	2:50 PM
TDC (µg/L)	As	nd	0.79	0.16	0.24	0.54
	Se	nd	1.93	0.07	0.07	0.07
	Sb	nd	1.26	0.05	0.23	0.18
	Ge	nd	0.10	0.08	nd	nd
Nuts (µM)	PO₄	nd	nd	nd	nd	nd
	NH₄	nd	nd	nd	nd	nd
	NO₂	nd	nd	nd	nd	nd
	NO₂+NO₃	nd	nd	nd	nd	nd
	Si	nd	nd	nd	nd	nd
Sus. Solids (mg/kg)	Sus. Solid (mg/l)	nd	nd	nd	nd	nd
	As	nd	nd	nd	nd	nd
	Se	nd	nd	nd	nd	nd
	Sb	nd	nd	nd	nd	nd
	Ge	nd	nd	nd	nd	nd
WQ	pH	nd	nd	nd	nd	nd
	DO (%)	nd	nd	nd	nd	nd
	O₂ (uM)	nd	nd	nd	nd	nd
	Cond	nd	nd	nd	nd	nd
	Chlor	nd	nd	nd	nd	nd
	Turb	nd	nd	nd	nd	nd
	T	nd	nd	nd	nd	nd

5-22-2001, Tuesday Chattahoochee River

	R-Number		R-1027	R-1026	R-1025	R-1024	R-1023
	km downstream	20	96	105	112	129	172
Time			5:00 PM	4:15 PM	3:10 PM	2:15 PM	12:45 PM
TDC (µg/L)	As	nd	0.24	0.43	1.37	0.35	0.28
	Se	nd	0.95	1.10	1.40	0.96	1.02
	Sb	nd	0.22	0.32	0.61	0.35	3.99
	Ge	nd	0.70	1.22	2.31	0.95	nd
Nuts (µM)	PO₄	nd	nd	nd	nd	nd	nd
	NH₄	nd	nd	nd	nd	nd	nd
	NO₂	nd	nd	nd	nd	nd	nd
	NO₂+NO₃	nd	nd	nd	nd	nd	nd
	Si	nd	nd	nd	nd	nd	nd
Sus. Solids (mg/kg)	Sus. Solid (mg/l)	nd	nd	nd	nd	nd	nd
	As	nd	nd	nd	nd	nd	nd
	Se	nd	nd	nd	nd	nd	nd
	Sb	nd	nd	nd	nd	nd	nd
	Ge	nd	nd	nd	nd	nd	nd
WQ	pH	nd	nd	nd	nd	nd	nd
	DO (%)	nd	nd	nd	nd	nd	nd
	O₂ (uM)	nd	nd	nd	nd	nd	nd
	Cond	nd	nd	nd	nd	nd	nd
	Chlor	nd	nd	nd	nd	nd	nd
	Turb	nd	nd	nd	nd	nd	nd
	T	nd	nd	nd	nd	nd	nd

8-2-2001, Thursday Etowah River

	R-Number	R-1040	R-1039	R-1038	R-1036	R-1034
	km downstream	0	11	25	83	113
Time		12:50 PM	11:40 AM	10:55 AM	9:40 AM	8:00 AM
TDC (µg/L)	As	0.18	0.62	0.24	0.21	0.36
	Se	0.40	1.71	0.55	0.06	0.08
	Sb	0.04	0.99	0.10	0.06	0.41
	Ge	nd	0.10	0.44	nd	nd
Nuts (µM)	PO₄	nd	nd	nd	nd	nd
	NH₄	nd	nd	nd	nd	nd
	NO₂	nd	nd	nd	nd	nd
	NO₂+NO₃	nd	nd	nd	nd	nd
	Si	nd	nd	nd	nd	nd
Sus. Solids (mg/kg)	Sus. Solid (mg/l)	nd	nd	nd	nd	nd
	As	nd	nd	nd	nd	nd
	Se	nd	nd	nd	nd	nd
	Sb	nd	nd	nd	nd	nd
	Ge	nd	nd	nd	nd	nd
WQ	pH	nd	nd	nd	nd	nd
	DO (%)	nd	nd	nd	nd	nd
	O₂ (uM)	nd	nd	nd	nd	nd
	Cond	nd	nd	nd	nd	nd
	Chlor	nd	nd	nd	nd	nd
	Turb	nd	nd	nd	nd	nd
	T	nd	nd	nd	nd	nd

8-6-2001, Monday Chattahoochee River

	R-Number		R-1045	R-1044	R-1043	R-1042	R-1041
	km downstream	20	96	105	112	129	172
Time			12:05 PM	11:40 AM	10:45 AM	9:40 AM	8:20 AM
TDC (µg/L)	As	nd	0.28	0.71	1.89	0.60	0.82
	Se	nd	0.25	0.66	1.25	0.74	0.40
	Sb	nd	0.27	0.38	0.68	0.43	0.17
	Ge	nd	0.80	1.01	3.02	1.41	nd
Nuts (µM)	PO₄	nd	nd	nd	nd	nd	nd
	NH₄	nd	nd	nd	nd	nd	nd
	NO₂	nd	nd	nd	nd	nd	nd
	NO₂+NO₃	nd	nd	nd	nd	nd	nd
	Si	nd	nd	nd	nd	nd	nd
Sus. Solids (mg/kg)	Sus. Solid (mg/l)	nd	nd	nd	nd	nd	nd
	As	nd	nd	nd	nd	nd	nd
	Se	nd	nd	nd	nd	nd	nd
	Sb	nd	nd	nd	nd	nd	nd
	Ge	nd	nd	nd	nd	nd	nd
WQ	pH	nd	nd	nd	nd	nd	nd
	DO (%)	nd	nd	nd	nd	nd	nd
	O₂ (uM)	nd	nd	nd	nd	nd	nd
	Cond	nd	nd	nd	nd	nd	nd
	Chlor	nd	nd	nd	nd	nd	nd
	Turb	nd	nd	nd	nd	nd	nd
	T	nd	nd	nd	nd	nd	nd

9-15-2001, Saturday Chattahoochee River

	R-Number	R-1051	R-1050	R-1049	R-1048	R-1047	R-1046
	km downstream	20	96	105	112	129	172
Time		2:30 PM	12:05 PM	11:30 AM	10:45 AM	10:00 AM	8:30 AM
TDC (µg/L)	As	0.07	0.25	0.50	5.60	1.12	0.37
	Se	0.15	0.63	1.21	3.01	1.09	0.39
	Sb	0.02	0.22	0.45	1.41	0.53	0.19
	Ge	0.02	0.28	0.85	1.87	0.87	nd
Nuts (µM)	PO₄	nd	nd	nd	nd	nd	nd
	NH₄	nd	nd	nd	nd	nd	nd
	NO₂	nd	nd	nd	nd	nd	nd
	NO₂+NO₃	nd	nd	nd	nd	nd	nd
	Si	nd	nd	nd	nd	nd	nd
Sus. Solids (mg/kg)	Sus. Solid (mg/l)	nd	nd	nd	nd	nd	nd
	As	nd	nd	nd	nd	nd	nd
	Se	nd	nd	nd	nd	nd	nd
	Sb	nd	nd	nd	nd	nd	nd
	Ge	nd	nd	nd	nd	nd	nd
WQ	pH	nd	nd	nd	nd	nd	nd
	DO (%)	nd	nd	nd	nd	nd	nd
	O₂ (uM)	nd	nd	nd	nd	nd	nd
	Cond	nd	nd	nd	nd	nd	nd
	Chlor	nd	nd	nd	nd	nd	nd
	Turb	nd	nd	nd	nd	nd	nd
	T	nd	nd	nd	nd	nd	nd

11-9-2001, Friday Chattahoochee River

	R-Number	R-1057	R-1056	R-1055	R-1054	R-1053	R-1052
	km downstream	20	96	105	112	129	172
Time		5:00 PM	1:45 PM	12:55 PM	11:25 AM	10:00 AM	8:10 AM
TDC (µg/L)	As	0.07	0.24	0.46	3.72	0.63	0.27
	Se	0.17	0.34	1.09	2.02	1.07	0.44
	Sb	0.02	0.21	0.42	1.11	0.47	0.24
	Ge	0.01	0.25	0.76	1.16	0.53	
Nuts (µM)	PO₄	nd	1.15	1.10	0.90	0.55	0.45
	NH₄	nd	nd	nd	nd	nd	nd
	NO₂	nd	1.65	0.87	0.98	0.78	0.67
	NO₂+NO₃	nd	nd	nd	nd	nd	nd
	Si	99.05	119.41	116.48	107.50	75.93	127.00
Sus. Solids (mg/kg)	Sus. Solid (mg/l)	5.75	6.50	5.25	2.75	13.75	3.25
	As	19.10	23.20	387.37	502.89	9.79	374.24
	Se	0.00	11.25	72.48	8.77	0.00	1.10
	Sb	9.77	6.88	2.49	13.75	0.99	10.64
	Ge	nd	nd	nd	nd	nd	Nd
WQ	pH	7.07	6.89	6.92	6.95	6.90	6.70
	DO (%)	0.97	0.91	0.99	0.96	0.90	0.65
	O₂ (uM)	296	272	290	281	275	190
	Cond	511	221	227	207	194	135
	Chlor	nd	nd	nd	nd	nd	Nd
	Turb	nd	nd	nd	nd	nd	nd
	T	15.30	16.00	16.90	16.90	15.20	16.60

12-18-2001, Monday Chattahoochee River

	R-Number	R-1063	R-1062	R-1061	R-1060	R-1059	R-1058
	km downstream	20	96	105	112	129	172
Time		4:30 PM	1:15 PM	12:10 PM	10:45 AM	9:35 AM	7:15 AM
TDC (µg/L)	As	0.10	0.21	0.28	1.73	0.74	0.23
	Se	0.13	0.24	0.42	0.98	0.63	0.32
	Sb	0.05	0.16	0.21	0.52	0.35	0.56
	Ge	0.02	0.35	0.46	0.88	0.68	nd
Nuts (µM)	PO₄	0.23	1.19	1.14	0.91	0.68	0.46
	NH₄	4.29	6.01	3.42	0.49	2.75	0.28
	NO₂	0.72	2.39	2.43	1.55	1.15	0.80
	NO₂+NO₃	22.8	207.2	182.2	160.7	134.7	61.9
	Si	113	157	158	153	154	152
Sus. Solids (mg/kg)	Sus. Solid (mg/l)	28.25	53.25	130.00	30.50	29.25	18.00
	As	5.95	3.99	6.51	39.38	20.88	3.03
	Se	2.74	1.76	1.61	2.12	0.29	0.00
	Sb	0.00	0.27	0.95	0.67	4.00	0.09
	Ge	nd	nd	nd	nd	nd	nd
WQ	pH	7.52	7.35	1.37	7.47	7.45	7.28
	DO (%)	84	82	82	86	86	70
	O₂ (uM)	270	250	250	259	259	210
	Cond	0.06	0.18	0.17	0.17	0.15	0.13
	Chlor	3.53	4.42	5.32	-0.23	3.59	2.62
	Turb	100	77	149	52	228	18
	T	12.13	15.33	15.36	15.29	14.65	14.79

3-6-2002, Wednesday Chattahoochee River

	R-Number	R-1070	R-1069	R-1068	R-1067	R-1066	R-1065
	km downstream	20	96	105	112	129	172
Time		4:20 PM	2:10 PM	1:00PM	11:20 AM	10:00AM	8:10AM
TDC (µg/L)	As	0.30	0.22	0.31	0.40	0.27	0.25
	Se	0.03	0.22	0.71	0.64	0.49	0.34
	Sb	0.19	0.12	0.20	0.24	0.18	0.19
	Ge	nd	nd	nd	nd	nd	nd
Nuts (µM)	PO₄	0.13	0.27	0.31	0.31	0.31	0.12
	NH₄	nd	nd	nd	nd	nd	nd
	NO₂	0.18	1.30	0.93	0.38	0.32	0.59
	NO₂+NO₃	22.3	102.0	103.4	87.8	73.7	75.4
	Si	129	141	154	152	159	94
Sus. Solids (mg/kg)	Sus. Solid (mg/l)	2.75	20.50	16.00	66.00	30.25	8.75
	As	6.19	4.29	21.85	5.24	6.47	2.50
	Se	65.60	16.64	19.07	3.01	1.82	14.27
	Sb	0.00	0.00	0.00	0.04	0.00	0.00
	Ge	nd	nd	nd	nd	nd	nd
WQ	pH	nd	nd	nd	nd	nd	nd
	DO (%)	nd	nd	nd	nd	nd	nd
	O₂ (uM)	nd	nd	nd	nd	nd	nd
	Cond	nd	nd	nd	nd	nd	nd
	Chlor	nd	nd	nd	nd	nd	nd
	Turb	nd	nd	nd	nd	nd	nd
	T	nd	nd	nd	nd	nd	nd

5-6-2002, Monday Chattahoochee River

	R-Number	R-1084	R-1083	R-1082	R-1081	R-1080	R-1079
	km downstream	20	96	105	112	129	172
Time		4:15 PM	2:15 PM	12:45 PM	11:45 AM	10:30 AM	9:00 AM
TDC (µg/L)	As	0.145	0.320	0.406	0.937	0.628	0.254
	Se	0.183	0.242	0.450	0.560	0.482	0.358
	Sb	0.035	0.132	0.226	0.325	0.272	0.175
	Ge	nd	nd	nd	nd	nd	Nd
Nuts (µM)	PO₄	0.09	0.57	0.52	0.52	0.57	0.38
	NH₄	2.55	5.94	6.11	4.38	4.44	4.77
	NO₂	0.33	1.29	1.95	0.65	0.52	0.43
	NO₂+NO₃	24.8	100.3	98.3	74.4	62.1	61.9
	Si	104	168	164	160	147	164
Sus. Solids (mg/kg)	Sus. Solid (mg/l)	17.50	37.75	32.75	50.50	23.25	2.75
	As	4.77	5.28	14.44	19.94	21.61	3.38
	Se	8.76	9.23	9.10	8.19	19.39	13.58
	Sb	0.00	0.00	0.28	0.16	0.52	0.00
	Ge	nd	nd	nd	nd	nd	Nd
WQ	pH	nd	nd	nd	nd	nd	Nd
	DO (%)	nd	nd	nd	nd	nd	Nd
	O₂ (uM)	nd	nd	nd	nd	nd	nd
	Cond	nd	nd	nd	nd	nd	nd
	Chlor	nd	nd	nd	nd	nd	nd
	Turb	nd	nd	nd	nd	nd	nd
	T	nd	nd	nd	nd	nd	nd

6-5-2002, Wednesday Chattahoochee River

	R-Number	R-1093	R-1092	R-1090	R-1089	R-1088	R-1087	R-1086	R-1085
	km downstream	0	20	50	96	105	112	129	172
Time		7:30 PM	5:45 PM	2:10 PM	1:00 PM	11:30 AM	10:20 AM	9:20 AM	7:30 AM
TDC (µg/L)	As	0.162	0.157	0.641	0.525	2.873	5.671	1.742	0.302
	Se	0.094	0.142	0.427	0.320	1.029	1.990	0.967	0.261
	Sb	0.029	0.048	0.542	0.260	0.494	1.071	0.574	0.404
	Ge	nd	nd	nd	nd	nd	nd	nd	nd
Nuts (µM)	PO₄	0	0.00	0.30	0.75	0.89	0.45	0.21	0.11
	NH₄	0.52	0.61	7.86	4.08	1.41	1.55	2.97	6.27
	NO₂	0.077	0.18	1.60	3.10	3.14	1.31	0.78	0.99
	NO₂+NO₃	nd	nd	nd	nd	nd	nd	nd	nd
	Si	64	79	113	122	116	107	89.00	133
Sus. Solids (mg /kg)	Sus. Solid (mg / L)	1.00	0.00	29.25	95.25	5.25	10.75	24.50	9.75
	As	2.85	0.00	6.94	2.00	44.33	73.45	17.88	2.10
	Se	139.21	0.00	18.73	2.30	24.83	24.73	2.48	5.40
	Sb	39.76	0.00	3.18	0.06	0.03	0.51	0.00	0.00
	Ge	nd	nd	nd	nd	nd	nd	nd	nd
WQ	pH	nd	nd	nd	nd	nd	nd	nd	nd
	DO (%)	nd	nd	nd	nd	nd	nd	nd	nd
	O₂ (uM)	nd	nd	nd	nd	nd	nd	nd	nd
	Cond	nd	nd	nd	nd	nd	nd	nd	nd
	Chlor	nd	nd	nd	nd	nd	nd	nd	nd
	Turb	nd	nd	nd	nd	nd	nd	nd	nd
	T	nd	nd	nd	nd	nd	nd	nd	nd

APPENDIX II

This appendix contains flux calculations based on my analytical data and river flow data from the United States Geological Survey National Water Information System program. Each table represents a sampling sequence (one day or contiguous dates). Column headers are the same as Appendix I

Flow Data: River flow data collected from the USGS NWIS web site.

(<http://www.water.usgs.gov/usa/nwis/sw>)

USGS Gaging Station: The eight-digit number used to identify the gaging stations utilized in this study. In some cases the USGS no longer maintains gaging stations at or near the sampling sites and flow must be estimated using historical data. These sites are denoted with “estimate”* in the data cell.

Flow (CFS): River flow in cubic-feet per second (ft³/s) directly from the USGS. Data obtained directly (not estimated) from the NWIS site is the 24-hour average of the flow on date the sample was taken.

Flow (L/s): River flow Converted from CFS to L/s
 $\text{Ft}^3/\text{s} \times 28.357 \text{ L}/\text{ft}^3 = \text{L}/\text{s}$

Riverine Flux: The flux of metalloids in the river in mg/s.

$\mu\text{g}/\text{L}$ (concentration) $\times 10^{-3} \text{ mg}/\mu\text{g} \times \text{L}/\text{s}$ (flow) = mg/s (flux)

As, Se, Sb, Ge: The flux of a particular metalloid element in the river at the sampling location (mg/s).

Δ Flux: The difference in upstream and downstream river flux calculated between sampling locations in mg/s . Calculated by subtracting the upstream flux from the downstream flux. A negative Δ flux indicates a net loss of metalloids from the river between the two locations. A positive flux indicates net input of metalloids into the river.

As, Se, Sb, Ge: The Δ flux of each metalloid element in the river between sampling locations (mg/s).

TRI Estimate: The metalloid flux estimate released by coal fired power plants in their Toxic Release Inventory (http://www.epa.gov/enviro/html/tris/tris_query.html) “NA” indicates an inventory of the element is required by the EPA but is not available in the TRI estimate. “NR” indicates that an inventory of the element is not required based on the peak mega-wattage rating of the power plant.

As, Se, Sb, Ge: The TRI estimate of the power plant aquatic emission of metalloid elements in mg/s.

$\text{Lbs}/\text{year} \times 1 \text{ kg}/2.2 \text{ lbs} \times 10^6 \text{ mg}/\text{kg} \times 1\text{year}/3.15 \times 10^7 \text{ s} = \text{mg}/\text{s}$

* Estimated flows were determined by comparing historical flow data with recent flow data. The USGS publishes the historical data for stations that are inactive as well as those online now. Flows at inactive sites are estimated by comparing the difference between the flows for the day of the year the sample was taken, averaged over the entire history of the station, at an active station and the inactive station. The percent difference between the flows in historical data is scaled to the flow at an active station of the data the sample was taken.

Average flow for Station 1 (active) on June 15th (life of station) = 1000CFS
Average flow for Station 2 (inactive) on June 15th (life of station) = 500CFS

Difference = -50%

Daily average flow for Station 1 June 15th 2001 = 1500 CFS
Estimated flow for Station 2 June 15th 2001 = 1500 CFS x -0.5 = 750 CFS

5-21-2001, Monday Etowah River

	R-Number km downstream	0	R-1017 11	R-1019 25	R-1020 83	R-1021 113	
Flow Data	USGS Gaging Station Flow (CFS) Flow (L/s)	nd nd nd	Estimate 1356 38398	Estimate 1549 43863	Estimate 1587 44939	2397000 3430 97127	
Riverine Flux (mg/s)	As Se Sb Ge	nd nd nd nd	30 74 48 4	7 3 2 3	11 3 11 nd	52 7 18 nd	
Δ Flux (mg/s)	As Se Sb Ge	nd nd nd nd	nd nd nd nd	-24 -71 -46 0	4 0 8 nd	42 4 7 nd	nd nd nd nd
Power Plants				Bowen		Hammond	
TRI Estimate (mg/s)	As Se Sb Ge			0 0 NR NR		NA NR NR NR	

5-22-2001, Tuesday Chattahoochee River

	R-Number km downstream	20	R-1027 96	R-1026 105	R-1025 112	R-1024 129	R-1023 172	
Flow Data	USGS Gaging Station	nd	2338000	2338000	2338000	2338000	2339500	
	Flow (CFS)	nd	1850	1850	1850	1850	4230	
	Flow (L/s)	nd	52386	52386	52386	52386	119781	
Riverine Flux (mg/s)	As	nd	13	22	72	18	34	
	Se	nd	50	58	73	50	122	
	Sb	nd	12	17	32	19	478	
	Ge	nd	37	64	121	50	nd	
Δ Flux (mg/s)	As	nd	nd	10	49	-54	16	nd
	Se	nd	nd	8	15	-23	72	nd
	Sb	nd	nd	5	15	-13	460	nd
	Ge	nd	nd	27	57	-71	nd	nd
Power Plants				Yates	Wansley			
TRI Estimate (mg/s)	As			0.057	0			
	Se			NA	6.5			
	Sb			NR	NR			
	Ge			NR	NR			

8-2-2001 Thursday Etowah River

	R-Number km downstream	R-1040 0		R-1039 11	R-1038 25	R-1036 83	R-1034 113	
Flow Data	USGS Gaging Station	2494000		Estimate	Estimate	Estimate	2397000	
	Flow (CFS)	2250		2422	2767	2970	5910	
	Flow (L/s)	63713		68584	78353	84101	167353	
Riverine Flux (mg/s)	As	11		43	17	18	60	
	Se	26		117	40	5	13	
	Sb	2		68	7	5	68	
	Ge	nd		7	34	nd	nd	
Δ Flux (mg/s)	As	nd	31	-25	0	43	nd	
	Se	nd	92	-77	-36	9	nd	
	Sb	nd	65	-60	-3	63	nd	
	Ge	nd	nd	27	nd	nd	nd	
Power Plants				Bowen		Hammond		
TRI Estimate (mg/s)	As			0		NA		
	Se			0		NR		
	Sb			NR		NR		
	Ge			NR		NR		

8-6-2001, Monday Chattahoochee River

	R-Number km downstream	20	R-1045 96	R-1044 105	R-1043 112	R-1042 129	R-1041 172	
Flow Data	USGS Gaging Station	nd	2338000	23380000	2338000	2338000	2339500	
	Flow (CFS)	nd	2020	2020	2020	2020	3620	
	Flow (L/s)	nd	57200	57200	57200	57200	102508	
Riverine Flux (mg/s)	As	nd	16	40	108	34	84	
	Se	nd	15	38	71	43	41	
	Sb	nd	16	22	39	25	17	
	Ge	nd	46	58	173	80	nd	
Δ Flux (mg/s)	As	nd	nd	24	68	-74	50	nd
	Se	nd	nd	23	34	-29	-2	nd
	Sb	nd	nd	6	17	-14	-7	nd
	Ge	nd	nd	12	115	-93	nd	nd
Power Plants				Yates	Wansley			
TRI Estimate (mg/s)	As			0.057	0			
	Se			NA	6.5			
	Sb			NR	NR			
	Ge			NR	NR			

9-15-2001, Saturday Chattahoochee River

	R-Number km downstream	R-1051 20	R-1050 96	R-1049 105	R-1048 112	R-1047 129	R-1046 172	
Flow Data	USGS Gaging Station	2335000	2338000	2338000	2338000	2338000	2339500	
	Flow (CFS)	1290	2170	1270	1270	1270	741	
	Flow (L/s)	36529	61448	35963	35963	35963	20983	
Riverine Flux (mg/s)	As	3	9	18	201	40	8	
	Se	5	23	43	108	39	8	
	Sb	1	8	16	51	19	4	
	Ge	1	17	30	67	31	nd	
Δ Flux (mg/s)	As	nd	6	9	183	-161	-33	nd
	Se	nd	17	21	65	-69	-31	nd
	Sb	nd	7	8	35	-32	-15	nd
	Ge	nd	17	13	37	-36	nd	nd
Power Plants				Yates	Wansley			
TRI Estimate (mg/s)	As			0.057	0			
	Se			NA	6.5			
	Sb			NR	NR			
	Ge			NR	NR			

11-9-2001, Friday Chattahoochee River

	R-Number	R-1057 20	R-1056 96	R-1055 105	R-1054 112	R-1053 129	R-1052 172	
	km downstream							
Flow Data	USGS Gaging Station	2335000	2338000	2338000	2338000	2338000	2339500	
	Flow (CFS)	977	1030	1030	1030	1030	2580	
	Flow (L/s)	27666	29167	29167	29167	29167	73058	
Riverine Flux (mg/s)	As	2	7	13	108	18	20	
	Se	5	10	32	59	31	32	
	Sb	1	6	12	32	14	18	
	Ge	1	10	13	26	20	nd	
Δ Flux (mg/s)	As	nd	5	6	95	-90	1	nd
	Se	nd	5	22	27	-28	1	nd
	Sb	nd	5	6	20	-19	4	nd
	Ge	nd	9	3	12	-6	nd	nd
Power Plants				Yates	Wansley			
TRI Estimate (mg/s)	As			0.057	0			
	Se			NA	6.5			
	Sb			NR	NR			
	Ge			NR	NR			

12-18-2001, Monday Chattahoochee River

	R-Number km downstream	R-1063 20		R-1062 96		R-1061 105		R-1060 112		R-1059 129		R-1058 172	
Flow Data	USGS Gaging Station	2335000		2338000		2338000		2338000		2338000		2339500	
	Flow (CFS)	880		3920		3870		3650		3350		1040	
	Flow (L/s)	24954		111159		109742		103503		94996		29491	
Riverine Flux (mg/s)	As	4		33		43		252		99		10	
	Se	3		27		46		101		60		9	
	Sb	1		18		23		54		33		17	
	Ge	1		38		50		91		65			
Δ Flux (mg/s)	As	nd	29	10		209		-153		-90		nd	
	Se	nd	24	19		56		-41		-51		nd	
	Sb	nd	16	6		31		-21		-17		nd	
	Ge	nd	38	11		41		-26		-65		nd	
Power Plants						Yates		Wansley					
TRI Estimate (mg/s)	As					0.057		0					
	Se					NA		6.5					
	Sb					NR		NR					
	Ge					NR		NR					

3-6-2002, Wednesday Chattahoochee River

	R-Number km downstream	R-1070 20		R-1069 96	R-1068 105	R-1067 112	R-1066 129	R-1065 172
Flow Data	USGS Gaging Station	2335000		2338000	2338000	2338000	2338000	2339500
	Flow (CFS)	696		2160	2180	2190	2170	8690
	Flow (L/s)	19736		61251	61818	62102	61535	246422
Riverine Flux (mg/s)	As	6		13	19	25	17	61
	Se	1		13	44	40	30	84
	Sb	4		7	12	15	11	47
	Ge	nd		nd	nd	nd	nd	nd
Δ Flux (mg/s)	As	nd	8	6	5	-8	44	nd
	Se	nd	13	30	-4	-10	53	nd
	Sb	nd	4	5	3	-4	36	nd
	Ge	nd	nd	nd	nd	nd	nd	nd
Power Plants				Yates	Wansley			
TRI Estimate (mg/s)	As			0.057	0			
	Se			NA	6.5			
	Sb			NR	NR			
	Ge			NR	NR			

5-6-2002, Monday Chattahoochee River

	R-Number km downstream	R-1084 20		R-1083 96	R-1082 105	R-1081 112	R-1080 129	R-1079 172
Flow Data	USGS Gaging Station	2335000		2338000	2338000	2338000	2338000	2339500
	Flow (CFS)	696		2120	2130	2160	2170	996
	Flow (L/s)	19945		60753	61039	61899	62186	28542
Riverine Flux (mg/s)	As	3		19	25	58	39	7
	Se	4		15	27	34	30	10
	Sb	1		8	14	20	17	5
	Ge	nd		nd	nd	nd	nd	nd
Δ Flux (mg/s)	As	nd	17	5	33	-19	-32	nd
	Se	nd	11	13	7	-5	-20	nd
	Sb	nd	7	6	6	-3	-12	nd
	Ge	nd	nd	nd	nd	nd	nd	nd
Power Plants				Yates	Wansley			
TRI Estimate (mg/s)	As			0.057	0			
	Se			NA	6.5			
	Sb			NR	NR			
	Ge			NR	NR			

6-5-2002, Wednesday Chattahoochee River

	R-Number km downstream	R-1093 0		R-1092 20	R-1090 50	R-1089 96	R-1088 105	R-1087 112	R-1086 129	R-1085 172
Flow Data	USGS Gaging Station			2335000	2338000	2338000	2338000	2338000	2338000	2339500
	Flow (CFS) Flow (L/s)	482 13668		670 18999	3610 102369	2920 82802	2610 74012	2280 64654	2020 57281	877 24869
Riverine Flux (mg/s)	As	2		3	66	43	213	367	100	8
	Se	1		3	44	27	76	129	55	15
	Sb	0		1	55	22	37	69	33	23
	Ge	Nd		nd	nd	nd	nd	nd	nd	nd
Δ Flux (mg/s)	As	nd	1	63	-22	169	154	-267	-92	nd
	Se	nd	1	41	-17	50	53	-73	-40	nd
	Sb	nd	1	55	-34	15	33	-36	-10	nd
	Ge	nd	nd	nd	nd	nd	nd	nd	nd	nd
Power Plants						Yates	Wansley			
TRI Estimate (mg/s)	As					0.057	0.00			
	Se					NA	6.70			
	Sb					NR	NR			
	Ge					NR	NR			

APPENDIX III

Appendix III contains specific driving direction to each sampling location. For both transects the directions start on Interstate 75-85 in downtown Atlanta and proceed to the first sample site of the sequence. Following directions are from one sample site to another.

Chattahoochee Transect (Figure 2-6)

Km marker 172 (West Point): Drive south on Interstate 75-85 and take the I-85 south split. Proceed south on I-85 to Exit 2 (GA 18). Take GA 18 west toward Alabama. Turn right immediately after the Chattahoochee River bridge into parking lot of the Interstate Telephone Company. Sample location is underneath the overpass. West Bank

Latitude-32° 52.670' N
Longitude- 85° 10.882' W
USGS gaging station- 02339500 (active)

Km marker 129 (Franklin): From the Interstate Telephone Company turn back onto GA 18 headed east. Turn left onto US 29 North toward La Grange. In La Grange turn onto US 27 North towards Franklin. In Franklin cross the bridge over the Chattahoochee River and make the first left after the bridge into the parking lot with the softball field. Sample from the boat dock near the bridge. West Bank

Latitude-33° 16.663' N
Longitude- 85° 06.114' W
USGS gaging station (inactive)

Km marker 112 (Below Wansley / Yates): Turn back onto US 27 N. Proceed north to Central Hatchee. App. 2 miles past Central Hatchee turn right at the large white sign for the concrete plant and Yellow Dirt Baptist Church. Follow this road past the four-way intersection, church and onto the dirt road. You will pass the entrance to Plant Wansley. The road ends in a boat ramp on the Chattahoochee River. Sample from this boat ramp. West Bank

Latitude-33° 23.674' N
Longitude- 85° 02.007' W

Km marker 105 (Between Wansley / Yates): Follow the dirt road back to the four-way intersection. At the intersection turn right. This road will lead back to US 27. Turn right onto US 27 headed north. At the intersection of GA 5 turn right (east). Proceed east until mile marker 22. Between mile marker 22 and 23 turn right into the McIntosh Reserve at McIntosh Road. Follow this road until it ends at the

information center. Turn right onto the dirt path and follow it a very short distance to the bottom of the hill. Walk along the riverbank back toward the information center and sample from the rocks jutting into the river. West Bank

Latitude-33° 26.403' N
Longitude- 84° 57.173' W

Km Marker 96 (Above Wansley / Yates) Proceed back to GA 5 and turn right (east). Head east to the intersection of GA 5 and US 27 Alt. Turn right onto US 27 Alt (south). After a short distance you will cross the bridge over the Chattahoochee. Make an immediate left after the bridge. Park in the parking lot and sample from the boat ramp. East Bank

Latitude-33° 28.563' N
Longitude- 84° 54.012' W
USGS gaging station- 02338000 (active)

Km marker 20 (Holcomb Bridge): Turn back onto US 27 Alt. Headed south. Follow signs back to I-85 N through Newnan, GA. In Newnan, get on I-85 N. Follow I-85 N back through Atlanta. Merge onto I-75-85. At the I-75-85 split, follow I-85 N. Proceed north to the Clairemont Road exit. Turn left onto Clairemont Road (north) and follow it until ends at Peachtree Industrial Drive. Turn right onto Peachtree Industrial and follow it to the exit at Jimmy Carter Blvd. After the exit turn left (north) onto Jimmy Carter Blvd. Follow this road north. It will turn into Holcomb Bridge Road. At the border of Gwinnett County Holcomb Bridge Road crosses the Chattahoochee River. Turn left immediately after the bridge into the front drive of the North Atlanta Raw Water Uptake. Park and sample from the stream-bank. This is the last sample site for the Chattahoochee Transect. East Bank

USGS Gaging Station- 02335000

Etowah River Transect (Figure 2-3)

Km marker 113 (Coosa outside Rome): Drive north on Interstate 75-85. Take the 75 N split. Drive app. 40 miles north to the GA 20 West (toward Rome) exit. Take this exit. Drive through Rome towards the Alabama border. Outside Rome turn left onto GA 100 S. Cross the bridge over the Coosa River and make an immediate right. There is a small path down to the river. Sample from this shore.

Latitude-34° 14.887' N
Longitude- 85° 21.320' W
USGS gaging station- 02397000 (active)

Oostanuala River in Rome: Turn left onto GA 100 N. Turn right onto GA 20 E. In Rome make a right immediately before crossing the bridge over the Oostanuala River. This leads into the parking lot of the Floyd County Library. Park in the lot and sample from the river bank.

Latitude-34° 15.542' N
Longitude- 85° 10.170' W

Km marker 83 (The Shrimp Boat): From the library get on GA 20 E. Turn right onto North Broad Street. Navigate to East 2nd Avenue. Turn right into the Shrimp Boat Restaurant. Sample underneath the overpass.

Latitude-34° 14.780' N
Longitude- 85° 10.091' W

Km Marker 25 (Etowah below Euharlee Creek): Navigate back to GA 20 E. Turn onto GA 20 headed east and proceed out of Rome. At the intersection of US 411 and GA 20, take US 411 east towards Cartersville. Turn right onto Harden Bridge Road. Follow this road app. 4 miles until it intersects Chulio Road. Follow Chulio Road until it crosses the Etowah River. Make an immediate right after the bridge. On this road make the first right. This leads into a small dirt parking area by the river bank. Sample from the shore.

Latitude-34° 08.859' N
Longitude- 84° 55.179' W

Covered Bridge over Euharlee Creek: Turn left onto Chulio Road. Drive west to the fork that leads towards the covered bridge. Follow this road to the covered bridge, which is on the right side of the road. Turn into the parking lot. Sample at the creek underneath the bridge.

Latitude-34° 08.573' N

Longitude- $84^{\circ} 55.934'$ W

Km Marker 11 (61-113): Turn left out of the covered bridge parking lot. Make and drive south. Make the first right you come to. Follow this road past Bowen power plant and through the plant grounds. Follow this road to GA 113 and turn left (east). Proceed east until GA 61 and GA 113 merge. Continue northeast. After crossing the bridge over the Etowah River make an immediate right into a dirt parking area underneath the bridge. Sample at the stream bank.

Latitude- $34^{\circ} 08.574'$ N

Longitude- $84^{\circ} 50.297'$ W

Km marker 0 (Allatoona Dam): Return to 61-113 headed northeast. Follow this road through Cartersville to US 41. Take US 41 South. After crossing the Etowah River, take a short spur road (GA 293) to the bank of the Etowah. Sample underneath the bridge.

Latitude- $34^{\circ} 09.198'$ N

Longitude- $84^{\circ} 46.310'$ W

USGS gaging station- 02494000 (active)

REFERENCES

- Anderson, L.C.D. and Bruland, K.W. (1991) Biogeochemistry of Arsenic in Natural Waters: The Importance of Methylated Species. *Environmental Science and Technology*, **25**, 420-427
- Andreae, M.O. (1978) Distribution and Speciation of Arsenic in Natural Waters and Some Marine Algae. *Deep Sea Research*, **25**, 391-402.
- Andreae, M.O. and Froelich, P.N. (1981) Determination of Germanium in Natural Water by Graphite Furnace Atomic Adsorption Spectrometry with Hydride Generation. *Analytical Chemistry*, **53**, 287-291.
- Andreae, M.O. and Froelich, P.N. (1984) Arsenic, Antimony, and Germanium Biogeochemistry in the Baltic Sea, *Tellus*, **36B**, 101-117.
- Andrewes, P. Cullen, W.R., Polishchuk, E. (2000) Antimony Biomethylation by *Scopulariopsis Brevicaulis*: Characterization of Intermediates and the Methyl Donor. *Chemosphere*, **41**, 1717-1725.
- Baines, S.B., Fisher N.S., Doblin, M.A. Cutter, G.A. (2001) Uptake of Dissolved organic Selenides by Marine Phytoplankton. *Limnology and Oceanography*, **46**, 1936-1934.
- Bhumbala, D.K. and Keefer, R.F. Arsenic Mobilization and Bioavailability in Soils. *Arsenic in the Enviroment Part I: Cycling and Characterization*. Ed. Nriagu J.O. New York: John Wiley & Sons, Inc., 1994.
- Brookins, D.G. *Eh-pH Diagrams for Geochemistry*. New York: Springer-Verlag, 1988.
- Byrd, J.T. and Andreae, M.O. (1982) Tin and Methyltin Species in Seawater: Concentrations and Fluxes. *Science*, **218**, 565-569.
- Chowns, T.M. (1983) *Geology of Paleozoic Rocks in the Vicinity of Rome, Georgia*. Georgia Geological Society, Georgia.
- Cooke, T.D. and Bruland, K.W. (1987) Aquatic Chemistry of Selenium: Evidence of Biomethylation. *Environmental Science and Technology*, **21**, 1214-1219.
- Crutchfield, J.U. (2000) Recovery of a Power Plant Cooling Reservoir From Selenium Bioaccumulation. *Environmental Science and Policy*, **3**, 145-163.
- Cutter, G. A. and Bruland, K.W. (1984) The Marine Biogeochemistry of Selenium: A re-evaluation. *Limnology and Oceanography*, **29(6)**, 1179-1192.

- Eisler, R. A Review of Arsenic Hazards to Plants and Animals with an Emphasis on Fishery and Wildlife Resources *Arsenic in the Environment Part II: Human Health and Ecosystem Effects*. Ed. Nriagu J.O. New York: John Wiley & Sons, Inc., 1994.
- Filella, M., Belzile, N., and Chen, W. (2002) Antimony in the Environment: A review focused on Natural Waters I. Occurrence. *Earth Science Reviews*, **57**, 125-176.
- Francesconi, K.A. and Kuehnelt, D. Arsenic Compounds in the Environment. *Environmental Chemistry of Arsenic*. Ed. Frankenburger, W.T. Marcel Dekker, Inc: New York, 2002.
- Grasshoff, K., Kremling, K., and Ehrhardt, M. (1999) *Methods of Seawater Analysis*. Wiley-Vich, Germany.
- Hambrick, G.A., Froelich, P.N., Andrea, M.O., Lewis, B.L. (1984) Determination of Methylgermanium Species in Natural Waters by Graphite Furnace Atomic Absorption Spectrometry with Hydride Generation. *Analytical Chemistry*, **56**, 421-424
- Klien, C. and Hulbut, C.S. (1993) *The Manual of Mineralogy*, 21st Edition. John Wiley & Sons, Inc., New York.
- Le, X.C., Cullen, W.R., Reimer, K.J. (1994) Effect of Cysteine on the Speciation of Arsenic by Using Hydride Generation Atomic Absorption Spectrometry. *Analytica Chimica Acta*, **285**, 277-285.
- Milne, J.B. The Uptake and Metabolism of Inorganic Selenium Species. *Environmental Chemistry of Selenium*. Ed. Frankenburger, W.T, and Engberg, R.A. Marcel Dekker, Inc: New York, 1998.
- Mok, W.M. and Wai C.M. Mobilization of Arsenic in Contaminated River Waters. *Arsenic in the Environment Part I: Cycling and Characterization*. Ed. Nriagu J.O. New York: John Wiley & Sons, Inc., 1994.
- Murphy, Riley. (1962) Analysis of Dissolved Reactive Phosphate in Natural Waters. *Analytica Chimica Acta*, **29**, 31.
- Morris, Rilet, (1963) Analysis of Nitrite in Natural Waters. *Analytica Chimica Acta*. **30**, 272.
- Newman, D.K., Ahmann, D., Morel, F.M.M. (1998) A Brief Review of Microbial Arsenate Respiration. *Geomicrobiology*, **15**, 255-268.
- Oldfield, J.E. Environmental Implications of Uses of Selenium with Animals. *Environmental Chemistry of Selenium*. Ed. Frankenburger, W.T, and Engberg, R.A. Marcel Dekker, Inc: New York, 1998.

- Ormland, R.S., Dowdle, P.R., Hoefft, S., Sharp, J.O., Schaefer, J.K., Miller, L.G., Blum, J.S., Smith, R.L., Bloom, N.S., Wallschlager, D. (2000) Bacterial Dissimilatory Reduction of Arsenate and Sulfate in Meromictic Mono Lake, California. *Geochemica et Cosmochemica Acta*, **64**, 3073-3084.
- Rubin, E. (1999) Toxic Releases from Power Plants. *Environmental Science and Technology*, **33**, 3062-3067.
- Ryan, Dave. *Whitman Annouces Transistion From Consumer Use of Wood Containing Arsenic*. (12 Feb. 2002): 1pp. Online. Internet. 14 Oct. 2002.
- Sandelin, K. and Backman, R. (1999) A Simple Two-Reactor Method for Predicting Distribution of Trace Elements in Combustion Systems. *Environmental Science and Technology*, **33**, 4508-4513.
- Sanders, J.G. (1981) Role of Marine Phytoplankton in Determining the Chemical Speciation and Biogeochemical Cycling of Arsenic. *Canadian Journal of Fisheries and Aquatic Science*. **40**, 192-196.
- Sordo, M. Herrera, L.A., Ostrosky-Wegman, P., Rojas, E. (2001) Cytotoxic and Genotoxic Effects of As, MMA, and DMA on Leukocytes and Stimulated Human Lymphocytes. *Teratogenesis, Carcinogenesis, and Mutagenesis*. **21**, 249-260.
- Stephens, D.W. and Waddel, B. Selenium Sources and Effects in Biota in the Green River Basin of Wyoming, Colorado, and Utah. *Environmental Chemistry of Selenium*. Ed. Frankenburger, W.T, and Engberg, R.A. Marcel Dekker, Inc: New York, 1998.
- Takayanagi, K. and Wong, G.T.F. (1985) Dissolved Inorganic and Organic Selenium in the Orca Basin, *Geochemica and Cosmochemica Acta*, **49**, 539-546.
- Yamauchi, H. and Fowler, B.A. (1994) Toxicity and Metabolism of Inorganic and Methylated Arsenicals. *Arsenic in the Enviroment Part II: Human Health and Ecosystem Effects*. Ed. Nriagu J.O. New York: John Wiley & Sons, Inc., 1994.
- Yan, R., Gauthier, D., and Filles, G. (2001) Volatility and chemistry of trace elements in a coal combuster, *Fuel*, **80**, 2217-2226.
- Yan, R., Gauthier, D., and Filles, G. (1999) Possible Interactions Between As, Se, and Hg During Coal Combustion. *Combustion and Flame*, **120**, 49-60.
- Zeng, T., Sarofim, A.F., and Senior, C.L. (2001) Vaporization of Arsenic, Selenium, and Antimony during Coal Combustion, *Combustion and Flame*, **126**, 1714-1724